UNIVERSITÀ DEGLI STUDI DI UDINE
hic sunt futura

www.uniud.it

Doctor of Philosophy degree in

Environmental and Energy Engineering Science

Cycle XXXI

Title of the thesis

"Effect of Neodymium on the development of Ni supported catalysts for carbon dioxide reforming of methane."

Ph.D. candidate

Rabil Razzaq

Polytechnic Department of Engineering and Architecture,

University of Udine, Italy

2021

ACKNOWLEDGEMENT

First and foremost, I would like to acknowledge and express my deepest gratitude to my research supervisor for her benevolence, dedicated advice, warmest treatments beside their invaluable ideas and suggestions.

I want to give my special thanks to Professor Alessandro Trovarelli, coordinator of heterogeneous catalysis group, University of Udine, Italy, for his cooperation extended during my PhD studies. I thank him from the core of my heart for all his deeds that are difficult to express in words.

A special thanks to Professor Thomas Etsell, Dr Amir Reza and Sajad university of Alberta, Canada for providing me a great opportunity to work with them in a friendly environment.

Thanks must go to Professor Frederic Meunier university of Lyon, France for helping me during my research stay and to complete some important DRIFT experiments.

Next, I would like to acknowledge my colleagues and friends for their help and encouragement in hard times during my PhD studies. I am also very grateful for the overall support that I have received from the staff of University of Udine, Italy.

Finally, I am deeply appreciative to my parents, brothers and sisters and my beloved husband Muhammad Haseeb Mir Ahmed who have provided me with a loving, supportive relation and climate needed to complete this project.

Rabil Razzaq

Introduction

In this work the most important issues regarding DRM reaction namely; high cost, low process efficiency and carbon deposition have been addressed by developing novel Ni based catalysts. Many attempts have been made to develop catalytic systems for DRM process. The catalysts with characteristics such as strong resistance towards carbon deposition and higher CH_4 and CO_2 activation in DRM process are highly desirable. Catalysts incorporating noble metals (Pt, Pd, Rh, Ru) are more active and selective towards DRM. However, the high cost associated to such catalysts virtually prohibits their use on industrial scale. Therefore, considerable attention has been devoted in developing catalysts containing transition metals (Ni, Co, Fe). Ni based catalyst has been found to be more attractive for industrial scale applications because of high activity even at low temperature and economic feasibility.

The main focus of current research is to develop Ni based catalysts which can be employed in multiple applications. Another objective is to run targeted catalytic processes especially fuel cell technology at relatively low temperatures (600-800ºC). However, Ni based catalysts are more prone to deactivation at low temperatures because of carbon deposition over catalyst surface. This problem can be resolved by impregnating the catalyst over suitable support; more precisely supports with high oxygen storage capacity and high thermal stability.

Thesis outline

Current research is divided into following categories;

Chapter 1: This section describes the general introduction regarding the consumption of fossil fuels, emission of greenhouse gases in open atmosphere and use of different reforming technologies specially DRM which consume two major greenhouse gases (CH_4 and CO_2) to valuable products.

Chapter 2: This section is dedicated for literature review regarding active metals for the preparation of DRM catalysts and choice of support.

Chapter 3: This section describes the synthesis procedure of Ni based catalysts, supported on ceria-zirconia doped with neodymium. Further, the catalysts are characterized using analytical techniques such as X-ray diffraction (XRD), Brunauer Emmett Teller (BET), Temperature Programmed Reduction (TPR), CHNS, SEM and chemisorption. Catalytic testing was carried out in a laboratory scale fixed bed reactor in a temperature range of 550-750^{o}C.

Chapter 4: This part illustrates the role of surfactant to improve the surface properties of catalyst.

Chapter 5: This section describes the effect of neodymium doping onto ceria-zirconia support towards the activity of Ni catalysts in DRM reaction.

Chapter 6: In this section Zirconia and Ceria are separately doped with neodymium and their comparative activities in finally prepared Ni catalysts are outlined.

Appendix section shows the activities carried out in University of Alberta, Canada. This section investigates the effect of neodymium on the performance of Ni-ceria and/or Ni-zirconia based anode for IT-SOFCs.

Abstract

Rapid increase in population, growing energy demands and dependence on fossil fuels have been a major subject of discussion for researcher and scientists. Global climate changes related to the emission of greenhouse gases (CH_4 and CO_2) increasing rapidly due to fast consumption of fossil fuel. Therefore, for environmental protection, it is urgent to control the emission of greenhouse gases and to introduce new economic technologies for the energy production.

In this work the most important issues regarding DRM reaction namely; high endothermic nature, low process efficiency and carbon deposition have been addressed by developing novel Ni based catalysts. Our main research goal is to develop Ni based catalysts operating at low temperature (600-800ºC) which can further be used for other industrial application and fuel cell technology specially IT-SOFCs. The main disadvantage of Ni is the carbon formation specially at low temperature (600-800ºC). Therefore, nickel catalyst supported on CeO_2 and CeO_2-ZrO_2 solid solutions were selected due to their high oxygen storage capacity and high thermal stability. Neodymium (Nd) has been demonstrated as an effective dopant to improve the support properties, therefore, CeO_2, ZrO_2, and CeO_2-ZrO_2 supports doped with Nd are synthesized using a surfactant assisted co-precipitation method. All catalysts have been physicochemical characterized by several techniques such as isothermal N_2 adsorption/desorption (BET and BJH analysis), X-ray diffraction (XRD), temperature programmed reduction/oxidation (TPR/TPO), desorption of CO_2 (CO_2-TPD) and CO-pulse chemisorption, elemental analysis (CHNS) and scanning electron microscopy (SEM). All catalysts were tested in dry reforming of methane reaction with a typical biogas composition (0.66) in a temperature range of 550-750°C.

It has been observed that addition of surfactant (lauric acid) with surfactant/cation (S/C) molar ratio of 0.25 in the synthesis of support materials improves the morphological properties of the finally prepared catalyst. However, more prominent results regarding catalytic activity of Ni catalysts are obtained when ceria, zirconia and ceria-zirconia supports are doped with Nd compared to undoped supports. The physiochemical properties and catalytic activities of all synthesized catalysts are

compared at different and same surface area. XRD results has shown the presence of cubic fluorite structure for all ceria-based materials and Ni is well dispersed on support materials. TPR results reveals that degree of reduction of Ni/CeZrNd$_{0.07}$ catalyst is higher (83%) in comparison to Ni/CeZr(53%) and Ni/CeZrNd$_{0.2}$ (42%) at higher surface area. Catalytic results show that Ni/CeZrNd$_{0.07}$ has highest CH_4 and CO_2 conversion with higher H_2/CO ratio (≈ 1) and reached the thermodynamic value. This means that the co-presence of Zr and Nd inhibits the reverse water gas shift reaction and increase the H_2/CO ratio. A comparative study between CeNd$_{0.2}$ and ZrNd$_{0.2}$ has shown that Nd affects more on the morphological and texture properties of Zr as compared to Ce. Higher catalytic activity and stability has been observed for Ni/ZrNd$_{0.2}$. Long term durability tests show that all catalysts are stable and TPO analysis reveals that the gasification of carbon occurred between 450-600^{o}C which means that the presence of Zr and/or Nd contributes to depress the carbon formation.

Keywords: Neodymium doping; Ceria-Zirconia; dry reforming of methane

TABLE OF CONTENTS

CHAPTER 1

Part A: General Introduction

1. Introduction

From the standpoint of a global sustainable energy strategy, and bearing in mind the threats of climate change, diminished oil availability and increased pollution, are the major issues to be resolved. Rapid increase in population resulting in growing energy demands and will increase 57% from 2004 to 2030 [1]. Fossil fuels possess a fundamental energy resource in present era. But this endless increase in the consumption of fossil fuels will result in depletion of energy and can also cause severe environmental problems including global warming. The dependence on fossil fuels has created major environmental issues by the production of greenhouse gases (GHG). Among GHG, methane (CH_4) and carbon dioxide (CO_2) constitute a major part and have a key contribution in climate changes, forecasted in terms of major incidence and magnitude of hurricanes, droughts and floods, affecting natural ecosystem, agriculture, forestry and society. In the 20^{th} century, an increase of 0.8^oC has occurred and further increase upto $1.4\text{-}5.8^oC$ has been predicted in 21^{st} century [1]. According to the World Meteorological Organization (WMO), although the concentration of CH_4 is lower than CO_2 but it constituted about 20% of global warming [2]. Based on the assessment of 2011, the concentrations of CH_4 and CO_2 were 1.813 and 390.5 ppm respectively [1]. CH_4 is the major component of natural gas (NG) obtained from petroleum reserves [3] and land fill gas [4, 5] also contains low balances of other hydrocarbons such as ethane, propane and butane [6]. Apart from NG, biogas produced from anaerobic decomposition of organic matter is also a source of with almost the equal concentrations of CH_4 and CO_2 [7]. Therefore, the major concern related to the utilization of fossil fuels is the increased concentration of CH_4 and CO_2 emission in an open atmosphere which ultimately have a negative impact on the climate, causing the global surface temperature to increase [1]. Therefore, the development of a new economic paradigm based on the sustainability via the use of renewable resources is an important target of the modern societies. It requires new technologies as well as the upgrading and the innovation of traditional processes for the conversion and storage of energy [8, 9].

Keeping in view the above scenario, researchers are investigating different processes by which the parts of the CO_2 could be utilized, for example by application in enhanced oil recovery or by converting them into fuels and chemicals.

One strategy to reduce the emissions of CO_2 is carbon capture and storage (CCS) which involves capturing of CO_2 from natural gas fields or large industrial pants, compressing it for transportation and then injecting it into a safe location for storage. Although CCS provides a relatively effective option for CO_2 emission reduction, but it has certain limitations [10]. It requires a high geological storage capacity and a method of transporting the CO_2 from the source to the storage location, as well a high capture cost, which could require a high capital investment cost. Biocatalytic process can also be employed for the valorization of CO_2 in which biochemical agents such as enzymes are used for breaking down carbon dioxide and water and combine carbon and hydrogen to form liquid fuel (methanol) [11]. Production of methane via reduction of CO_2 with H_2 also got attraction since last year. The first scientist who studied the reaction was Sabatier, which discovered that one mole of methane can be obtained by the reaction of one mole of carbon dioxide and four moles of hydrogen ($CO_2 + 4H_2 \rightarrow CH_4 + 2H_2O$). Among these technologies for the valorization of CO_2, the carbon dioxide reforming of methane (dry reforming) has got a much attention since the early work of Fischer and Tropsch. In this process carbon dioxide reacts with methane to produce syngas, a mixture of carbon monoxide and hydrogen. The syngas mixture can further be used for the production of synthetic fuels by the Fischer-Tropsch synthesis or for the production of compounds as the methanol or the dimethyl ether (DME) [12-16].

There are various reforming technologies available which can be used to produce syngas. The processes such as partial oxidation of methane, steam reforming of methane and carbon dioxide reforming of methane (dry reforming) yield different H_2/CO ratios [17]. There are three oxidizing agents used in reforming processes, (i) H_2O in steam methane reforming (SRM), (ii) O_2 in partial oxidation of methane (POX) and (iii) CO_2 in dry reforming of methane (DRM). Autothermal reforming (ATR) can be considered as a combination of partial oxidation and steam reforming.

SMR is energy intensive method due to the endothermic nature of reaction, which is widely used in the industry. It produces syngas by reacting high temperature steam with natural gas on catalytic surface (Eq. 1). Furthermore, H_2 is produced through shift reactions following the main reactor, one high temperature shift reaction and another is low temperature shift reaction, where the water gas shift reaction (Eq. 1.1) takes place to increase the yield of H_2.

$$CH_4 + H_2O \rightarrow CO + 3H_2 \qquad \Delta H = 206 kJmol^{-1} \quad (1)$$

Steam reforming generally produces higher ratio of syngas (H_2/CO = 3) which is normally higher than the needed ratio for Fischer -Tropsch or methanol synthesis (H_2/CO = 2). To produce the higher yield of H_2, a higher ratio of H_2O/CH4 is required which makes the SR energetically unfavorable and leads to the deactivation of catalyst. Apart from this, SR can face corrosion issues and requires desulphurization unit [1]. A high heat is required to drive the endothermic reaction, and operational costs and energy consumption are also increased when excess of steam is used to inhibit catalyst deactivation due to carbon deposition onto the surface of catalysts [18].

Partial oxidation of methane (POX) is an exothermic reaction (Eq. 2) which is suitable for the production heavier hydrocarbons and naphtha. POX yields a H_2/CO ratio of about 2 [15]. The major advantage of POX is its very short residence time and high conversion rates and higher selectivity.

$$CH_4 + \frac{1}{2}O \rightarrow CO + 2H_2 \qquad \Delta H = -32 kJmol^{-1} \quad (2)$$

The exothermic nature is one of the drawbacks of this process because it induces hot spots on the catalytic surface arising from the poor heat removal rate which can makes the operation difficult to control. In most cases, pure O_2 source is needed, which could lead to higher costs of O_2 and necessary precautionary measures related to the risk of explosion. Desulphurization unit does not require but a cryogenic unit is necessary for the separation of oxygen from air [19, 20].

Autothermal reforming (ATR) is more flexible reforming process compared to the other reforming technologies [21]. ATR generally produce a syn gas (H_2/CO) ratio

between 1 to 2. The compact reactor proposes a moderate cost, size and weight requirements. To avoid the soot formation, steam must be added during combustion, and it contributes to the higher costs which is one of the drawbacks of ATR. Furthermore, an extensive control system for mixing the gases is also required to control the reaction. In addition, the high temperature of the gas mixture entering the catalyst bed requires a catalyst and carrier system with high thermal stability [22].

Among steam reforming, partial oxidation and autothermal reforming of methane, dry reforming of methane (DRM) (Eq. 3) has got an industrial advantage. DRM offers many valuable environmental benefits including, (i) biogas utilization [13, 23] (ii) removal of greenhouse gases (CH_4 and CO_2) and (iii) conversion of NG with high CO_2 content to valuable syngas with H_2/CO ratio close to unity which is suitable for the production of liquid hydrocarbons and oxygenates [14].

$$CH_4 + CO_2 \rightarrow 2CO + 2H_2 \quad \Delta H = 247.3\ kJmol^{-1} \qquad (3)$$

The reaction is highly endothermic and usually carried out at temperature higher than 800°C.

Part B: Dry Reforming of Methane (DRM)

1.1. Dry reforming of methane

Carbon dioxide reforming of methane also known as dry reforming of methane has got a significant importance because of following reasons. Firstly, it utilizes two abundantly greenhouse gases, CH_4 and CO_2 and could provide a way to reduce greenhouse effect [24-27]. Secondly, CH_4 and CO_2 also produced in the pyrolysis of biomass, hence the utilization of CH_4 and CO_2 could make more valuable the pyrolysis gases and makes the whole process more practical [28-30]. Thirdly, as CH_4 and CO_2 are the main components of marsh gas, so the utilization of CH_4 and CO_2 could provide a way to make biogas value added [31, 32]. Hence the DRM has got much attention because this process not only consume two major greenhouse gases (CH_4 and CO_2) but also produce a valuable product of syngas (mixture of CO and H_2) with H_2/CO ratio closer to unity which is desirable for the production of liquid hydrocarbons and oxygenates via Fischer- Tropsch synthesis (Eq. 4). [12, 33].

$$nCO + (2n+1)H_2 \rightarrow C_nH_{2n+2} + nH_2O \qquad \text{Fischer-Tropsch reaction (4)}$$

DRM is an endothermic reaction and usually carried out at higher temperature (> 800^{o}C). Therefore, in order to lower process costs and to favor its integration with fuel cell technology or other fuel production processes, several studies have been recently focused on developing systems and catalysts to decrease the operating temperature in the range of 600-800°C [14, 34]. At these temperatures, the main reaction (Eq. 5) is accompanied by other parallel-side reactions: reverse water gas reaction (Eq. 6), Boudoured reaction (Eq. 7 and methane cracking (Eq. 8) which can cause a decrease in the yield of products and the deactivation of catalysts due to the carbon deposition [35-37].

$$CH_4 + CO_2 \rightarrow 2CO + 2H_2 \quad \Delta H = 247.3\ kJmol^{-1} \qquad (5)$$

$$\Delta G^o = 61770 - 67.32T$$

$$CO_2 + H_2 \rightarrow CO + H_2O \quad \Delta H = 41\ kJmol^{-1} \qquad (6)$$

$$\Delta G^o = -8545 + 7.84T$$

$$CO_2 + C \rightarrow 2CO \quad \Delta H = -172\ kJmol^{-1} \qquad (7)$$

$$\Delta G^o = -39810 + 40.87T$$

$$CH_4 \rightarrow C + 2H_2 \qquad \Delta H = 74.9\ kJmol^{-1} \qquad (8)$$

$$\Delta G^o = 29960 - 26.45T$$

Based on Gibbs free energy, the thermodynamics of reaction involved in DRM at different temperatures (500-900°C) using a CO_2/CH_4 feed ratio of l/l at 1 atm are shown in Figure 1.

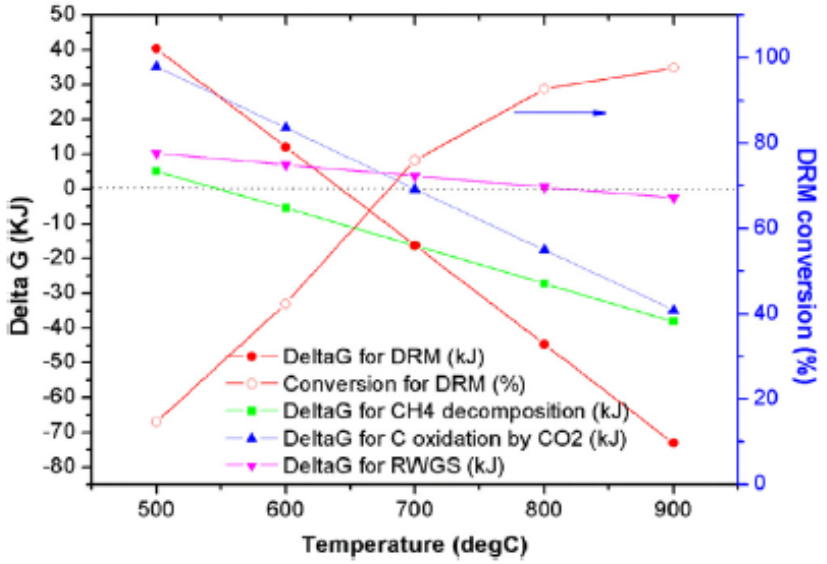

Figure 1. Illustrating the variation of Gibbs free energy (KJ) with temperature (°C) based on dry reforming of methane (DRM), methane decomposition, Boudouard reaction and reverse water gas shift (RWGS) [38].

It can be seen that when DRM reaction operating at lower temperature (< 800°C) the carbon formation occurs due to methane cracking and Boudouard reaction while at high operating temperature (>800°C) the carbon deposition mainly occurs due to methane cracking and these carbon species are more active than those are originates from Boudouard reaction. Furthermore, reverse water gas reaction (RWGS) and Boudoured reaction are less favored at high temperature. It is noteworthy to point out that at 700°C temperature, the CH_4 cracking is more spontaneous than carbon oxidation and RWGS reaction. However, the CO_2/CH_4 ratio generally closer to 1 because at 700°C, excess of

CO_2 would be consumed by RWGS reaction and H_2 production during DRM reaction and as a result less amount of H_2 with syngas ratio < 1 would be obtained [38].

Based on the calculated equilibrium conversions it was concluded that DRM has greater tendency to carbon formation, however, changing the operating conditions could maximize the H_2 yield by obtaining a desirable syngas ratio by minimizing the carbon formation during DRM reaction.

1.2. Reaction Mechanism

Both pressure and temperature have significant role in DRM reaction. Figure 2 represents the effect of temperature on a stoichiometric mixture at 0.1 MPa pressure with O/C =1. No significant conversion was observed below 500^{o}C because of most stable structure of CH_4 which need high temperature to break C-H bond. The higher CH_4 and CO_2 conversion and selectivity were observed at higher temperature. It can be seen that syngas ratio ≈ 1 can be obtained at 900^{o}C.

Figure 3 shows equilibrium conversions in a pressure range of 0.1-3 MPa. It can be seen that CH_4 and CO_2 conversion and H_2 and CO yield decreases with the increase of pressure [39].

Furthermore, to understand better the effect of temperature and pressure on DRM reaction, equilibrium study was conducted at different temperatures in the pressure range of 0.1-5 MPa and results are shown in Figure 4 (A, B). It can be seen from Figure 4A that at 900 K temperature, the CH_4 conversion is 98, 90, 82 and 58% at pressure of 0.1, 0.5, 1 and 5 MPa respectively. Moreover, H_2/CO ratio as found to be decreased with the increase of pressure (Figure 4B). This can be attributed to the conversion of CO_2 by Boudouard reaction ($2CO = C + CO_2$). In summary, it was concluded that DRM reaction is favored at high temperature and low pressure [40].

Figure 5 shows the effect of feed ratios (CO_2/CH_4) on limiting temperature of carbon formation and total pressure. It can be seen that for the same feed ratio, the temperature limit for carbon deposition increases with the increase of pressure. With CO_2/CH_4 feed ratio of 1:1, the carbon deposition is thermodynamically possible at 1143K at 1 atm and 1303K at 10 atm. Additionally, at given pressure, the temperature limit

increase as the CO_2/CH_4 feed ratio decreases. This means that by using excess of CO_2 in the feed may avoid carbon deposition at lower temperatures [41].

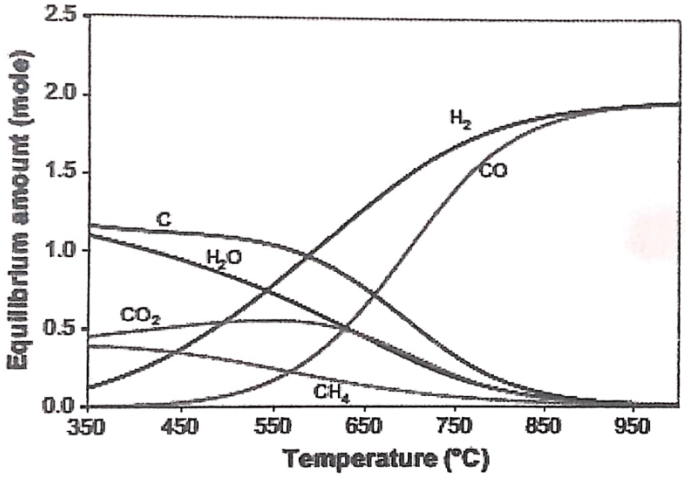

Figure 2. Effect of temperature on DRM reaction on equilibrium amount of product species [39].

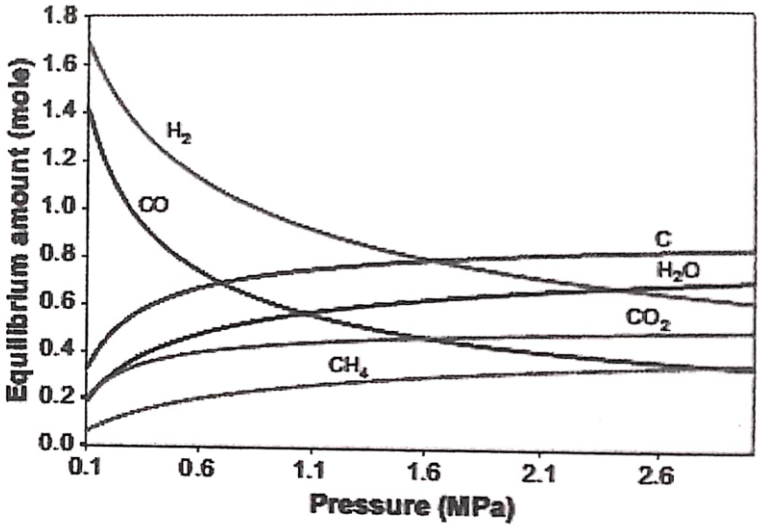

Figure 3. Effect of pressure on DRM reaction on equilibrium amount of product species [39].

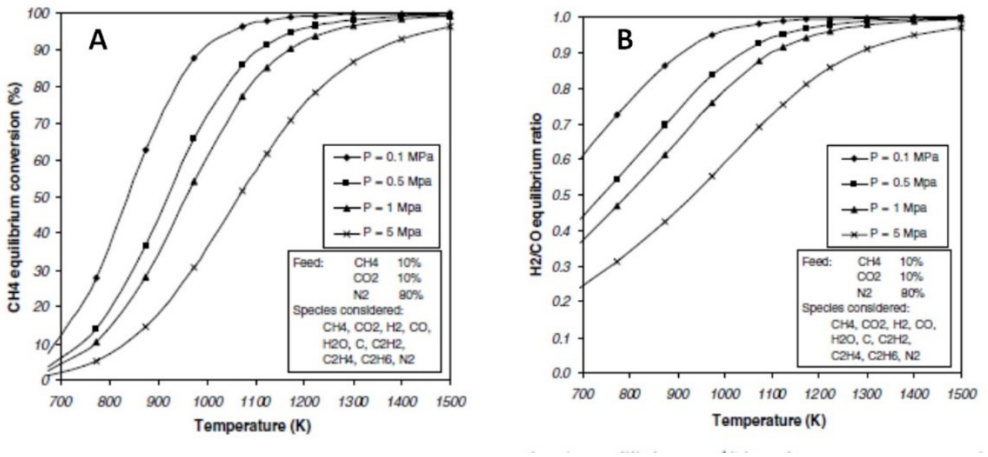

Figure 4. Equilibrium conversions (A) and equilibrium H_2/CO ratio (B); vs temperature and pressure [40].

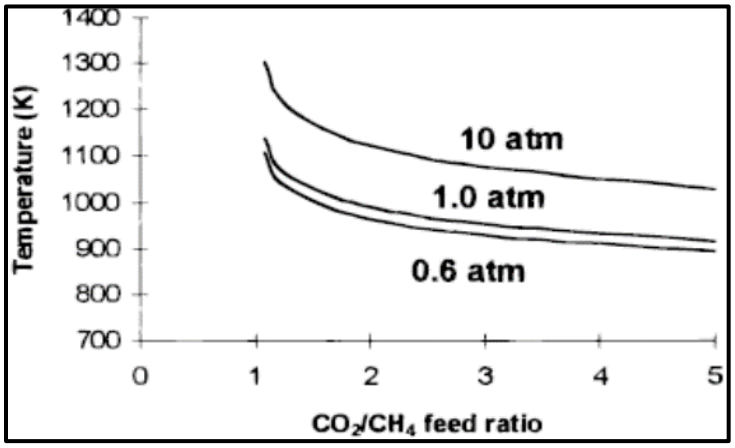

Figure 5. Effects of CO_2/CH_4 feed ratio on limiting temperature at various pressures [41].

1.3. Reaction kinetics

In order to understand the kinetics of reforming process, kinetic models are considered as a useful tool for giving a deep interpretation of experimental data. Power la model, Eley-Rideal model and Langmuir Hinshelwood-Hougen Watson (LHHW) model are typically considered for DRM reactions. In comparison to other models, most of the reaction mechanisms proposed for DRM reaction are based on LHHW model. Based on LHHW model it is assumed that on reaction step is rate determining step while others are in thermodynamic equilibrium. LHHW model has got considerable attention because

most of the proposed steps are confirmed by using different experimental techniques such as XRD, XPS, DRIFT and TGA analysis [37].

Figure 6 describes the mechanism of CO_2 reforming of methane over Ni based catalysts. The reaction involves the following steps [41]:

1. Dehydrogenation of methane to form H and C
2. Dissociation of CO_2 to form CO and O.
3. Combination of O with H to form OH
4. Reaction of OH group with CH_x intermediates to form CH_xO (CH_xO species can be produced either via CH_x adsorption with O which is originating from CO_2 or from the direct cleavage of OH groups)
5. Decomposition of CH_xO to H_2 and CO

The possible mechanism is described as follows:

$$CH_4 \rightarrow C(s) + 4H(s) \qquad (9)$$

$$CO_2\,(g) \rightarrow CO(s) + O(s) \qquad (10)$$

$$C(s) + O(s) \rightarrow CO(s) \qquad (11)$$

$$CO(s) \rightarrow CO(g) \qquad (12)$$

$$2H(s) \rightarrow H_2(g) \qquad (13)$$

The kinetic mechanism of CO_2 reforming reaction over Ni/La_2O_3 catalysts is described as follow. It is known that CH_4 is only weakly adsorbs on La_2O_3 while at high temperature it can easily cracks on metallic Ni, so it may be predicted that the breaking of C-H bond of CH_4 favorably occurs on Ni crystallites with or without assistance of CO_2. On the other hand, CO_2 preferentially adsorb on La_2O_3 to form $La_2O_2CO_3$ and FTIR results has confirmed the formation of $La_2O_2CO_3$ on Ni/La_2O_3 catalysts.

$$CH_4 + Ni_n \rightarrow C + Ni_n + 2\,H_2 \qquad (14)$$

$$CO_2 + La_2O_3 \rightarrow La_2O_2CO_3 \qquad (15)$$

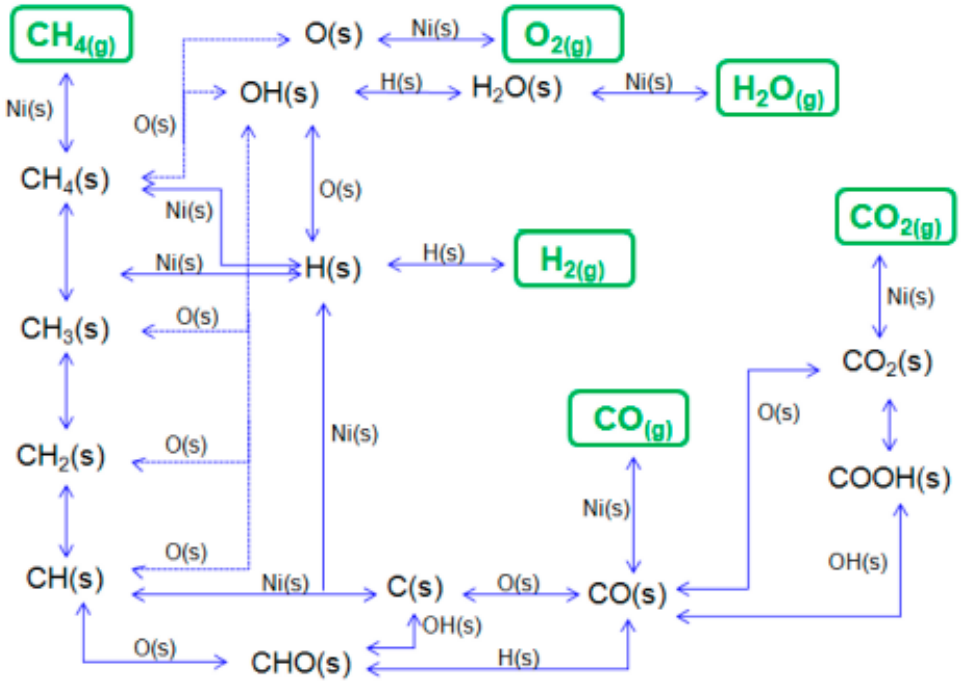

Figure 6. Reaction pathway for methane oxidation and reforming [42].

For CH_4/CO_2 reaction at high temperature the $La_2O_2CO_3$ tend to attack on C-Ni_n species producing two CO molecules while La_2O_3 acts as an intermediate, promoting a reaction between C species and CO_2 by storing CO_2 from gas phase and releasing if to the reaction sites.

$$C - Ni_n + La_2O_2CO_3 \rightarrow 2CO + Ni_n + La_2O_3 \qquad (16)$$

The presence of formate species on Ni/La_2O_3 catalysts were indicated by FTIR and XPS results, so an alternative mechanism could be, the involvement of formate species for the removal of carbon formation originating from CH_4 cracking. CO_2 adsorption on La_2O_3 or $La_2O_2CO_3$ and H_2 spillover from Ni crystallites on the support resulting the formation of formats on the support.

$$CO_2(a) + H^+ \rightarrow HCOO^-(support) \qquad (17)$$

Afterwards, formate species decompose into H_2 and CO due to the interaction with another H_2 atom.

$$HCOO^- + H^+ \rightarrow H_2O + CO \quad (18)$$

The resulting H_2O may then react with C species on Ni crystallites to form one CO and one H_2 molecule.

$$H_2O + CO \rightarrow CO + H_2 \quad (19)$$

On the basis of both processes described above, the C species on Ni crystallites of Ni/La_2O_3 catalysts are favorably removed by H_2O or CO_2 oxidants originating from support side. This offers a superior pathway in comparison to the conventional Ni based catalysts on which CO_2 attacks on C species on Ni crystallites' directly from gas phase [43].

In summary, the kinetic mechanism of CO_2 reforming reaction depends on the type of catalyst and the mechanism can probably change with the change of temperature.

CHAPTER 2

Catalytic Technology and Literature Review

2.1. Why we need a catalyst

Dry reforming has been a challenge for researchers for decades. Keeping in mind the fact that the DRM reaction is more endothermic than SRM or ATR, the required aspect of an optimal catalyst would be to induce high conversions of CH_4 and CO_2 by lowering the activation energy. Numerous studies have been devoted to develop a catalyst for DRM which can resist the deactivation due to the sintering and carbon deposition. The overall activity of DRM depends on the type of metal, nature of support and the interaction between metal and support.

2.1.1. Noble Metals

Numerous studies have been devoted to develop a suitable catalyst for DR which can resist the deactivation due to the sintering and carbon deposition. The overall activity of DRM depends on the type of metal, nature of support and the interaction between metal and support. DRM has been investigated with noble metals (Pt, Pd, Ru, Rh) and non-noble metals (Ni, Co, Fe). Noble metals catalysts have drawn much attention due to their higher resistance to carbon deposition and higher catalytic and stability, specially at low operation temperature. Among Pt, Pd, Ru and Rh; Pt and Rh are most suitable for dry reforming reaction. It is reported in literature that noble metal catalysts have revealed inconsistencies in the results presented by different groups [44].

Hou et al; (2006) [45] made a comparison between noble metal (5 wt%) supported on Al_2O_3 support and has been concluded that these catalysts showed high coke resistance and stability in the order of $Rh/\alpha Al_2O_3$ > $Ru/\alpha Al_2O_3$ > $Ir/\alpha Al_2O_3$ > $Pd/\alpha Al_2O_3$ > $Pt/\alpha Al_2O_3$. The amount of carbon deposition was found to be zero (0.00) for all catalysts except $Pd/\alpha Al_2O_3$. This study was in agreement with the findings of Matsui [46]. The relatively lower stability of Pt and Pd supported catalysts can be attributed to the sintering of the metal particles at higher reaction temperatures [1].

Tsyganok et al; (2004) [47] investigated the effect of Rh, Ru, Ir, Pd, Pt and Au over Mg-Al mixed oxide support. The higher catalytic activity and stability towards DRM was observed for $Ru/MgAlO_x$, Rh/AlO_x and Ir/AlO_x. The results were verified through TEM characterization and showed that the presence of highly dispersed smaller metal particles can reduce the carbon deposition, agglomeration and sintering.

Wang et al; (2006) [48] explained catalytic behavior of Rh and CeO_2 over Al_2O_3 catalyst (Rh-CeO_2 over Al_2O_3) and concluded that coke resistance could be enhanced due to the strong interaction of Rh with CeO_2.

Breadford et al; (1998) [49] investigated and tested the catalytic activity of Pt onto TiO_2, ZrO_2, Cr_2O_3 and SiO_2 supports and concluded that TiO_2 and ZrO_2 are the promising supports for Pt based catalysts for DRM reaction due to the strong interaction of Pt with TiO_2 and ZrO_2 supports.

2.1.2. Non-noble metals

Due to the prohibitive cost and limited availability, noble metals are not generally seen as appropriate catalysts for dry reforming reaction. Therefore, for an industrial application and in order to lower the process cost, non-noble transition metals are preferred to use for DRM. Several studies have been focused to investigate a stable, active and coke resistant catalyst and transition metals of VIII-B group are found to be most active, cheap and stable for large industrial scale applications. Based on the literature regarding DRM, nickel (Ni) and cobalt (Co) were found to be most suitable catalysts.

2.1.2.1. Cobalt (Co) based catalysts

Although the catalytic activity of Co based catalysts is lower than noble metals and Ni based catalysts, but still cobalt (Co) is considered as an active transition metal and largely investigated for dry reforming reaction.

Ayodele and coworkers (2016) [50] investigated La_2O_3 supported Co catalyst for CO rich hydrogen production from methane dry reforming reaction. The catalyst was synthesized by wet-impregnation method and characterized by using different physio-chemical techniques such as N_2 adsorption-desorption, TGA, FTIR, XRD analysis. The kinetics behavior of the Co/La_2O_3 catalyst was investigated as a function of temperature and partial pressure of reactants (CH_4 and CO_2). The catalytic activity of Co/La_2O_3 catalyst yielded highest CH_4 and CO_2 conversion of 50% and 60% respectively at 800^oC while H_2 and CO yield was 45% and 58% respectively.

Ayodele et al; (2015) [51] synthesized 20 wt%Co/80 wt%Nd_2O_3 catalyst via wet-impregnation procedure for dry reforming of methane and characterized by TGA, XRD,

FESEM, EDX, FTIR, H2-TPR and TPD followed by activity testing in a fixed-bed reactor. The conversion efficiencies for CH_4 and CO_2 increased to 62.7% and 82% respectively. The results indicated that the formation of syngas with maximum yields of 59.91% and 62.02% for H_2 and CO respectively, leading to formation of syngas ratio of 0.97. The presence of carbon deposition on the surface of the catalyst is an indication of the possible influence of side reactions such as Boudouard reaction and methane cracking reactions during the CO_2 reforming of methane.

Ruckenstein and Wang [52] investigated the Co supported on γ-Al_2O_3 catalyst for carbon dioxide reforming of methane as a function of different Co loading (2-20 wt.%) and calcination temperature (500-1000^{o}C). Catalytic results showed the deactivation of catalyst either due to carbon deposition onto the surface of catalyst or oxidation of metallic (Co) sites. Consequently, the catalysts can be stable when there is a balance between the generation of carbon species and its oxidative removal.

2.1.2.2. Nickel (Ni) based catalysts

In recent years, Ni based catalysts have been investigated for industrial stand point due to their low prize, higher activity and better stability for DRM. However, one of the major drawbacks of Ni based catalysts is carbon deposition which can contribute to the deactivation of catalysts. Based on the specific reaction conditions and structure of the catalyst, different types of carbon deposited during dry reforming reaction. Methane adsorption normally occurs on Ni surface where it can decompose into C and H, where C atoms diffuse through the Ni particles and precipitate as carbon. The main types of carbon deposited on Ni based catalysts are categorized into, polymeric, filamentous (whisker carbon), graphitic and bulk carbon [53]. Polymeric type is derived from gas phase thermal decomposition of hydrocarbons, whereas, filamentous and graphitic forms of coke are generally accepted to occur on catalyst. It has been reported that the polymeric carbon is more active and can rapidly consumed by the Boudouard reaction (Eq. 1.7), whereas filamentous and graphitic types are proposed to not block active sites but are consumed at a lesser rate and normally needed higher temperature to be oxidized compared to amorphous carbon. On the other hand, bulk carbon causes a rapid loss of

activity due to the physical coverage of the active sites, and that cannot be consumed easily in the Boudouard reaction [54].

Several approaches have been proposed in order to decrease the carbon formation for Ni based catalysts and are summarized as follows:

- Addition of oxidizing agents (water or oxygen)
- Suitable support materials
- Appropriate method of preparation

Previous literature related to Ni based catalysts revealed that the catalytic activity, stability and carbon deposition over catalytic surface is strongly depend on the nature and type of support material. Research is being done using different types of supports to improve the catalytic activity [55, 56]. It is reported that under dry reforming conditions, migration of adsorbed species from the active metal to the support and vice versa can take place [57]. For example, carbon deposition is favored on acidic supports, such as SiO_2, whereas basic supports having opposite effect, as high affinity towards CO_2 chemisorption and high oxygen mobility between support and active metal phase [58] which can lead to the gasification of deposited carbon and thereby enhance the durability of reforming process. The size of the Ni particles is suggested to be connected to the overall participation of the support through the metal-support interfacial zone [59] and it is reported that smaller Ni particles are more resistant to carbon formation [60, 61]. Smaller the particles size, lower is the coke formation and higher catalytic activity.

Further improvements can be done through catalyst promoters and dopants which offer a diversity of effects, including enhanced metal dispersion over support,[34] blocking step sites on the nickel particles thereby disrupting coke formation, improving regasification rate of carbon, improving stability of the active metal and altering the type of formed coke [62].

2.1.3. Supports for nickel (Ni) based catalysts

Many efforts have been made to improve catalytic activity of Ni based catalysts by minimizing the carbon deposition. In order to hinder carbon formation and to optimize both CH_4 and CO_2 conversion, Ni can be supported on different types of supports such as, SiO_2, La_2O_3, Al_2O_3, MgO, CeO_2, ZrO_2 and CeO_2-ZrO_2 [63, 64]. The effect of La_2O_3,

Al_2O_3, MgO, CeO_2 and CeO_2-ZrO_2 supports have been investigated in dept and it was concluded that these supports react with CO_2 to form oxygen storing complexes on catalytic surface in the form of carbonates and therefore favoring the oxidation of carbon formed during methane decomposition and Bouduard reaction and improving activity and stability. On the other hand, acidic supports like SiO_2 favors the carbon deposition. The type of the support and the nature of metal-support interaction plays an important role in the activity and stability of the catalysts. Strong metal-support interactions advantage the dispersion of Ni, increasing activity, while oxygen transfer properties of the support limit the carbon buildup, thus improving stability.

2.1.3.1. Alumina and magnesia support for Ni based catalysts

Kang and his coworkers (2011) [61] have synthesized Ni supported catalysts with core/shell structure of Ni/Al_2O_3 and Ni/MgO-Al_2O_3 under multi-bubble sonoluminescence (MBSL) conditions and tested for dry reforming of methane (DRM). High operating cost and high temperature operation usually caused Ni metal sintering and carbon formation which lead to the catalyst deactivation. Some efforts such as core/shell structure catalysts have been made in solving this problem. Core/shell structures have been designed in such a way that the shell material can improve the reactivity, thermal stability, or stability of the core material [65-69]. Catalysts were characterized by using different techniques such as XRD, TPR. XPS and SEM. The catalytic performance of Ni supported catalysts Ni/Al_2O_3 and Ni/MgO-Al_2O_3 was tested for steam reforming of methane, partial oxidation of methane and methane dry reforming. All catalysts, Ni/Al_2O_3 and Ni/MgO-Al_2O_3 with core/shell structures has shown good thermal stability and high catalytic yield and carbon deposition on the surfaces of catalysts did not influence the activity or thermal stability of the catalysts.

Yang et al; (2012) [70] synthesized Ni/MgO-ZrO_2 catalysts by using coprecipitation and impregnation method. Several characterization techniques such as X-ray diffraction (XRD), Scanning electron microcopy (SEM) were employed to understand the structural morphology of Ni/MgO-ZrO_2 catalyst. It was concluded that with the rise of mole ratios of Zr/Mg, the addition of Mg^{2+} transformed the monoclinic ZrO_2 to tetragonal ZrO_2 and these changes enhanced the thermal stability of the catalysts.

ZrO_2 exhibits both acidity and basicity, and active in many heterogeneous catalytic systems. Carbon deposition needs a certain size of metal Ni, so the formation of mixed oxide phase of NiO-MgO inhibited Ni agglomeration and prevent the deactivation of catalyst.

Titus et al; (2016) [21] have synthesized NiO-MgO-ZrO_2 catalysts by using melt impregnation technique on a zirconia support impregnated with an equimolar amount of Ni and Mg in the range of 2–35 mol%. Several characterization techniques were employed to characterize the prepared catalysts such as TPDA, TPR, PXRD, TEM and EDX. It was observed that Ni and Mg are homogeneously distributed over the zirconia support and metallic Ni is highly dispersed on the support together with a solid solution of NiO–MgO. NiO-MgO-ZrO_2 catalysts showed a high activity in DRM at 850^{o}C. The high activity was achieved for catalysts with Ni and Mg contents of 8–20 mol%. The catalysts were subjected to severe carbon deposition which leads to the pronounced deactivation by increasing the Ni and Mg contents ≥22 mol%. The presence of MgO leads to a suppression of carbon formation, especially when compared to Ni supported on Mg free zirconia. The overall conclusion was, the basic nature and high thermal stability of NiO-MgO-ZrO_2 catalysts could lead to the low coking tendency for reforming reactions.

Koo et al; (2008) [71] have been studied the MgO-promoted Ni/Al_2O_3 catalysts by varying the MgO contents using incipient wetness method. X-ray diffraction (XRD), BET surface area, H_2-temperature programmed reduction (TPR), H_2-chemisorption and CO_2-temperature programmed desorption (TPD) were used for the characterization of the prepared catalysts. It was concluded that the catalysts prepared with 20 wt.% MgO exhibit the highest catalytic performance and have high coke resistance due to $MgAl_2O_4$ spinel phase, which is stable at high temperatures. The basic strength of catalyst prevents coke formation by increasing CO_2 adsorption.

Luna et al; (2008) [60] has proposed the influence of K, Sn, Mn and Ca (0.5 wt.%) on the behavior of a Ni-Al_2O_3 catalyst for CO_2 reforming of methane. The catalysts were synthesized by a sol-gel method and characterized by using XRD, TPR, TPH, TPD and TEM. The preparation method allowed to obtain a massive catalyst with a small and homogeneous nickel particle size (TEM:5-7 nm) and no effect of sintering was

observed. The catalytic tests showed that the activity of unmodified catalyst is constant during 30 h of operation with low carbon deposition. It was observed that the K modified catalyst showed low carbon deposition and high stability during 30 h of operation while Ca, Sn and Mn modified catalysts has shown a dramatic reduction of catalytic activity and a significant increase in carbon deposition were observed during the period of time under study. The catalytic activity was constant for the unmodified and the K-modified catalyst which indicate that the incorporation of potassium hinders the accumulation of carbon on the catalyst surface, increases the reducibility without modifying the the size and the structure of nickel particles.

2.1.3.2. Lanthanum support for Ni based catalysts

Pereniguez et al; (2012) [72] investigated the physio-chemical and catalytic properties of Ni/La_2O_3 catalysts using different preparation methods. Ni/La_2O_3 catalysts were prepared by Hydrothermal synthesis (HT), Combustion (CM), Spray pyrolysis (SP) and Spray pyrolysis-combustion (SPCM) and characterized by using SEM, XRD, XAS, TPR and TPO. XRD results found the crystalline rhombohedral phase of $LaNiO_3$ and an amorphous NiO phase, normally not detectable by XRD but evidenced by XAS. The catalytic tests were performed in the temperature range of 420-1120K. It was observed that the systems synthesized by HT and SPCM present the best catalytic performances compared to SP and CM. In case of $LaNiO_3$ prepared by CM method induced low activity for DRM due to the formation of big Ni^0 particles.

2.1.3.3. Effect of promotors on support materials for Ni based catalysts

Promotors could enhance the catalytic activity of Ni based catalyst via different ways. Firstly, they could increase the reduction degree of NiO to Ni^0 species. These Ni^0 species improve the direct decomposition of methane which in turn enhance the H_2/CO ratio with the time on stream. Secondly, promotors could increase the basic sites and thereby enhancing the ability of CO_2 adsorption. Thirdly, promotors could facilitate the formation of active sites at low temperature. It is reported that presence of La as a promotor could enhance the reduction of NiO and Ni^0 species activate the CH_4 decomposition. Presence of Ce could increase the basic properties and thereby increase the ability of CO_2 adsorption. Furthermore, Zr promoted the low temperature active sites and hence decrease the reaction temperature [34].

2.1.3.3.1. Co and Cu promoters for alumina and zirconia supported Ni catalysts

Sharifi and his coworkers (2014) [73] used impregnation method of preparation and investigated the effects of Cu and Co as promoters over Ni/Al_2O_3-ZrO_2 nanocatalyst in reforming of biogas. The synthesized nanocatalysts were characterized using XRD, FESEM, BET and FTIR analysis. The XRD patterns revealed that the active phases promoters could be effective for the dispersion of nanoparticles. The catalytic activity was observed in the temperature range of 550-850°C with the feed gas ratio of CO_2/CH_4= 1. The results revealed that the best activity was gained for Ni Co/Al_2O_3-ZrO_2 nanocatalyst compared to Ni-Cu/Al_2O_3-ZrO_2 probably due to the sintering of Cu active phase. Presence of ZrO_2 as a promoter led to the stability of all nanocatalysts at 850°C for 24 h during reforming reaction.

2.1.3.4. Ceria and zirconia support for Ni based catalysts

CeO_2-ZrO_2 (CeZr) mixed oxides have been often selected for Ni based catalysts owning to their higher oxygen storage capacity and their higher thermal stability as compared to other supports**.** These properties are related to their rapid oxidation and reduction capability due to releasing and up taking of oxygen species. Furthermore, during DRM CeO_2 reacts with CH_4 to produce syngas and reduced phase of Ce (Ce_2O_3) which can be reoxidized to CeO_2 by reacting CO_2. As a lattice oxygen provider, CeO_2 facilitate the oxidation of carbon which is formed due to the CH_4 decomposition reaction and Boudouard reaction. In addition, CeO_2 oxidize NiO to Ni^0 which possess the higher activity as compared to NiO. Moreover, the addition of ZrO_2 to CeO_2 improves the CH_4 conversion at lower temperature which is an important characteristic to overcome the endothermic nature of DR process.

Roh et al; (2004) [74] employed co-precipitation/digestion method for the synthesis of $Ce_{0.8}Zr_{0.2}O_2$, $Ce_{0.5}Zr_{0.5}O_2$ and $Ce_{0.2}Zr_{0.8}O_2$ supports followed by the 15% Ni (w/w) co-precipitation. The synthesized Ni-Ce-ZrO_2 catalysts were characterized by various physico-chemical characterization techniques such as XRD, BET surface area, hydrogen chemisorption, SEM, TPR and XPS. The results demonstrated that 15% Ni (w/w) co-precipitated with $Ce_{0.8}Zr_{0.2}O_2$ having cubic phase structure and contributed syn gas with CH_4 conversion more than 97% at 800ºC and catalytic activity was maintained without significant loss during the reaction for 100 h. On the contrary, $Ni/Ce_{0.2}Zr_{0.8}O_2$

tetragonal phase and mixed phase Ni/$Ce_{0.5}Zr_{0.5}O_2$ catalysts deactivated during DR reaction due to the significant amount of carbon formation. The nano-crystalline nature of cubic $Ce_{0.8}Zr_{0.2}O_2$ support and the finely dispersed nano-sized NiO_x crystallites resulting in the enhanced catalytic activity and stability of Ni-$Ce_{0.8}Zr_{0.2}O_2$ catalyst due to the high oxygen storage capacity which results in increasing the availability of surface oxygen by a release mechanism during dry reforming reaction.

Prashant et al; (2007) [75] studied the catalytic activity of ZrO_2, ceria-doped ZrO_2 and $Ce_xZr_{1-x}O_2$ ($Ce_{0.6}Zr_{0.4}O_2$) solid solution for carbon dioxide reforming of methane (CDRM). Different techniques were employed for the synthesis of support materials having different physiochemical properties. Different preparation methods were used to prepare supports materials and various characterization techniques were employed to study the different physicochemical properties. Based on the catalytic experiments, $Ce_xZr_{1-x}O_2$ ($Ce_{0.6}Zr_{0.4}O_2$) solid solution as a support was found to be more active and stable for low temperature DRM. H_2-TPR analysis also showed enhanced reducibility of $Ce_xZr_{1-x}O_2$ solid solution at lower temperatures as compared to either pure ceria or ceria-doped ZrO_2 which is an important function of stability for reforming processes. Long term durability test showed that 5% Ni-$Ce_{0.6}Zr_{0.4}O_2$ catalyst was stable for up to 100 h at 650 and 700ºC and activity remained stable for more than 200 h at 800ºC. TPO results indicated the excellent resistance toward carbon formation for Ni supported on $Ce_xZr_{1-x}O_2$ as compared to the other catalysts.

Prashant and coworkers (2008) [63] synthesized various Ni-based catalysts on CeO_2-ZrO_2, CeO_2-Al_2O_3, and La_2O_3-Al_2O_3 mixed oxide supports. Surfactant assisted method was employed for synthesis and catalytic characterization was done by BET, XRD and H_2-TPR. XRD patterns revealed that homogeneous CeO_2-ZrO_2 solid oxide exhibit cubic phase after calcination at 650°C while CeO_2 appears as cubic fluorite structure in CeO_2-Al_2O_3 binary oxides and hexagonal La_2O_3 formed in case of La_2O_3-Al_2O_3 which means that Al_2O_3 exists in an amorphous state in both mixed oxides. TPR the results demonstrate that the presence of Ce and/or La leads to the enhancement of Ni reducibility which is an important indicator for catalytic activity and stability for dry reforming of methane. Furthermore, higher oxygen storage capacity of CeO_2 might help in gasification of deposited carbon and therefore improve catalyst stability during the

course of catalytic reaction. The presence of alumina could contribute to provide the mechanical strength to the catalyst.

Roh et al; (2009) [64] have synthesized Ni-CeO_2, Ni-ZrO_2 and Ni-$Ce_{0.8}Zr_{0.2}O_2$ using conventional impregnation and co-precipitation method to develop a suitable catalyst for synthesis gas production for gas to liquid (GTL) process. Catalytic activity was tested with time on stream at 800^oC and results confirmed that the co-precipitated Ni-CeO_2 and Ni-$Ce_{0.8}Zr_{0.2}O_2$ catalysts showed relatively high activity and stability in comparison to impregnated Ni/CeO_2 and Ni/$Ce_{0.8}Zr_{0.2}O_2$ catalysts. Ni-$Ce_{0.8}Zr_{0.2}O_2$ catalyst showed higher reactants conversion in the temperature range from 700 to 750^oC and the enhanced catalytic activity and stability was related to the nano-crystalline nature of cubic $Ce_{0.8}Zr_{0.2}O_2$ support as well as higher oxygen storage capacity and finely dispersed nano-sized NiO crystallites.

Quiroga and coworkers (2010) [76] synthesized Ni based catalyst onto Al_2O_3, CeO_2, La_2O_3, ZrO_2 supports via wet impregnation method. All catalysts were tested for dry reforming of methane using a fixed bed reactor. Among all prepared catalyst, Ni/ZrO_2 showed the highest activity and stability during catalytic reaction. Furthermore, Ni supported catalysts onto CeO_2 has relatively high activity, but significant deactivation was observed after certain period of time. In order to improve the catalytic activity, Li and K (0.5 wt%) were chosen as modifiers and it was observed that addition of modifiers could possibly enhance the stability. Although the modified catalyst has shown low reactants (CH_4 and CO_2) conversions.

Naseem et al; (2013) [58] investigated the comparative behavior of Ni supported on Al_2O_3, ZrO_2 and CeO_2 nano-supports for dry reforming of methane. Catalysts were synthesized via polyol method (ethylene glycol medium with polyvinylpyrrolidone as a nucleation-protective agent) and characterized by using various catalytic techniques. The catalytic tests were evaluated in the temperature range 500-800°C. The obtained results revealed that the performance of a catalyst depends on the nature of support. Ni-Zr showed highest catalytic activity (87.2%) compared to Ni-Al (84.8%) and Ni-Ce (83.2%). On the other hand, higher tendency towards coke resistance was observed for Ni-Al catalyst due to its higher basicity and smaller Ni crystallites.

Naeem et al; (2014) [33] synthesized ceramic oxides of Ni-Zr, Ni-Ce and Ni-Al by using polyol (ethylene glycol (EG) medium with polyvinylpyrrolidone (PVP) as a nucleation protective agent) and surfactant-assisted (cetyl trimethyl ammonium bromide (CTAB)) methods and subsequently tested for dry reforming reaction. The prepared materials were characterized by various techniques, such as BET, H_2-TPR, CO_2-TPD, XRD, TGA, SEM, HRTEM and CO pulse chemisorption. It was observed that polyol catalysts showed high catalytic activity while surfactant-assisted catalysts exhibited high resistance towards carbon deposition under similar reaction conditions. Among all tested catalysts, the highest activity was observed for Ni-Zr Pol and lowest activity was observed over Ni-Zr Srf catalysts. Moreover, H_2/CO product ratio was found to be smaller in case of surfactant-assisted catalysts than their corresponding polyol catalysts. All results demonstrated that the method of preparation has a significant effect on the redox properties and better Ni dispersion which can enhance the catalytic performance for dry reforming of methane.

Wolfbeisser et al; (2016) [77] studied the textural and adsorption properties of ceria-zirconia mixed oxide, ceria and zirconia support materials and corresponding Ni impregnated catalysts for dry reforming reaction. Textural properties were studied by N_2 adsorption and it was observed that mixed oxide prepared by co-precipitation, resulted in catalysts with higher surface area than that of pure ZrO_2 or CeO_2. The catalyst prepared by using surfactant assisted co-precipitation was not active for DRM, probably due to the encapsulation of Ni particles by ceria-zirconia particles. They have concluded that using ceria-zirconia as a support material for Ni based catalysts hinders the formation of filamentous carbon and decreases the risk of reactor blocking during dry reforming reaction.

Goula and coworkers (2017) [59] studied the catalytic efficiencies of Ni supported catalysts onto ZrO_2, La_2O_3-ZrO_2 and CeO_2-ZrO_2 supports via dry reforming reaction. The catalytic tests were performed in in the temperature range of 500-800^oC with a CH_4/CO_2 ratio equal to 1.5. Various techniques, like N_2 physisorption-desorption (BET method), XRD, H_2-TPR, SEM, TEM, Raman spectroscopy, potentiometric titration and inductively coupled plasma emission spectroscopy (ICP), were applied to understand

the morphology, texture and other physio-chemical properties of the materials. The enhanced basicity and Ni dispersion on Ni/LaZr and Ni/CeZr catalysts have shown the superior efficiency and durability in comparison to Ni/Zr catalyst. Furthermore, small amount of carbon formation was detected on spent Ni/CeZr catalyst due to the higher oxygen storage capacity CeZr support.

2.1.3.5. Ceria and zirconia support for bimetallic Ni/Co based catalysts

Dijinovic et al; (2015) [57] investigated the various bimetallic NiCo/$CeZrO_2$ materials for methane dry reforming reaction. This purpose of the study was to investigate that how morphology, active metal content and oxygen storage capacity can influence the catalytic activity and stability during dry reforming of methane reaction. It was observed that Oxygen storage capacity of the $CeZrO_2$ catalyst support played a vital role in retarding carbon accumulation over the tested NiCo/$CeZrO_2$ materials. This property can be fully developed when a nanocrystalline solid solution of $CeO_2$and $ZrO_2$is formed. It was concluded that oxygen species originating from the CeZr support migrate to the NiCo bimetallic clusters and act as oxidative scavengers for carbon precursors and prevent their polymerization to coke. It has been seen that the catalysts which contain larger NiCo bimetallic particles (for example with 12–18 wt.% active metal loading) exhibit a low metal-support interphase that results in enhanced coke formation rates. The results revealed that a NiCo/$CeZrO_2$ catalyst under relevant operating conditions after 400 h TOS maintains 79 and 84% conversion of CH_4 and CO_2 respectively, with negligible coke deposition onto the surface of catalyst.

Vasiliades et al; (2017) [78] have been used hydrothermal method (HT) and ethylene glycol (EG) methods for the synthesis of $Ce_{0.75}Zr_{0.25}O_{2-x}$ solid solution. 3 wt% NiCo (nickel 1.2 wt% and cobalt 1.8 wt%) were dispersed over $Ce_{0.75}Zr_{0.25}O_{2-x}$ and tested for DRM at 750°C. The structural, morphological, textural and redox properties were probed by XRD, HAADF/STEM and SAED, N_2 adsorption/desorption at 77 K, H_2-chemisorption, H_2-TPR and H_2 transient isothermal reduction (H_2-TIR) techniques. The catalytic results revealed that the rate and kind of carbon deposition formed due to CH_4 decomposition, mainly depend on the structure of the ceria-zirconia support. The $Ce_{0.75}Zr_{0.25}O_{2-x}$ support prepared by EG method promotes the rate of CH_4 decomposition

and at the same time carbon removal takes place via the participation of mobile lattice oxygen to a greater extent than the $Ce_{0.75}Zr_{0.25}O_{2-x}$ support prepared by HT method.

2.1.3.6. Effect of dopant for ceria-zirconia based support

The modification of supports through doping with rare earth (RE) metals is an effective way to alter support's properties and the interactions with the metal catalyst. The addition of rare earth metals (RE=La, Pr, Nd, Sm, Eu, Gd, Tb) as a dopant not only improve the redox properties and thermal resistance of ceria zirconia support but cases also exhibited higher oxygen storage capacity (OSC) of CeO_2 based materials [9]. Cao et al (2009) [10] reported that, every RE^{+3} ions can replace Ce^{+4} and hence one oxygen vacancy is needed to balance the charge, in this way the oxygen vacancies can increase the diffusion rate of oxygen which leads to the higher OSC. Moreover, RE metals having larger ionic radii than Zr^{4+} ion (0.084 nm), which can provide more effective stabilization of fluorite type structure. RE ions also showed an enhancement of the textural properties (larger BET areas and smaller grain sizes) [62].

Rcently, neodymium (Nd^{3+}) has been demonstrated to be an effective dopant to stabilize the cubic phase of ceria-zirconia solid solutions in all range of compositions [27], and to improve the catalytic activity of CeZr in the removal of soot and other automotive exhausts [28,29].

Jorge Gonzalez Mira et al; (2015) [79] synthesized $Ce_{0.64}Zr_{0.27}Nd_{0.09}O$ mixed oxides by nitrates calcination, co-precipitation and microemulsion method and tested for soot combustion. The $Ce_{0.64}Zr_{0.27}Nd_{0.09}O$ catalyst synthesized via microemulsion showed higher surface area (147 m^2/g) and low crystalline size compared to the catalysts prepared by nitrates calcination and co-precipitation method. All the three catalysts lower the soot combustion temperature with respect to uncatalyzed reaction. Furthermore, the higher catalytic activity was also observed with the catalyst prepared via microemulsion. The sequence of catalytic activity was observed as; microemulsion > nitrates calcination > coprecipitation >> No catalyst. Although the catalytic activity of $Ce_{0.64}Zr_{0.27}Nd_{0.09}O$ catalyst synthesized by nitrates calcination is slightly lower than the catalyst synthesized by microemulsion method, but the method of synthesis is very simple without any

surfactant and/or other chemicals. Therefore, it is very convenient for scaling up and practical utilization. Moreover, the better activity of $Ce_{0.64}Zr_{0.27}Nd_{0.09}O$ catalyst synthesized by nitrates calcination could be attributed to the introduction of better Nd cations to ceria framework which promotes the creation of more oxygen vacancies.

Gimenez and coworkers (2013) [80] investigated the effect of Nd doping for CeO_2 and CeO_2-ZrO_2 mixed oxides to study physicochemical and catalytic properties for soot combustion. CeO_2, $Ce_{0.9}Nd_{0.1}O_2$, $Ce_{0.73}Zr_{0.27}O_2$ and $Ce_{0.64}Zr_{0.27}Nd_{0.09}O_2$ have been prepared by co-precipitation method, calcined at 800°C and characterized by XRD, raman spectroscopy, N_2 adsorption and H_2-TPR and finally tested for soot combustion with NO_x/O_2. It was concluded that Zr doping can improve the thermal stability as well as redox properties of ceria framework while Nd doping has an additional effect to improves the oxygen mobility of CeO_2 and CeO_2-ZrO_2 mixed oxides. The best catalytic activity for soot combustion was observed with both Nd and Zr doped CeO_2 ($Ce_{0.6}4Zr_{0.27}Nd_{0.09}O_2$), and it was observed for the first time that the soot combustion activity of a CeO_2-ZrO_2 mixed oxides was improved by Nd doping. Wang et al; (2012) [81] investigated the similar effect of Nd on ceria-zirconia solid solution for gasoline engine exhaust reduction.

2.2. Conclusions

In terms of catalysts reported to be efficient for DRM reaction, Ni based catalysts is one of the most promising choice. Many researchers reported that the utilization of Ni catalyst can lower the energy demand to activate the dry reforming to the higher conversion level for both CH_4 and CO_2. However, the major obstacle with Ni based catalyst is the carbon formation. A brief literature survey regarding Ni based catalyst has shown that researchers are trying to prepare a suitable support material for Ni based catalyst which could increase the dry reforming activity by lowering the carbon formation but still is a challenge for scientific community. By comparing the different properties of support materials, ceria-zirconia solid solution was found to be most suitable support material owning to their higher oxygen storage capacity and their higher thermal stability, thereby enhancing the ability of CO_2 adsorption which is contributed to eliminate carbon deposition and as a consequence, enhance the stability of Ni based

catalysts. Our main research goal is to optimize Ni supported catalyst active at lower temperature (600-800ºC), therefore it was decided to continue the research activity by considering Ni catalyst supported on ceria, zirconia, and ceria-zirconia based materials. In order to improve the ceria-zirconia support and to enhance their catalytic properties, interactions with the metal, and their tolerance towards carbon formation, neodymium has been demonstrated as a dopant owing to its high basic properties.

References

1. Usman, M., W.W. Daud, and H.F. Abbas, *Dry reforming of methane: Influence of process parameters—A review.* Renewable and Sustainable Energy Reviews, 2015. **45**: p. 710-744.
2. Popa, M., et al., *Vehicle emissions of greenhouse gases and related tracers from a tunnel study: CO: CO. sub. 2, N. sub. 2O: CO. sub. 2, CH. sub. 4: CO. sub. 2, O. sub. 2: CO. sub. 2 ratios, and the stable isotopes. sup. 13C and. sup. 18O in CO. sub. 2 and CO.* Atmospheric Chemistry and Physics, 2014. **14**(4): p. 2105-2105.
3. Iyer, M.V., et al., *Kinetic modeling for methane reforming with carbon dioxide over a mixed-metal carbide catalyst.* Industrial & engineering chemistry research, 2003. **42**(12): p. 2712-2721.
4. Barrai, F., et al., *The role of carbon deposition on precious metal catalyst activity during dry reforming of biogas.* Catalysis Today, 2007. **129**(3-4): p. 391-396.
5. Kohn, M.P., M.J. Castaldi, and R.J. Farrauto, *Auto-thermal and dry reforming of landfill gas over a $Rh/\gamma Al_2O_3$ monolith catalyst.* Applied Catalysis B: Environmental, 2010. **94**(1-2): p. 125-133.
6. Karavalakis, G., et al., *Air pollutant emissions of light-duty vehicles operating on various natural gas compositions.* Journal of Natural Gas Science and Engineering, 2012. **4**: p. 8-16.
7. Izquierdo, U., et al., *Tri-reforming: a new biogas process for synthesis gas and hydrogen production.* International journal of hydrogen energy, 2013. **38**(18): p. 7623-7631.
8. Ghoneim, S.A., R.A. El-Salamony, and S.A. El-Temtamy, *Review on innovative catalytic reforming of natural gas to syngas.* World Journal of Engineering and Technology, 2015. **4**(01): p. 116.
9. Monaco, F., A. Lanzini, and M. Santarelli, *Making synthetic fuels for the road transportation sector via solid oxide electrolysis and catalytic upgrade using recovered carbon dioxide and residual biomass.* Journal of Cleaner Production, 2018. **170**: p. 160-173.
10. Styring, P., et al., *Carbon Capture and Utilisation in the green economy*. 2011: Centre for Low Carbon Futures New York.

11. Karthikeyan, C., et al., *Biogenic ammonia for CO2 capturing and electrochemical conversion into bicarbonate and formate.* Journal of CO2 Utilization, 2014. **6**: p. 53-61.
12. Oyama, S.T., et al., *Dry reforming of methane has no future for hydrogen production: Comparison with steam reforming at high pressure in standard and membrane reactors.* International journal of hydrogen energy, 2012. **37**(13): p. 10444-10450.
13. Kohn, M.P., M.J. Castaldi, and R.J. Farrauto, *Biogas reforming for syngas production: The effect of methyl chloride.* Applied Catalysis B: Environmental, 2014. **144**: p. 353-361.
14. Lunsford, J.H., *Catalytic conversion of methane to more useful chemicals and fuels: a challenge for the 21st century.* Catalysis Today, 2000. **63**(2-4): p. 165-174.
15. Elvidge, C., et al., *A fifteen year record of global natural gas flaring derived from satellite data.* Energies, 2009. **2**(3): p. 595-622.
16. Pen, M., J. Gomez, and J.G.a. Fierro, *New catalytic routes for syngas and hydrogen production.* Applied Catalysis A: General, 1996. **144**(1-2): p. 7-57.
17. Gaddalla, A.M. and M.E. Sommer, *Carbon dioxide reforming of methane on nickel catalysts.* Chemical Engineering Science, 1989. **44**(12): p. 2825-2829.
18. Rostrup-Nielsen, J.R., J. Sehested, and J.K. Nørskov, *Hydrogen and synthesis gas by steam-and C02 reforming.* 2002.
19. Djinović, P., et al., *Influence of active metal loading and oxygen mobility on coke-free dry reforming of Ni–Co bimetallic catalysts.* Applied Catalysis B: Environmental, 2012. **125**: p. 259-270.
20. Wilhelm, D., et al., *Syngas production for gas-to-liquids applications: technologies, issues and outlook.* Fuel processing technology, 2001. **71**(1-3): p. 139-148.
21. Titus, J., et al., *Dry reforming of methane with carbon dioxide over NiO–MgO–ZrO2.* Catalysis Today, 2016. **270**: p. 68-75.
22. Song, X. and Z. Guo, *Technologies for direct production of flexible H2/CO synthesis gas.* Energy Conversion and Management, 2006. **47**(5): p. 560-569.

23. Lucrédio, A.F., J.M. Assaf, and E.M. Assaf, *Reforming of a model biogas on Ni and Rh–Ni catalysts: Effect of adding La.* Fuel processing technology, 2012. **102**: p. 124-131.
24. Baudouin, D., et al., *Particle size effect in the low temperature reforming of methane by carbon dioxide on silica-supported Ni nanoparticles.* Journal of catalysis, 2013. **297**: p. 27-34.
25. Elsayed, N.H., et al., *Low temperature dry reforming of methane over Pt–Ni–Mg/ceria–zirconia catalysts.* Applied Catalysis B: Environmental, 2015. **179**: p. 213-219.
26. Dębek, R., et al., *A short review on the catalytic activity of hydrotalcite-derived materials for dry reforming of methane.* Catalysts, 2017. **7**(1): p. 32.
27. Gao, X., et al., *Ni/SiO2 catalyst prepared via Ni-aliphatic amine complexation for dry reforming of methane: Effect of carbon chain number and amine concentration.* Applied Catalysis A: General, 2015. **503**: p. 34-42.
28. Beneroso, D., et al., *Comparing the composition of the synthesis-gas obtained from the pyrolysis of different organic residues for a potential use in the synthesis of bioplastics.* Journal of analytical and applied pyrolysis, 2015. **111**: p. 55-63.
29. He, X., et al., *Integrated process of coal pyrolysis with CO2 reforming of methane by dielectric barrier discharge plasma.* Energy & Fuels, 2011. **25**(9): p. 4036-4042.
30. Valin, S., et al., *Upgrading biomass pyrolysis gas by conversion of methane at high temperature: experiments and modelling.* Fuel, 2009. **88**(5): p. 834-842.
31. Kim, Y.J., Y.S. Nam, and Y.T. Kang, *Study on a numerical model and PSA (pressure swing adsorption) process experiment for CH4/CO2 separation from biogas.* Energy, 2015. **91**: p. 732-741.
32. Ryckebosch, E., M. Drouillon, and H. Vervaeren, *Techniques for transformation of biogas to biomethane.* Biomass and bioenergy, 2011. **35**(5): p. 1633-1645.
33. Naeem, M.A., et al., *Hydrogen production from methane dry reforming over nickel-based nanocatalysts using surfactant-assisted or polyol method.* International Journal of Hydrogen Energy, 2014. **39**(30): p. 17009-17023.

34. Wang, Y., et al., *Low-temperature catalytic CO2 dry reforming of methane on Ni-based catalysts: a review.* Fuel Processing Technology, 2018. **169**: p. 199-206.
35. Nikoo, M.K. and N. Amin, *Thermodynamic analysis of carbon dioxide reforming of methane in view of solid carbon formation.* Fuel Processing Technology, 2011. **92**(3): p. 678-691.
36. Shah, Y.T. and T.H. Gardner, *Dry reforming of hydrocarbon feedstocks.* Catalysis Reviews, 2014. **56**(4): p. 476-536.
37. Xu, J. and G.F. Froment, *Methane steam reforming, methanation and water-gas shift: I. Intrinsic kinetics.* AIChE journal, 1989. **35**(1): p. 88-96.
38. Kathiraser, Y., et al., *Kinetic and mechanistic aspects for CO2 reforming of methane over Ni based catalysts.* Chemical Engineering Journal, 2015. **278**: p. 62-78.
39. Ishihara, T., *Perovskite oxide for solid oxide fuel cells*. 2009: Springer Science & Business Media.
40. Haghighi, M., et al., *On the reaction mechanism of CO2 reforming of methane over a bed of coal char.* Proceedings of the Combustion Institute, 2007. **31**(2): p. 1983-1990.
41. Wang, S., G. Lu, and G.J. Millar, *Carbon dioxide reforming of methane to produce synthesis gas over metal-supported catalysts: state of the art.* Energy & fuels, 1996. **10**(4): p. 896-904.
42. Delgado, K., et al., *Surface reaction kinetics of steam-and CO2-reforming as well as oxidation of methane over nickel-based catalysts.* Catalysts, 2015. **5**(2): p. 871-904.
43. Zhang, Z., et al., *Comparative study of carbon dioxide reforming of methane to synthesis gas over Ni/La2O3 and conventional nickel-based catalysts.* The Journal of Physical Chemistry, 1996. **100**(2): p. 744-754.
44. Ferreira-Aparicio, P., A. Guerrero-Ruiz, and I. Rodrıguez-Ramos, *Comparative study at low and medium reaction temperatures of syngas production by methane reforming with carbon dioxide over silica and alumina supported catalysts.* Applied Catalysis A: General, 1998. **170**(1): p. 177-187.

45. Hou, Z., et al., *Production of synthesis gas via methane reforming with CO2 on noble metals and small amount of noble-(Rh-) promoted Ni catalysts.* International journal of hydrogen energy, 2006. **31**(5): p. 555-561.
46. Matsui, N.-o., et al., *Reaction mechanisms of carbon dioxide reforming of methane with Ru-loaded lanthanum oxide catalyst.* Applied Catalysis A: General, 1999. **179**(1-2): p. 247-256.
47. Crisafulli, C., et al., *Ni–Ru bimetallic catalysts for the CO2 reforming of methane.* Applied Catalysis A: General, 2002. **225**(1-2): p. 1-9.
48. Wang, R., et al., *Role of redox couples of Rh0/Rhδ+ and Ce4+/Ce3+ in CH4/CO2 reforming over Rh–CeO2/Al2O3 catalyst.* Applied Catalysis A: General, 2006. **305**(2): p. 204-210.
49. Huygh, S., et al., *High Coke Resistance of a TiO2 Anatase (001) Catalyst Surface during Dry Reforming of Methane.* The Journal of Physical Chemistry C, 2018. **122**(17): p. 9389-9396.
50. Ayodele, B.V., et al., *Production of CO-rich hydrogen from methane dry reforming over lanthania-supported cobalt catalyst: kinetic and mechanistic studies.* international journal of hydrogen energy, 2016. **41**(8): p. 4603-4615.
51. Ayodele, B.V., M.R. Khan, and C.K. Cheng, *Syngas production from CO2 reforming of methane over ceria supported cobalt catalyst: Effects of reactants partial pressure.* Journal of Natural Gas Science and Engineering, 2015. **27**: p. 1016-1023.
52. Ruckenstein, E. and H. Wang, *Carbon deposition and catalytic deactivation during CO2 reforming of CH4 over Co/γ-Al2O3 catalysts.* Journal of Catalysis, 2002. **205**(2): p. 289-293.
53. Bartholomew, C.H. and J.B. Butt, *Catalyst Deactivation 1991*. Vol. 68. 1991: Elsevier.
54. Asai, K., et al., *Decomposition of methane in the presence of carbon dioxide over Ni catalysts.* Chemical Engineering Science, 2008. **63**(20): p. 5083-5088.
55. Fan, M.S., A.Z. Abdullah, and S. Bhatia, *Catalytic technology for carbon dioxide reforming of methane to synthesis gas.* ChemCatChem, 2009. **1**(2): p. 192-208.

56. Al-Fatesh, A.S., et al., *Sustainable production of synthesis gases via state of the art metal supported catalytic systems: an overview.* Journal of the Chinese Chemical Society, 2013. **60**(11): p. 1297-1308.
57. Djinović, P., I.G.O. Črnivec, and A. Pintar, *Biogas to syngas conversion without carbonaceous deposits via the dry reforming reaction using transition metal catalysts.* Catalysis Today, 2015. **253**: p. 155-162.
58. Naeem, M.A., et al., *Syngas production from dry reforming of methane over nano Ni polyol catalysts.* International Journal of Chemical Engineering and Applications, 2013. **4**(5): p. 315.
59. Goula, M., et al., *Syngas production via the biogas dry reforming reaction over Ni supported on zirconia modified with CeO2 or La2O3 catalysts.* international journal of hydrogen energy, 2017. **42**(19): p. 13724-13740.
60. Luna, A.E.C. and M.E. Iriarte, *Carbon dioxide reforming of methane over a metal modified Ni-Al2O3 catalyst.* Applied Catalysis A: General, 2008. **343**(1-2): p. 10-15.
61. Kang, K.-M., et al., *Catalytic test of supported Ni catalysts with core/shell structure for dry reforming of methane.* Fuel Processing Technology, 2011. **92**(6): p. 1236-1243.
62. Cao, L., et al., *Correlation between catalytic selectivity and oxygen storage capacity in autothermal reforming of methane over Rh/Ce0. 45Zr0. 45RE0. 1 catalysts (RE= La, Pr, Nd, Sm, Eu, Gd, Tb).* Catalysis Communications, 2009. **10**(8): p. 1192-1195.
63. Kumar, P., Y. Sun, and R.O. Idem, *Comparative study of Ni-based mixed oxide catalyst for carbon dioxide reforming of methane.* Energy & Fuels, 2008. **22**(6): p. 3575-3582.
64. Roh, H.-S., K.Y. Koo, and W.L. Yoon, *Combined reforming of methane over co-precipitated Ni–CeO2, Ni–ZrO2 and Ni–Ce0. 8Zr0. 2O2 catalysts to produce synthesis gas for gas to liquid (GTL) process.* Catalysis Today, 2009. **146**(1-2): p. 71-75.

65. Li, Z., et al., *Yolk–satellite–shell structured Ni–yolk@ Ni@ SiO2 nanocomposite: superb catalyst toward methane CO2 reforming reaction.* Acs Catalysis, 2014. **4**(5): p. 1526-1536.
66. Li, Z., Y. Kathiraser, and S. Kawi, *Facile synthesis of high surface area yolk–shell Ni@ Ni embedded SiO2 via Ni phyllosilicate with enhanced performance for CO2 reforming of CH4.* ChemCatChem, 2015. **7**(1): p. 160-168.
67. Bian, Z., I.Y. Suryawinata, and S. Kawi, *Highly carbon resistant multicore-shell catalyst derived from Ni-Mg phyllosilicate nanotubes@ silica for dry reforming of methane.* Applied Catalysis B: Environmental, 2016. **195**: p. 1-8.
68. Mo, L., K.K.M. Leong, and S. Kawi, *A highly dispersed and anti-coking Ni–La 2 O 3/SiO 2 catalyst for syngas production from dry carbon dioxide reforming of methane.* Catalysis Science & Technology, 2014. **4**(7): p. 2107-2114.
69. Li, Z., et al., *Simultaneous tuning porosity and basicity of nickel@ nickel–magnesium phyllosilicate core–shell catalysts for CO2 reforming of CH4.* Langmuir, 2014. **30**(48): p. 14694-14705.
70. Yang, M., et al. *Characterization of Nano Ni/MgO-ZrO2 Catalysts*. in *Advanced Materials Research*. 2013. Trans Tech Publ.
71. Koo, K.Y., et al., *Coke study on MgO-promoted Ni/Al2O3 catalyst in combined H2O and CO2 reforming of methane for gas to liquid (GTL) process.* Applied Catalysis A: General, 2008. **340**(2): p. 183-190.
72. Pereñiguez, R., et al., *LaNiO3 as a precursor of Ni/La2O3 for CO2 reforming of CH4: Effect of the presence of an amorphous NiO phase.* Applied Catalysis B: Environmental, 2012. **123**: p. 324-332.
73. Sharifi, M., et al., *Reforming of biogas over Co-and Cu-promoted Ni/Al2O3-ZrO2 nanocatalysts synthesized via sequential impregnation method.* Journal of Renewable Energy and Environment, 2014. **1**(1): p. 53.
74. Roh, H.-S., et al., *Carbon dioxide reforming of methane over Ni incorporated into Ce–ZrO2 catalysts.* Applied Catalysis A: General, 2004. **276**(1-2): p. 231-239.
75. Kumar, P., Y. Sun, and R.O. Idem, *Nickel-based ceria, zirconia, and ceria–zirconia catalytic systems for low-temperature carbon dioxide reforming of methane.* Energy & Fuels, 2007. **21**(6): p. 3113-3123.

76. Delimitis, A., *IV Yentekakis, G. Goula, P. Panagiotopoulou, A. Katsoni, E. Diamadopoulos, D. Mantzavinos &.* Top Catal, 2015. **58**: p. 1228-1241.
77. Wolfbeisser, A., et al., *Methane dry reforming over ceria-zirconia supported Ni catalysts.* Catalysis Today, 2016. **277**: p. 234-245.
78. Vasiliades, M.A., et al., *The effect of CeO 2–ZrO 2 structural differences on the origin and reactivity of carbon formed during methane dry reforming over NiCo/CeO 2–ZrO 2 catalysts studied by transient techniques.* Catalysis Science & Technology, 2017. **7**(22): p. 5422-5434.
79. Mira, J.G., V.R. Pérez, and A. Bueno-López, *Effect of the CeZrNd mixed oxide synthesis method in the catalytic combustion of soot.* Catalysis Today, 2015. **253**: p. 77-82.
80. Hernández-Giménez, A.M., L.P. dos Santos Xavier, and A. Bueno-López, *Improving ceria-zirconia soot combustion catalysts by neodymium doping.* Applied Catalysis A: General, 2013. **462**: p. 100-106.
81. Wang, Q., et al., *The effect of Nd on the properties of ceria–zirconia solid solution and the catalytic performance of its supported Pd-only three-way catalyst for gasoline engine exhaust reduction.* Journal of hazardous materials, 2011. **189**(1-2): p. 150-157.

Chapter No: 03

Experimental

3. Experimental

3.1. Fundamental aspects of catalyst synthesis

3.1.1. Preparation of catalysts

CeO_2 (Ce), $Ce_{0.8}Zr_{0.2}O_2$ (CeZr), $Ce_{0.8}Nd_{0.2}O_{1.9}$ ($CeNd_{0.2}$), $Zr_{0.8}Nd_{0.2}O_{1.9}$ ($ZrNd_{0.2}$) $Ce_{0.64}Zr_{0.16}Nd_{0.2}O_{1.9}$ ($CeZrNd_{0.2}$) and $Ce_{0.8}Zr_{0.13}Nd_{0.07}O_{1.9}$ ($CeZrNd_{0.07}$) were prepared via surfactant assisted co-precipitation method of synthesis as previously reported [1]. Briefly, the method of preparation is described below;

Stoichiometric amounts of metal precursor such as $Ce(NO_3)_3*6H_2O$, $ZrO(NO_3)_2$ and $Nd(NO_3)_3*6H_2O$ (Treibacher AG) were dissolved in demineralized water to obtain a 0.2 M solution. After that, concentrated H_2O_2 (35% Sigma-Aldrich) (molar ratio H_2O_2/total metal ions = 3) was added to the reaction mixture under continuous stirring for 45 min at room temperature. After 45 mins the concentrated ammonium hydroxide (28% Sigma-Aldrich) was added dropwise until the pH of the solution reached a value of 10.5. At the end, lauric acid (LA) (Sigma-Aldrich) was added to the mixture and continuously stirred for 4 h. An optimal LA/cations molar ratio of 0.25 was individuated after preliminary experiments in which the ratio was varied from 0.25 to 0.98. Finally, the solution was filtered, and the obtained solid were dried at 100^oC temperature overnight.

3.1.2. Calcination

Calcination has a significant on the performance of materials and/catalysts. Calcination at higher temperature is important because the precursors used for the synthesis might result in nitrates, carbonates or hydroxides which are not desired for catalyst. So, it is necessary to decompose and volatilized the precursors which are formed during preparation method to get rid of all impurities and unwanted compositions from the catalysts. In addition, the stability and chemical properties of a catalyst also depends on calcination [2]. Furthermore, the formation of new compounds and change in surface morphology can occur during calcination process which depends on the metal components in the system, calcination atmosphere, temperature and duration [3]. For Ni based catalysts, the surface area, dispersion and reducibility decrease with the increase of

calcination temperature. The most stable Ni based catalysts were obtained at a calcination temperature of 700-800°C.

In current study, the synthesizes materials were calcined at 500°C/4 h (fresh samples). Afterwards the samples were calcined at 800°C/3 h or at higher temperatures. Supports materials were loaded with 3.5wt% of Ni by incipient wetness impregnation method using $Ni(NO_3)_2*H_2O$ (Sigma-Aldrich) as precursor. Some supports were also impregnated with different wt% of Ni (1%, 7%). After impregnation, the samples were dried at 100°C overnight followed by calcination at 800°C for 1 h in order to get a stable structure for DRM reaction.

3.1.3. Activation

The activation of catalysts can be done by reduction and temperature is a crucial parameter for reduction process because it can affect the surface properties, dispersion and extent of reduction for metal support system. The main purpose of reduction is to convert the metal oxides into active metals using different reducing agents such as hydrogen. Moreover, the optimal reduction temperature can be different for different catalysts, depends on the component of catalysts. Therefore, all Ni catalysts were reduced at 800°C/1h to convert nickel oxide (NiO) to metallic Ni (Ni^0).

3.2. Fundamental aspects of catalyst characterization

3.2.1. Structural and textural properties

3.2.1.1. BET

Specific surface area and porosity of the support materials and/catalysts was measured by using a Micromeritics surface area and porosity analyzer. Surface area was calculated by Brunauer-Emmett-Teller (BET) method while pore size distribution was obtained from the N_2 desorption isotherm using Barrett-Joyner-Halenda (BJH) method. Prior to adsorption process, the samples were degassed at 150°C for 1.5 h to remove moisture and volatile adsorbates.

3.2.1.2. XRD

X-ray diffraction is used to characterize the crystallinity of catalysts and to determine their structure. Every crystalline solid has its unique characteristics X-ray patterns. XRD patterns of synthesized materials were obtained by using a X'Pert X-ray diffractometer with a Ni-filtered Cu K_α radiation source (λ = 1.540598 A^o) equipped with an X'Celerator detector. The operating voltage and current were 40 kV and 40 mA respectively. X'Pert High score software was used for phase analysis and the Scherrer equation (1) with corrected line broadening was used to calculate crystallite size.

$$dc = \frac{k\lambda}{\beta cos\theta} \qquad (1)$$

Where d_c: average crystalline size, K: dimensionless shape factor depending on the actual shape of the crystallite, λ: X-ray wavelength, β: line broadening at half of the maximum intensity, θ: Bragg angle.

3.2.2. TPR, TPD and plus chemisorption analysis

The temperature programmed reduction (method yields the quantitative information regarding surface of metal oxide as well as heterogenicity of reducible surfaces. This technique is really useful to determine the no. of reducible sites present in the catalyst and also reveals the temperature at which reduction takes place.

The temperature programmed desorption (TPD) technique is employed to determine the strength of basic site of a catalyst by using CO_2 as analysis/probe gas. The CO_2 desorption peaks at different temperature determine the strength of basic sites.

The activity of a catalyst also depends on the dispersion of metal onto the surface of catalyst. CO-plus chemisorption can be valid strategy to understand the dispersion of metal over support material. The Ni metal dispersion of the catalysts was estimated by CO-chemisorption using a stoichiometry of 1:1 for the calculations [4].

For the analysis of synthesized support materials and catalysts, Micromeritics apparatus (Autochem II 2990) equipped with a TCD detector was used to perform temperature programmed H_2 reduction (H_2-TPR), CO-chemisorption and temperature programmed CO_2 desorption (CO_2-TPD) measurements.

3.2.2.1. H_2-TPR

H_2-TPR experiments were conducted using 5% H_2 in N_2 flow and temperature was ramped from ambient to 950ºC, at a rate of 10ºC/min. About 0.05g of sample was used for each measurement. All samples were pre-treated in air at 500ºC/1 h and then cooled down to room temperature under N_2 flow for the removal surface carbonates and adsorbed impurities from the surface. The H_2 consumption was measured by TCD detector.

3.2.2.2. CO_2-TPD

In CO_2-TPD measurements were performed with 5%H_2/N_2 flow (35 cc/min) and cooled down at room temperature under He flow. About 0.05g of samples were used for each analysis and reduced at 800ºC/1 h. CO_2 was left to be adsorbed at 50ºC for 1 h with continuous flow of 20% CO_2/He gas mixture (30 ml/min) and then desorbed with a linear increase of temperature up to 800ºC under He flow.

3.2.2.3. CO-chemisorption

The Ni metal dispersion of the catalysts was estimated by CO-chemisorption using a stoichiometry of 1:1 for the calculations [4]. Prior to each analysis, all samples were reduced in 5% H_2/N_2 at 800ºC/1 h and cooled down to 35ºC under He flow. About 5% CO/He was pulsed over the catalyst recording the pulses until the peaks' area became constant. The percent dispersion was calculated by using following formula;

$$PD = 100[\frac{V_S * SF_{calc}}{SW * 22414}]\mathrm{GMW_{calc}} \qquad (2)$$

Where PD: percent dispersion, V_s: volume sorbed (mL at STP), SF_{calc}: calculated stoichiometric factor, SW: sample weight, GMW_{calc}: gram molecular weight g/g mol^{-1}.

3.2.2.4. CHNS analysis

Organic carbon (OC) content was determined for desiccated samples on a Carlo Erba elemental analyzer (Flash EA1112, ThermoQuest/CE Elantech, Lakewood, NJ). Pulverized samples (1-5 mg) were placed in preweighted tin combustion boats supplied

by the manufacturer, sealed, reweighted, and stored in a desiccator until analysis. Elemental analysis was conducted using automated combustion/reduction (at 900°C) followed by molecular sieve gas chromatography (at 90°C) and thermal conductivity detection system. Software used is Thermo Quest CE Instrument Eager 300 ver 1.01.

3.3. Scanning Electron Microscopy (SEM)

SEM images were collected on a Zeiss sigma 300 VP-FESEM with Bruker EDS. The acceleration voltage was 15kV. The SEM measurements were carried out by Prof. Thomas Etsell at the University of Alberta, Canada.

3.4. Dry reforming of methane reaction (DRM)

3.4.1. Experimental setup

A schematic diagram of the experimental setup for DRM reaction is shown in Figure 1. The feed units consist of four gas feed lines for CH_4, CO_2, N_2 and H_2. The mass-flow controllers regulate the flow rate of each gas according to the set flow rate. A pressure gauge is installed prior to the reactor to monitor the pressure. A quartz microreactor was used to carry out the catalytic experiments. The gas mixture (CH_4, CO_2 and N_2) was passing through reactor and the concentration of effluent gases (CO, H_2, CO_2 and CH_4) then analyzed by using a micro-gas chromatograph (GC, Varian model CP-4900) equipped with two columns (a molecular sieve and PPQ column) and with a thermal conductivity detector (TCD).

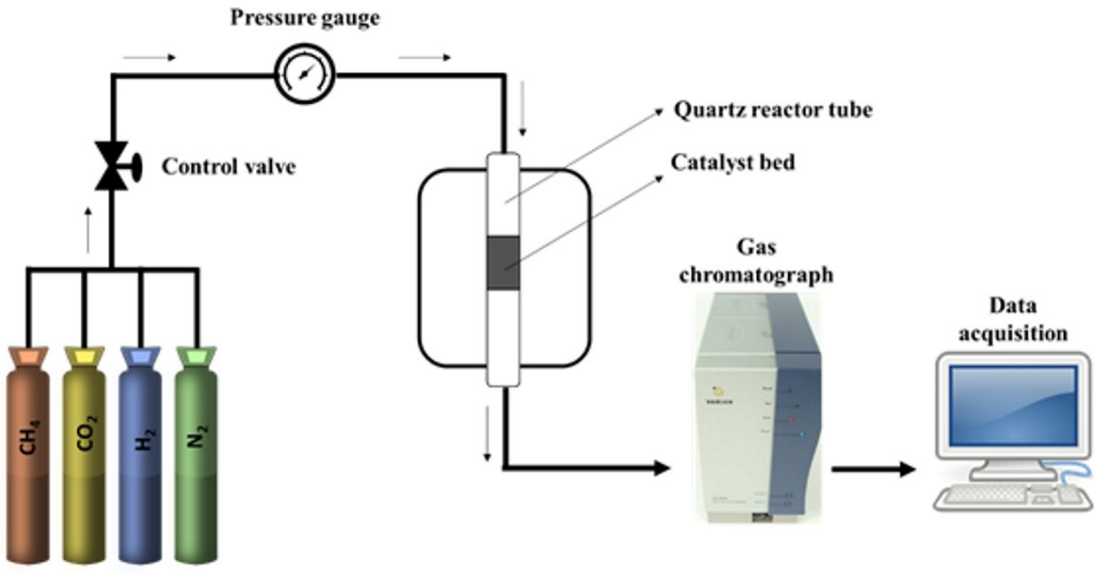

Figure 1. Schematic diagram of experimental setup used for DRM reaction.

3.4.2. Catalytic tests

The catalytic activities in term of dry reforming of methane were conducted in a fixed bed reactor (i.d.=4mm). For each run, 0.08 g of catalyst in powder form was diluted with quarts at a ratio of 1:1 to avoid the risk of blockage. The reactor was heated up to 800ºC at a rate of 10ºC/min with the flow rate of 50 ml/min of Helium. After that, each catalyst was reduced under hydrogen at 800ºC/1 h. Catalytic tests were conducted in the temperature range of 550-750ºC and pressure was maintained at 1 atmosphere throughout the process. Dry reforming tests were carried out with a 0.66 CO_2/CH_4 ratio with total volumetric flow of 80 mL/min, resulting in a GHSV of 8000 h^{-1}. Nitrogen was used as internal reference. The concentration of effluent gases (CO, H_2, CO_2 and CH_4) from reactor was analyzed by using a micro-gas chromatograph equipped with TCD detector. The conversions of CO_2 and CH_4 and H_2/CO ratios were calculated according to the following formulas, where the factor $\beta = [N_2]_{in}/[N_2]_{out}$ allows to take into account the changes of flow rate during the reaction.

$$X[CH_4]\% = ([CH_4]in - ([CH_4]out * \beta))/[CH_4]in) * 100$$

$$X[CO_2]\% = ([CO_2]in - ([CO_2]out * \beta))/[CO_2]in) * 100$$

$$H_2/CO = ([H_2]out* \beta) /([CO]out* \beta)$$

$$H_2 \text{ yield } \% = ([H_2]out* \beta)/(2*[CH_4]in)*100$$

$$CO \text{ yield } \% = ([CO]out* \beta)/([CH_4]in+[CO_2]in)*100$$

$$\text{Carbon balance} = ([CO]out* \beta)+([CH_4]out* \beta)+([CO_2]out* \beta))/ ([CH_4]in+[CO_2]in)*100$$

In order to check the accuracy of our GC data, we performed the carbon balance which shows that the error in our data was ± 5% (for more information please see appendix a table 1 and table 2).

3.5. Carbon analysis

Long term stability tests were conducted at 650°C for 8 h to the reactants mixture and cooled down to ambient temperature under inert atmosphere. To quantify the amount of coke formation, thermo gravimetric analysis (TGA) (SDT-Q-600 TA instruments) was conducted over spent catalysts. About 8-10 mg of the spent catalyst was heated in air from ambient temperature to 1000°C at a ramp rate of 10°C/min monitoring the loss of weight.

References

1. Pappacena, A., et al., *Development of a modified co-precipitation route for thermally resistant, high surface area ceria-zirconia based solid solutions*, in *Studies in Surface Science and Catalysis*. 2010, Elsevier. p. 835-838.
2. Bartholomew, C.H. and R.J. Farrauto, *Chemistry of nickel-alumina catalysts.* Journal of Catalysis, 1976. **45**(1): p. 41-53.
3. Deutschmann, O., et al., *Heterogeneous catalysis and solid catalysts, 3. industrial applications.* Ullmann's Encyclopedia of Industrial Chemistry, 2000.
4. Brooks, C. and G.L.M. Christopher, *Measurement of the state of metal dispersion on supported nickel catalysts by gas chemisorption.* Journal of Catalysis, 1968. **10**(3): p. 211-223.

Chapter No: 04

Results and Discussion

Part A: Effect of Surfactant (Lauric Acid)

4. Introduction

Many methods have been studied in order to obtain nanocrystalline powders with high surface areas for dry reforming catalytic applications. The use of surfactants during the precipitation could be a valid strategy in order to get nano crystalline metal oxide with high surface area [1]. Recently, we developed a new method of preparation in order to obtain nanocrystalline inorganic powders by using cationic surfactant (lauric acid) [2]. This study investigated the effect of surfactant (lauric acid) to improve the catalytic activities of dry reforming reaction. To improve the morphological and redox properties of supports is somehow controversial because some authors [3, 4] reported that the addition of surfactant during synthesis procedure could enhance the surface area, thermal stability and OSC properties of supports [5] while others [6] have shown the negative effect due to encapsulation phenomenon. Therefore, we have decided to study the role of surfactant on ceria-zirconia based materials to define a suitable morphology and porosity for the development of Ni catalysts for DRM reaction. This was done by preparing ceria-zirconia with varying surfactant/cation (S/C) ratio (S = lauric acid) in the range 0-0.98. Moreover, the modification of CeZr supports was carried out through La and Nd doping. The addition of rare earth metals (RE=La and Nd) as a dopant not only improve the redox properties and thermal resistance of ceria zirconia support, but also could exhibit higher oxygen storage capacity. After investigating the best S/C ratio and more effective dopant, the detailed experiments were conducted and explained in detail in chapter 5 and 6.

4.1. Results and discussions

4.1.1. BET surface area

The BET surface area, pore volume and pore size distribution by using a specific composition $Ce_{0.80}Zr_{0.13}Nd_{0.07}O_{1.96}$ ($CeZrNd_{0.07}$) prepared by varying S/C ratio in the range 0-0.98 are summarized in Table 1 together with corresponding nickel (Ni) catalysts. It is evident (Table 1) that BET surface area of the $CeZrNd_{0.07}$ supports calcined at 500ºC/4h show higher surface area compared to the supports calcined at 800ºC, and a further decrease was observed after Ni impregnation onto support materials. The BET surface area of $CeZrNd_{0.07}$ support (calcined at 800ºC/3h) with 0.25, 0.5 and 0.75 S/C ratios was equal to 46 m^2/g, while with 0.98 S/C ratio was found to be decreased down to

38 m^2/g, which is similar to that of $CeZrNd_{0.07}$ without surfactant (35 m^2/g). Hence it can be concluded that there is a threshold beyond which the amount of surfactant is not effective anymore and BET surface area decreases to the level of the support without the addition of lauric acid. Ni impregnation (3.5%) onto support materials leads to a significant decrease in the surface area, with $Ni/CeZrNd_{0.07}$ catalyst with 0.25 S/C ratio showing higher BET surface area (36 m^2/g) in comparison to the other catalysts.

Table 1. BET surface area of $CeZrNd_{0.07}$ ($Ce_{0.8}$ $Zr_{0.13}$ $Nd_{0.07}$ O_{2-x}) with different ratios of surfactant (0, 0.25, 0.5, 0.75 and 0.98), and corresponding Ni catalysts.

Sample Name	Temp/time Calcination (°C)	Surface Area (m^2/g)	Pore Volume (cm^3/g)	Pore Diameter (Å)
CeZrNd0.07_0	500/4h	63	0.18	104
CeZrNd0.07_0	800/3h	35	0.16	143
Ni/CeZrNd0.07_0	800/1h	24	0.14	175
CeZrNd0.07_0.25	500/4h	73	0.36	178
CeZrNd0.07_0.25	800/3h	45	0.30	223
Ni/CeZrNd0.07_0.25	800/1h	36	0.31	278
CeZrNd0.07_0.5	500/4h	124	0.19	62
CeZrNd0.07_0.5	800/3h	46	0.17	112
Ni/CeZrNd0.07_0.5	800/1h	29	0.14	141
CeZrNd0.07_0.75	500/4h	109	0.18	61
CeZrNd0.07_0.75	800/3h	46	0.15	99
Ni/CeZrNd0.07_0.75	800/1h	28	0.10	109
CeZrNd0.07_0.98	500/4h	119	0.17	63
CeZrNd0.07_0.98	800/3h	38	0.1	80
Ni/CeZrNd0.07_0.98	800/1h	22	0.08	97

Figure 4.1 reports the effect of S/C ratio on the morphological and textural properties of the supports calcined at 500°C (fresh support) and 800°C, along with the respective Ni-loaded catalysts. It is evident from Figure 4.1 that the catalyst with higher surface area (S/C = 0.25) shows a higher porosity and pores of larger dimension in comparison to the other samples. Moreover, Figure 4.2 shows that the pore size distribution in this catalyst is broad and ranges between 100 and 1000 Å, while the other catalysts are characterized by a bimodal distribution with a high fraction of micropores,

which decreases after calcination as micropores are more prone to collapsing at high temperature [7].

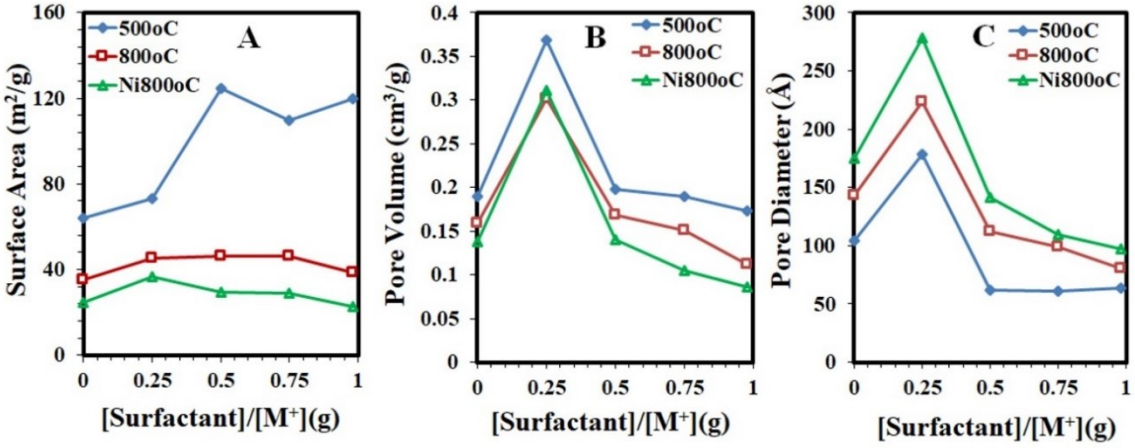

Figure 4.1. Effects of the amount of surfactant on the morphological properties of the ternary $CeZrNd_{0.07}$ composition in fresh state (calcined at 500°C), after calcination at 800°C and loaded with Ni followed by calcination at 800°C: (A) Surface Area; (B) Pore Volume, (C) Pore Diameter.

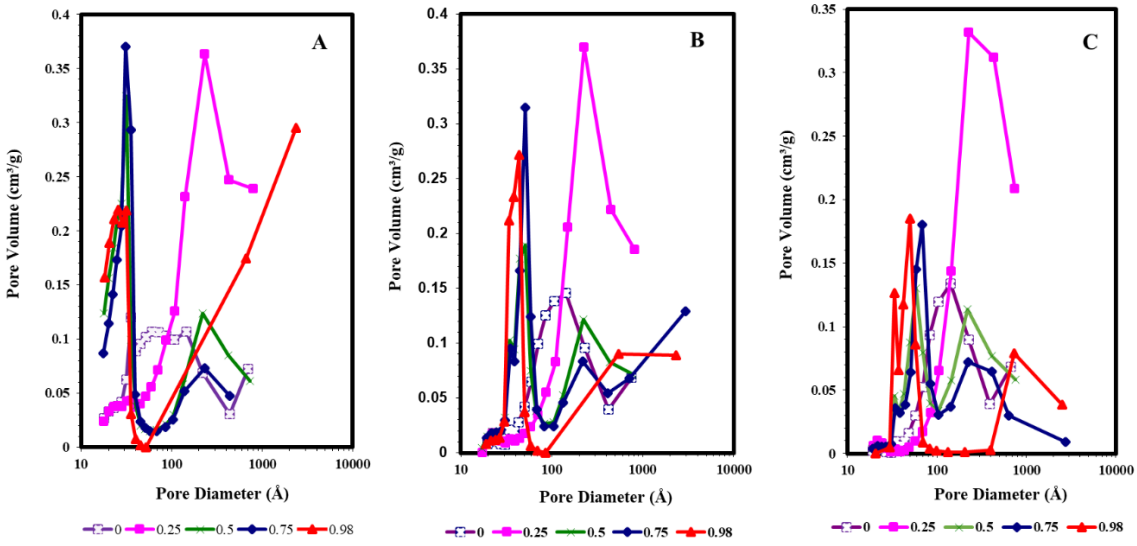

Figure 4.2. Comparison of pore size distribution of samples prepared with a S/C molar ratio of 0.25, 0.5, 0.75 and of 0.98: (A) after calcination at 500°C, (B) after calcination at 800°C, (C) after impregnation of Ni and calcination at 800°C.

In order to improve the surface morphology of zirconium oxide, Rezaei et al (2007) [8] investigated the effect of surfactant (hexadecyltrimethylammonium bromide) under basic conditions. The materials were synthesized with and without surfactant and a comparison was made under different experimental conditions. It was observed that the zirconia sample prepared with the addition of surfactant has higher surface area and pore size distribution which shows higher thermal stability at higher calcination temperatures than the sample without the addition of surfactant. Similar findings were also reported by Mustu et al (2015) and Yang et al (2016) [4, 9].

Alvar et al (2009) [1] synthesized mesoporous nanocrystalline $MgAl_2O_4$ by surfactant-assisted route using N-cetyl-N,N,N-trimethylammonium bromide (CTAB) as surfactant and employed as a support for Ni based catalyst in dry reforming reaction. They reported that the addition of surfactant (CTAB, S/C=0.3) led to an increase in the fraction of pores maintaining the meosporosity of synthesized materials which allow the higher Ni dispersion into the pores and shows positive effect for dry reforming reaction. It was also observed that the addition of surfactant has increased the specific surface area, showing high thermal stability of sample which remained relatively high at high calcination temperatures [10]. Moreover, the value of S/C molar ratio is 0.3 which is almost similar to our current study (S/C=0.25).

Therefore, on the basis of morphological study, it was concluded that in the presence of 0.25 S/C molar ratio of surfactant, ceria-zirconia crystallites can organize in a refractory structure with a broad mesoporosity which would favour the dispersion of Ni into the pores and its accessibility from the reactant mixture, while the supports with a large fraction of micropores are not stable, and during the calcination step micropores collapse encapsulating part of nickel crystallites [1]. Zhang et al (2015) [7] reported a bimodal distribution of micro and mesopores. They observed that the small pores resulted from the removal of CTAB (surfactant) during calcination, while the large pores may be due to the aggregation of the core–shell particles. As micropores are less stable and during the calcination process these pores collapse and encapsulated a part of Ni crystallites which would decrease the accessibility of Ni. Furthermore, it is reported in literature [11] that ceria and zirconia supported Ni based catalysts prepared via polyol method showing lower surface area, pore volume and pore diameter in comparison to

surfactant assisted method. Based on reported experimental results it was observed that during the preparation of polyol catalysts, a large number of Ni species succeeded to penetrate inside the pores of support which resulted in smaller pore volume due to the blockage of pores. On the other hand, in surfactant assisted method only a limited number of Ni species penetrate inside the pore and that is the reason why catalysts showed larger values of pore volume and pore diameter. Furthermore, the reported S/C molar ratio was 0.4 which is close to the S/C ratio (0.25) selected for the our current study which shows higher porosity and pores of larger dimension [11].

In conclusion, mesoporous material synthesized via surfactant assisted method exhibited promising textural properties such as high surface area and pore size distribution, showed good metal dispersion and higher stability for DR reaction [4, 6].

4.1.2. XRD

X-ray diffraction patterns were recorded for $CeZrNd_{0.07}$ support (calcined at 800°C) and related Ni catalysts with different S/C molar ratio of 0.25, 0.5, 0.75 and 0.98, and they are presented in Figure 4.3. It is confirmed from the diffractograms that all mixed oxides $CeZrNd_{0.07}$ (Figure 4.3A) are crystalline [12].

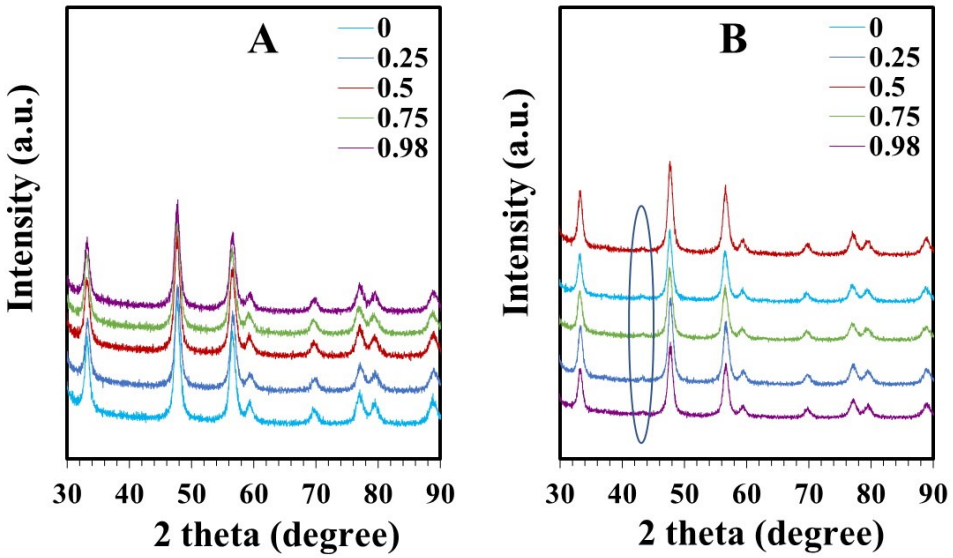

Figure 4.3. Comparison of XRD patterns of $CeZrNd_{0.07}$ ($Ce_{0.8}Zr_{0.13}Nd_{0.07}O_{2-x}$) support with different S/C molar ratio of 0.25, 0.5, 0.75 and 0.98: (A) after calcination at 800°C, (B) after impregnation of Ni and calcination at 800°C.

Ni impregnation (3.5%) onto support material (Figure 4.3B), did not affect the cubic structure of supports [13]. All spectra exhibited a very small peak at 2θ = 43.28 degrees corresponding to the (200) plane of cubic nickel oxide (PDF 78-0429). The small intensity of this peak suggests that NiO is well dispersed on the supports. These results are in good agreement with literature in which it is reported that Ni is better dispersed on cubic phases compared to other phase structures and Ni species are highly dispersed on support materials[4, 6, 14].

4.1.3. TPR

The TPR patterns obtained from CeO_2, CeZr (S/C=0.25) and $CeZrNd_{0.07}$ prepared with a S/C molar ratio of 0.25 and 0.98, were chosen as representative of the entire series and presented in Figure 4.4 [A, B and C]. It was observed that undoped materials showing a classical multi-model profiles [15, 16]. Figure 4.4A shows that CeO_2 support shows two distinct reduction peaks, a small peak at 500°C ascribable to the surface while second broad peak at 800°C related to the bulk reduction of the bulk Ce^{4+} ion. According to the proposed mechanism of Giordano et al (2000) [17] and Pias et al (2000) [18], the smaller crystallites of CeO_2 are reduced first at lower temperature due to the lower enthalpy of reduction while the bulk reduction of CeO_2 occurred at higher temperature (> 750ºC). CeZr, shows complex reduction pattern with overlapped peaks distinguishable at 400, 500 and 800°C related to nanostructural and compositional surface heterogeneity and the high temperature peak at 800°C attributed to the surface and in the bulk reduction of Ce [19]. $CeZrNd_{0.07}$ composition, on the other hand (Figure 4.4 A and B) illustrates that CeO_2 shows two distinct peaks centred at 550ºC and 700ºC attributed to surface and bulk reduction of ceria, respectively. Compared to the CeO_2 and CeZr, $CeZrNd_{0.07}$ composition showing lower degree of reduction of Ce^{4+} to Ce^{3+}. These results agree well with previous findings and requires further investigations to be fully understood [20, 21]. In these oxides the addition of extra vacancies due to the presence of Nd^{3+} may lead to a high vacancies concentration, which in turns may aggregate in less mobile clusters. TPR profiles of Ni catalysts (Figure 4.4 C) show also two peaks centred at 215 °C and 350 °C attributable to the reduction of NiO while the two peaks at 550 °C and 700 °C are again attributed to the surface and bulk reduction of ceria [22-25].

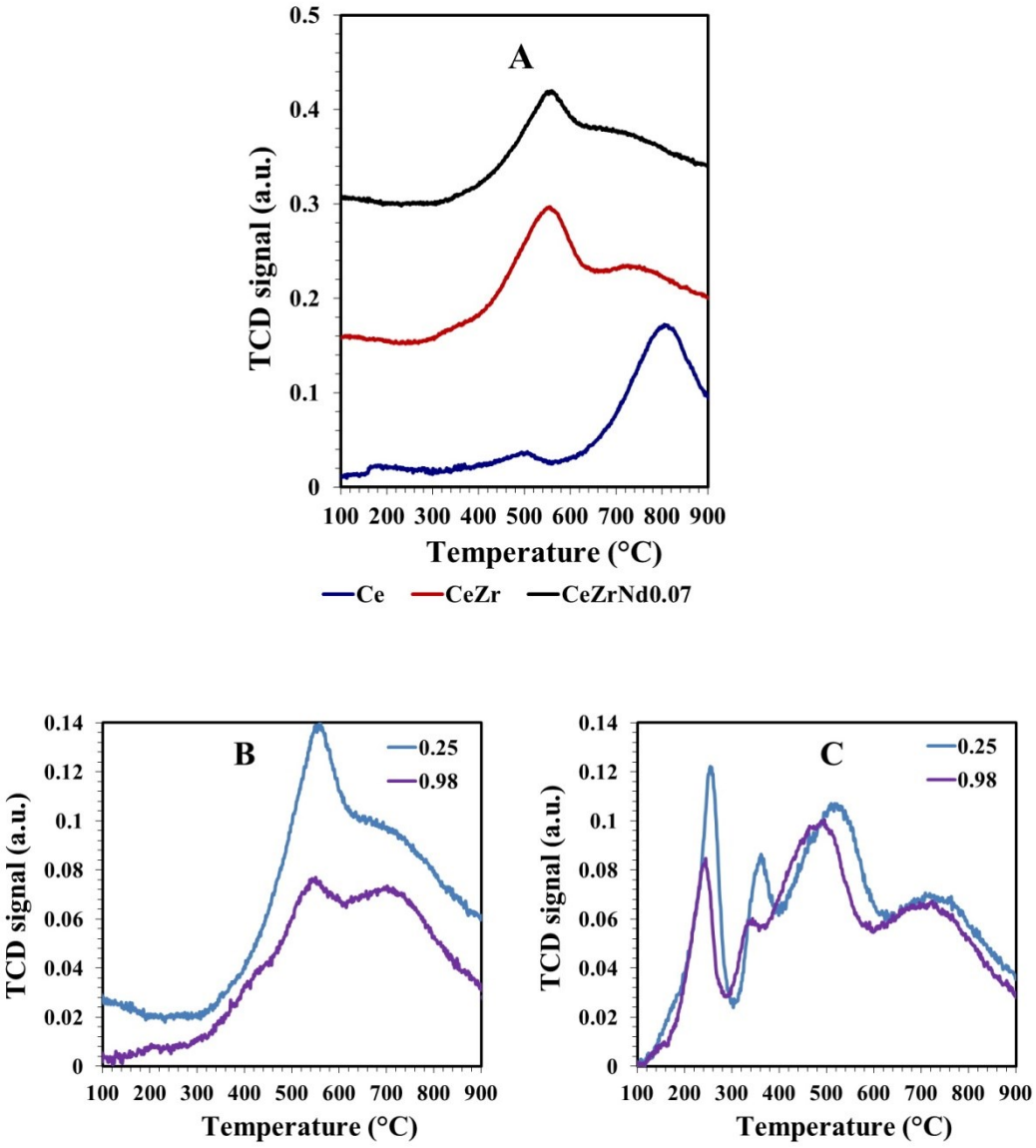

Figure 4.4. Comparison of TPR profiles of different samples calcined at 800°C (A) Ce, CeZr and $CeZrNd_{0.07}$ samples with S/C molar ratio of 0.25 without Ni, (B) $CeZrNd_{0.07}$ samples without nickel with S/C of 0.25 and 0.98, (C) $CeZrNd_{0.07}$ samples with nickel with S/C of 0.25 and 0.98.

The contribution of support to H_2 consumption (Table 2) is quite similar for both catalysts (26 ml/g vs. and 21 ml/g) as calculated from TPR of the support. Quantitatively the hydrogen consumption is 47.8 ml/g and 30.4 ml/g for the catalyst with S/C 0.25 and 0.98 respectively. It can be seen that the amount of hydrogen consumption increased for Ni catalysts compared to their bare supports. Moreover, the H_2 consumption for Ni

catalyst prepared with S/C 0.25 was found to be higher compared to the catalyst prepared with S/C 0.98. This difference in the H_2 consumption (Table 2) confirmed that the Ni/CeZrNd$_{0.07}$ catalyst prepared with S/C molar ratio of 0.25 has better reduction properties compared to 0.98.

Table 2. Quantitative results from TPR profiles of the CeZrNd$_{0.07}$ ($Ce_{0.8}Zr_{0.13}Nd_{0.07}O_{2-x}$) support with S/C molar ratio of 0.25 and 0.98 and Ni supported catalysts.

Sample Name	H_2 uptake without nickel (mL/g)	Degree of Reduction of supports (%)	H_2 uptake with nickel (mL/g)	Degree of Reduction of Ni catalysts (%)
Ni/CeZrNd$_{0.07}$_0.25	26.07	48	47.82	83
Ni/CeZrNd$_{0.07}$_0.98	21.69	40	30.46	51

4.1.4. CO-chemisorption

Metal dispersion is a fundamental characteristic of metal catalysts which can be defined as the fraction of active phase atoms present on the surface of support materials and therefore determines their catalytic properties**.** The chemisorption using hydrogen or carbon monoxide is the most widespread technique to measure dispersion, reported in many investigations because it can be carried out easily using simple apparatus. Furthermore, an appropriate procedure is established for each metal [26, 27].

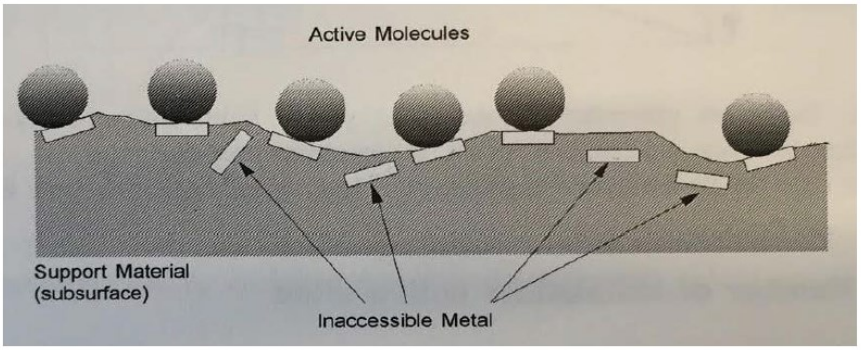

Figure 4.5. Pictorial representation of active metal dispersion.

The metal dispersion depends on the presence of active molecules accessible to the gas which in turn related to the available surface area. An increased number of active molecules would be lost inside the bulk which could decrease the dispersion if the

particle size increases and the inaccessible metal species decrease (Figure 4.5). Another possibility of low dispersion could be the higher stability of NiO crystallites on the surface of support material. Moreover, calcination temperature can also affect particle redistribution resulting in different dispersion for different calcination temperatures [1, 26].

CO pulse chemisorption experiments were conducted to gain insight into Ni metal dispersion on Ni/CeZrNd$_{0.07}$ catalyst prepared with S/C molar ratio of 0.25 and 0.98 and results are presented in Table 3. Ni dispersion resulted in 1.5% for Ni/CeZrNd$_{0.07}$ catalyst prepared with S/C 0.25 while it was 0.5% for Ni/CeZrNd$_{0.07}$ with S/C 0.98. The obtained results showed that the addition of surfactant i,e S/C 0.25 led to an increase in the fraction of pores which allow the higher Ni dispersion into the pores and shows positive effect towards dry reforming reaction [1]. The effect of dopant (Nd) onto CeZr support investigated for the first time and the given values of Ni dispersion is calculated with 3.5% loading of Ni metal onto CeZrNd supports. The dispersion value calculated for Ni/CeZr with 15% Ni metal loading was found to be 1.73 [28] while in case of Ni/CeZrNd$_{0.07}$ almost the same dispersion value (1.5%) was obtained with only 3.5% Ni metal loading which shows better characteristic of catalyst compared to literature. Italiano et al (2020) also reported lower chemisorption/g of Ni loading in CeO_2 compared to our reported values [29].

Table 3. Ni metal dispersion of Ni/CeZrNd$_{0.07}$ catalysts with S/C molar ratio of 0.25 and 0.98.

Sample Name	Dispersion (%)
Ni/CeZrNd$_{0.07}$_0.25	1.5
Ni/CeZrNd$_{0.07}$_0.98	0.5

4.1.5. Catalytic test

The catalytic performance of Ni/CeZrNd$_{0.07}$ catalysts with different S/C molar ratio of 0.25, 0.5, 0.75 and 0.98 was tested in a fixed bed reactor in the temperature range

of 550-750ºC (see Chapter 03 for Experimental procedure) and results are illustrated in Figure 4.6 (A, B).

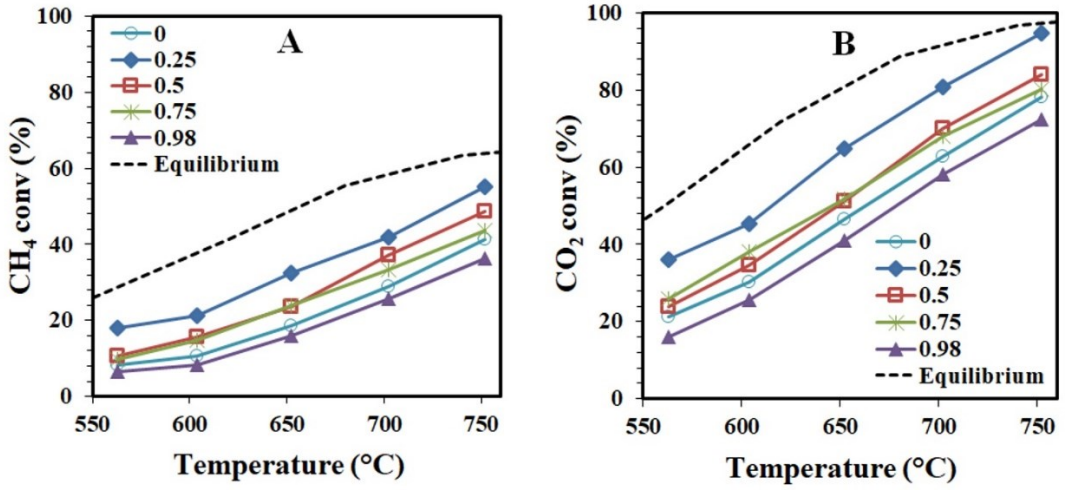

Figure 4.6. Comparison of catalytic activity of Ni/CeZrNd$_{0.07}$ ($Ce_{0.8}Zr_{0.13}Nd_{0.07}O_{2-x}$) catalyst with different S/C molar ratios (0.25, 0.5, 0.75 and 0.98): (A) CH_4 conv (%) (B) CO_2 conv (%).

The results were compared to investigate the best catalyst with respect to S/C molar ratio. During DR reaction it was found that the addition of surfactant remarkably improves the catalytic activity. However, the relationship between the amount of surfactant and the activity of the catalysts is not linear. It is obvious from the Figure 4.6 (A, B) that Ni/CeZrNd$_{0.07}$ without surfactant and with 0.5 and 0.75 S/C molar ratio show almost the same activity and the further addition of surfactant (0.98 S/C molar ratio) decreases the catalytic activity. It can be seen that the CH_4 conversion compared to CO_2 conversion is lower in the entire range of temperature (550-750ºC). It is evident from obtained results that, the overall conversion percent of CH_4 and CO_2 is increasing with the increase of reaction temperature and CO_2 conversion was higher than CH_4 conversion, which means that the DRM reaction is influenced by simultaneous occurrence of reverse water gas reaction (RWGS). Furthermore, RWGS reaction favored at low temperature (< 700ºC) and CO_2 can easily react with H_2 to give CO. The consumption of H_2 production due to RWGS resulted in H_2/CO product ratio less than unity. It should be noted that H_2/CO product ratio is also increasing with the increase of reaction temperature from 550-750ºC [30, 31]. Among all samples, CO_2 conversion was found to be higher for

Ni/$CeZrNd_{0.07}$ catalyst prepared with S/C molar ratio of 0.25 in comparison to 0.5, 0.75 and 0.98 and reached almost the thermodynamic value (equilibrium). In addition, the error between different runs was found to be negligible (0.5-2%), therefore, no error bar is mentioned in plots.

4.2. Conclusion

Nanocrystalline $CeZrNd_{0.07}$ supported Ni based catalysts were synthesized by surfactant assisted co-precipitation method by varying S/C ratio in the range of 0-0.98. On the basis of morphological study it was concluded that in the presence of 0.25 S/C ratio of surfactant, nanocrystallites of $CeZrNd_{0.07}$ can organize in a refractory structure with a broad mesoporosity such as high surface area and pore size distribution which would favour the dispersion of Ni into the pores of support. Chemisorption results revealed that Ni dispersion was found to be 1.5% for Ni/$CeZrNd_{0.07}$ catalyst prepared with S/C molar ratio of 0.25 while it was 0.5% for Ni/$CeZrNd_{0.07}$ with S/C ratio of 0.98. The obtained results showed that the addition of surfactant i,e S/C ratio 0.25 led to an increase in the fraction of pores which allow the higher Ni dispersion into the pores. XRD analysis confirmed that that all mixed oxides of $CeZrNd_{0.07}$ are crystalline and NiO is well dispersed on the supports. TPR profiles of Ni catalysts showed two peaks centred at 215 °C and 350 °C attributable to the reduction of NiO while the two peaks at 550 °C and 700 °C attributed to the surface and bulk reduction of ceria. Moreover, TPR analysis also revealed a strong metal-support interaction which could hinder the thermal agglomeration of Ni particles. It is evident from catalytic tests that, the overall conversion percent of CH_4 and CO_2 is increasing with the increase of reaction temperature and CO_2 conversion was higher than CH_4 conversion, which means that the DRM reaction is influenced by simultaneous occurrence of reverse water gas reaction (RWGS). Among all tested catalysts, CH_4 and CO_2 conversion was found to be higher for Ni/$CeZrNd_{0.07}$ catalyst prepared with S/C ratio of 0.25 in comparison to 0.5, 0.75 and 0.98 and CO_2 conversion reached almost the thermodynamic value (equilibrium). Therefore, on the basis of physio-chemical analysis, it was concluded that $CeZrNd_{0.07}$ prepared with 0.25 S/C molar ratio shows higher porosity, higher degree of reduction, high metal dispersion and exhibited good catalytic performance in term of DRM reaction. Therefore, further

investigation was carried out by considering only samples prepared with a S/C ratio of 0.25.

Chapter No: 04

Results and Discussion

Part B: Effect of dopants (Lanthanum (La) and Neodymium (Nd)

4.3. Effect of dopants (La and Nd)

In order to investigate the effect of dopants for catalytic activity of DRM, ceria zirconia doped with lanthanum, $CeZrLa_{0.07}$ ($Ce_{0.80}Zr_{0.13}La_{0.07}O_{2-x}$) was prepared with surfactant/cation (S/C) ratio of 0.25 and 0.75 and compared with $CeZrNd_{0.07}$ ($Ce_{0.8}Zr_{0.13}Nd_{0.07}O_{2-x}$) under the same conditions.

4.3.1. BET surface area

The BET surface area, pore volume and pore size distribution of $CeZrLa_{0.07}$ and $CeZrNd_{0.07}$ prepared by S/C ratio of 0.25 and 0.75 and corresponding nickel (Ni) catalysts are summarized in Table 4.

Table 4. BET surface area of $CeZrNd_{0.07}$ ($Ce_{0.8}$ $Zr_{0.13}$ $Nd_{0.07}$ O_{2-x}) and $CeZrLa_{0.07}$ ($Ce_{0.8}$ $Zr_{0.13}$ $La_{0.07}$ O_{2-x}) with different ratios of surfactant (0.25 and 0.75).

Sample Name	Temp/time Calcination (°C)	Surface Area (m^2/g)	Pore Volume (cm^3/g)	Pore Diameter (Å)
$CeZrNd_{0.07}$_0.25	500/4h	73	0.36	178
$CeZrNd_{0.07}$_0.25	800/3h	45	0.30	223
Ni/$CeZrNd_{0.07}$_0.25	800/1h	36	0.31	278
$CeZrLa_{0.07}$_0.25	500/4h	72	0.30	154
$CeZrLa_{0.07}$_0.25	800/3h	47	0.32	234
Ni/$CeZrLa_{0.07}$_0.25	800/1h	36	0.28	256
$CeZrNd_{0.07}$_0.75	500/4h	109	0.18	61
$CeZrNd_{0.07}$_0.75	800/3h	46	0.15	99
Ni/$CeZrNd_{0.07}$_0.75	800/1h	28	0.10	109
$CeZrLa_{0.07}$_0.75	500/4h	126	0.20	57
$CeZrLa_{0.07}$_0.75	800/3h	58	0.14	96
Ni/$CeZrLa_{0.07}$_0.75	800/1h	34	0.09	82

It is evident (Table 4) that BET surface area of the $CeZrNd_{0.07}$ and $CeZrLa_{0.07}$ supports prepared with S/C ratio of 0.25 and calcined at 500°C/4h (fresh samples), at 800°C and after Ni impregnation show very similar surface areas. Furthermore, the pore volume for supports and catalysts is also the same (≈ 0.3 cm^3/g). On the other hand, surface area of the $CeZrNd_{0.07}$ and $CeZrLa_{0.07}$ supports prepared with S/C ratio of 0.75 and calcined at 500°C/4h (fresh samples) and at 800°C show minor differences, as well as for Ni supported samples. This comparison between CeZr materials doped with La and Nd confirmed that the materials prepared with lower amount of surfactant show increased

pore volume and size compared to those prepared using S/C ratio of 0.75. The results are in good agreement with literature [1, 11]. Moreover, it was observed that mesoporous material synthesized via surfactant assisted method exhibited promising textural properties such as high surface area and pore size distribution, showed good metal dispersion and higher stability for DR reaction [4, 6].

4.3.2. XRD

XRD analysis confirmed that all mixed oxides of $CeZrNd_{0.07}$ and $CeZrLa_{0.07}$ (Figure 4.7(A)) are cubic [3]. Ni impregnation (3.5%) onto support material (Figure 4.7B), did not affect the cubic structure of supports [13]. All spectra exhibited a very small peak at $2\theta = 43.28$ degrees corresponding to the (200) plane of cubic nickel oxide. It is reported that Ni is better dispersed on cubic phases compared to other phase structures and Ni species are highly dispersed on support materials and the results are in good agreement with literature [4, 6, 14].

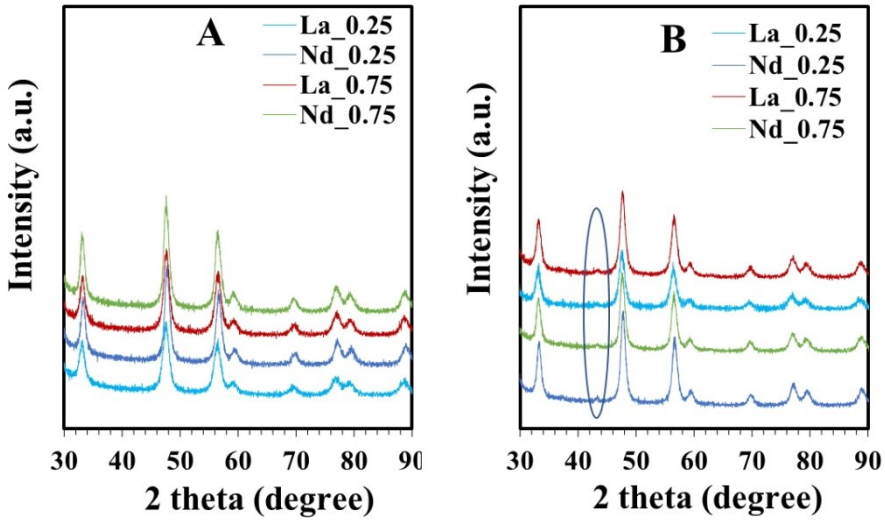

Figure 4.7. Comparison of XRD patterns of $CeZrNd_{0.07}$ and $CeZrLa_{0.07}$ supports with different S/C molar ratio of 0.25 and 0.75: (A) after calcination at 800°C, (B) after impregnation of Ni and calcination at 800°C.

($Ni/CeZrNd_{0.07}$_0.25 as Nd_0.25, $Ni/CeZrNd_{0.07}$_0.75 as Nd_0.75, $Ni/CeZrLa_{0.07}$_0.25 as La_0.25 and $Ni/CeZrLa_{0.07}$_0.75 as La_0.75)

4.3.3. Catalytic test

The catalytic performance of Ni/CeZrNd$_{0.07}$ and Ni/CeZrLa$_{0.07}$ catalysts with S/C molar ratio of 0.25 and 0.75 was tested in the temperature range of 550-750°C and results are illustrated in Figure 4.8 (A, B). In general, Nd containing samples are always better than those doped with La. Ni/CeZrNd$_{0.07}$ with S/C ratio of 0.25 showed similar activity in comparison to Ni/CeZrLa$_{0.07}$ at low temperature (≤600°C) while Ni/CeZrNd$_{0.07}$ with S/C 0.75 showed almost the same catalytic activity of Ni/CeZrLa$_{0.07}$ prepared with S/C 0.25. The catalytic behaviour of Ni/CeZrLa$_{0.07}$ prepared with S/C 0.75 was found to be very low in comparison to other catalysts.

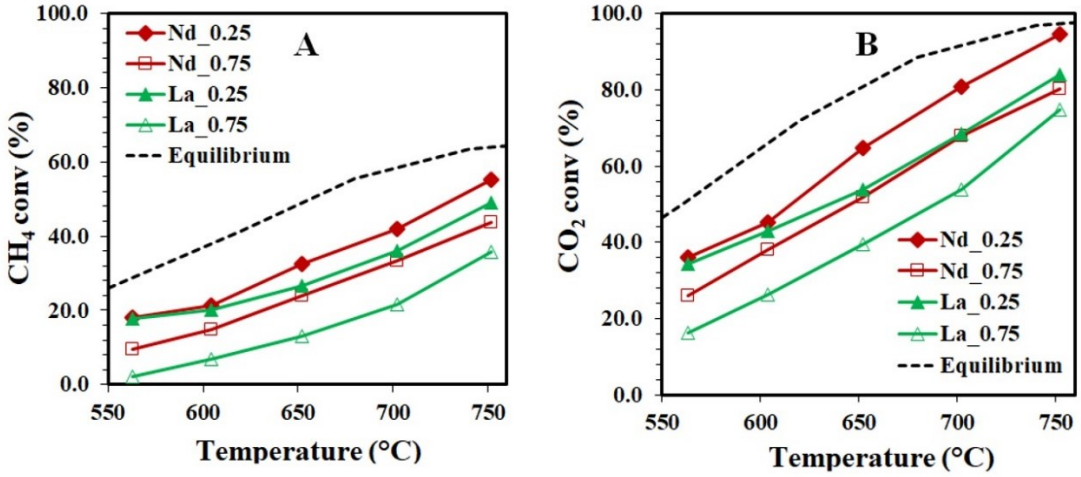

Figure 4.8. Comparison of catalytic activity of Ni/CeZrNd$_{0.07}$ ($Ce_{0.8}Zr_{0.13}Nd_{0.07}O_{2-x}$) and Ni/CeZrLa$_{0.07}$ ($Ce_{0.8}Zr_{0.13}La_{0.07}O_{2-x}$) catalysts with S/C molar ratios of 0.25 and 0.75): (A) CH_4 conv (%) (B) CO_2 conv (%)

(Ni/CeZrNd$_{0.07}$_0.25 as Nd_0.25, Ni/CeZrNd$_{0.07}$_0.75 as Nd_0.75, Ni/CeZrLa$_{0.07}$_0.25 as La_0.25 and Ni/CeZrLa$_{0.07}$_0.75 as La_0.75)

4.4. Main Conclusion

Based on the catalytic tests for DRM, it was concluded that ceria zirconia doped with neodymium showed better performance especially in term of CO_2 conversion as compared to ceria zirconia doped with lanthanum. Moreover, in literature, some studies were already conducted with La [12, 32-34] so it was decided to continue our research to gain insight into the effect of Nd as a dopant.

Note that the effect of surfactant (lauric acid) is the prime concern of current chapter while the detailed experiments in order to compare the Ni based catalysts with different compositions are explained in detail from chapter 5.

Chapter No: 05

Results and Discussion

Effect of neodymium (Nd_2O_3) doping on ceria and ceria-zirconia solid solutions for the development of Ni supported catalysts

5. Introduction

The support materials play a vital role in the catalytic activity and stability of DRM reaction towards carbon deposition. Ni has been supported on various supports such as MgO [35-39], Al_2O_3 [38, 40-43], SiO_2 [36, 44], La_2O_3 [30, 45]. CeO_2-ZrO_2 (CeZr) mixed oxides have been often considered as a promising support for Ni based catalysts owning to their higher oxygen storage capacity and their higher thermal stability**.** These properties are related to their capability of fast redox cycles due to releasing and up taking of oxygen species. Moreover, the addition of ZrO_2 to CeO_2 improves the CH_4 conversion at lower temperature which is an important characteristic to overcome the endothermic nature of DR process [3, 12, 16, 22, 23, 46-52]. Moreover, catalysts supported on CeZr material are more active and selective due to the increased number of active sites on the support surface. However, the catalytic activity of ceria-based materials is not directly related to bulk oxygen storage capacity. Therefore, in this section, much attention has been devoted to synthesize nickel (Ni) based catalysts supported on ceria-zirconia mixed oxide (CeZr) with neodymium (Nd) as dopant for DRM to investigate and improve the physiochemical properties of supports in order to optimize an innovative catalyst for dry reforming, active at lower temperature (600-800°C).

5.1. Results and Discussion

5.1.1. BET surface area

The results of texture properties of the supports prepared with a 0.25 molar ratio of surfactant (lauric acid, S/C=0.25) calcined at 800°C and together with corresponding nickel (Ni) catalysts are summarized in Table 1 and Table 2 and mesoporous structures are presented in Figure 5.1 and Figure 5.2. Brunauer, Emmet and Teller (BET) and Barret, Joyner and Halenda (BJH) methods were used for the determination specific surface area, pore volume and pore diameter of prepared catalysts. The BET surface area of CeZr, $CeZrNd_{0.2}$ and $CeZrNd_{0.07}$ was almost the same and found to be higher (41-45 m^2/g) compared to CeO_2 (22 m^2/g) and $CeNd_{0.2}$ (25 m^2/g) supports. On the other hand, ZrO_2 (6 m^2/g) and Nd_2O_3 (8 m^2/g) alone have very low surface areas (see chapter 6). It can be seen that loading of Ni metal onto support materials leads to a significant decrease

Table 1. Structural properties of CeO_2, CeZr, $CeNd_{0.2}$, $CeZrNd_{0.2}$ and $CeZrNd_{0.07}$ supports prepared with a S/C molar ratio of 0.25 and different calcination temperatures.

Composition	Name	Temp/time calcination (°C/h)	Surface Area (m^2/g)	Pore Volume (cm^3/g)	Pore Diameter (Å)	Crystallite size[1] (Å)
CeO_2	Ce	800/3	22	0.195	295	298
$Ce_{0.80}Zr_{0.20}O_2$	CeZr	800/3	44	0.374	270	58
$Ce_{0.80}Zr_{0.20}O_2$	CeZr_950	950/3	26	0.313	379	151
$Ce_{0.80}Nd_{0.20}O_{1.9}$	$CeNd_{0.2}$	800/3	25	0.221	280	178
$Ce_{0.64}Zr_{0.16}Nd_{0.2}O_{1.9}$	$CeZrNd_{0.2}$	800/3	41	0.310	249	77
$Ce_{0.64}Zr_{0.16}Nd_{0.2}O_{1.9}$	$CeZrNd_{0.2}$_990	990/3	22	0.282	384	134
$Ce_{0.80}Zr_{0.13}Nd_{0.07}O_{1,96}$	$CeZrNd_{0.07}$	800/3	45	0.301	223	87
$Ce_{0.80}Zr_{0.13}Nd_{0.07}O_{1,96}$	$CeZrNd_{0.07}$_1030	1030/3	20	0.259	395	170

[1] calculated with Scherrer equation from (111) peak of cubic phase of CeO_2 and of CeZr solid solutions.

Table 2. Structural properties of Ni/CeO_2, Ni/CeZr, $Ni/CeNd_{0.2}$, $Ni/CeZrNd_{0.2}$ and $Ni/CeZrNd_{0.07}$ catalysts prepared with a S/C molar ratio of 0.25 and different calcination temperatures.

Catalysts	Surface Area (m^2/g)	Pore Volume (cm^3/g)	Pore Diameter (Å)	Metal dispersion (%)	Support Crystallite size[1] (Å)
Ni/Ce	19	0.180	316	0.59	296
Ni/CeZr	34	0.261	255	1.08	100
Ni/CeZr-950	22	0.240	349	1.58	154
$Ni/CeNd_{0.2}$	19	0.196	307	0.58	195
$Ni/CeZrNd_{0.07}$	37	0.311	278	1.56	95
$Ni/CeZrNd_{0.2}$	32	0.311	309	1.28	86
$Ni/CeZrNd_{0.07}$-1030	19	0.243	382	1.93	170
$Ni/CeZrNd_{0.2}$-990	21	0.193	310	1.44	134

[1] calculated with Scherrer equation from (111) peak of cubic phase related to the supports.

in the surface area, so that the relative reduction of surface area with the loading of Ni metal can possibly increase the pore volume and pore diameter of catalysts compared to their pure supports [12].

In order to understand the effect of textural properties on the catalytic activity, the support materials, CeZr, $CeZrNd_{0.2}$ and $CeZrNd_{0.07}$ were subjected to higher calcinations temperatures at 950°C, 990°C and 1030°C respectively, to obtain the same surface area as CeO_2 (22 m^2/g). $CeNd_{0.2}$ (25 m^2/g) has comparable surface area with CeO_2. It was observed that with the increase of calcination temperature, the surface area of CeZr, $CeZrNd_{0.2}$ and $CeZrNd_{0.07}$ supports decreased to 20-25 m^2/g which is equal to the surface area of CeO_2 and $CeNd_{0.2}$ (22-25 m^2/g) calcined at 800°C. The calcined support materials were impregnated with Ni metal and again calcined at 800°C to get the stable structure for DRM reaction and results are illustrated in Table 2. CeZr, $CeZrNd_{0.2}$ and $CeZrNd_{0.07}$ were found to be stable even at relatively high calcination temperature (950°C-1030°C). Moreover, all materials exhibited IV-type isotherms and found to be mesoporous in nature (Figure 5.1 and Figure 5.2).

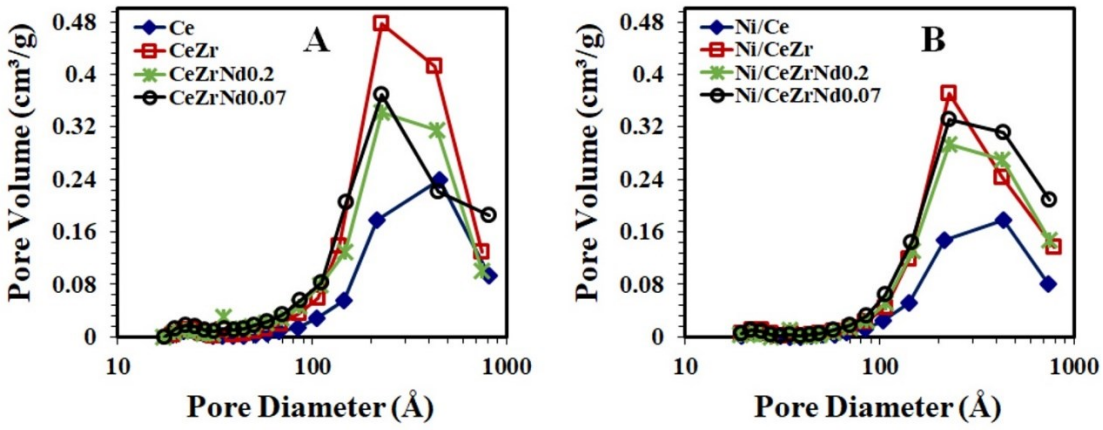

Figure 5.1. Comparison of pore size distribution of Ce, CeZr, $CeZrNd_{0.2}$ and $CeZrNd_{0.07}$ samples with and without nickel: (A) after calcination at 800°C, (B) after impregnation of Ni and calcination at 800°C.

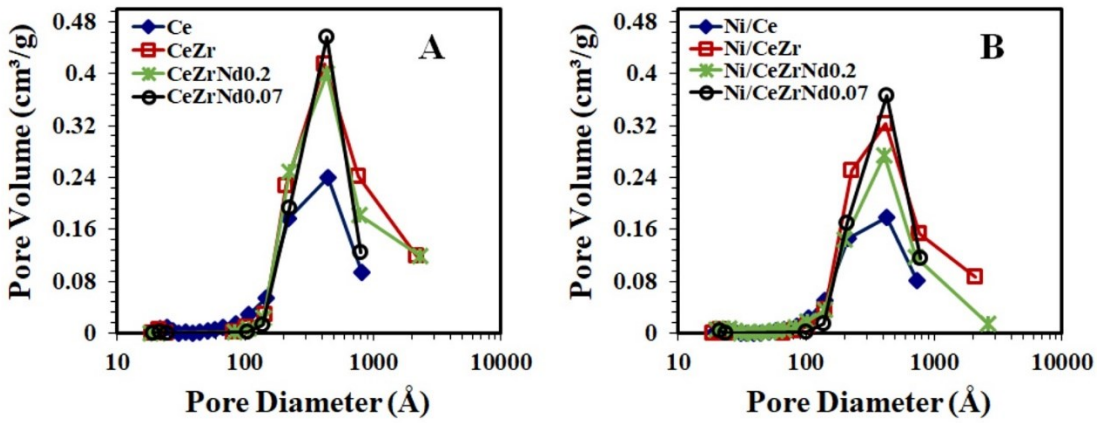

Figure 5.2. Comparison of pore size distribution of Ce, CeZr, $CeZrNd_{0.2}$ and $CeZrNd_{0.07}$ samples with and without nickel: (A) after calcination at different temperatures (800-1030ºC), (B) after impregnation of Ni and calcination at 800°C.

Based on the BET results it was found that addition of surfactant has a significant effect on textural properties. It was observed that the addition of surfactant led to an increase in the specific surface area and pore size distribution and to high thermal stability of sample which remained stable at relatively high calcination temperatures. Moreover, surfactant assisted method increases the fraction of pores maintaining the meosporosity of samples which allows higher Ni dispersion into the pores and shows positive effect towards dry reforming reaction (detailed discussion already explained in chapter 4) [1, 4, 6, 8-10]. It was also observed that Nd doping affects the textural properties and crystallinity of CeO_2 causing a decrease of the dimension of crystallites from 298 Å to 178 Å and an increase of the pore volume. Opposite and less significant effects were observed for CeZr where the addition of Nd leads to a coalescence of crystallites and merging of the pores.

5.1.2. XRD

XRD analysis was carried out for Ce, CeZr, $CeZrNd_{0.2}$ and $CeZrNd_{0.07}$ compositions (calcined at 800ºC) and related Ni catalysts, and their spectra are shown in Figure 5.3 (A, B). All diffractograms of mixed oxides (Figure 5.3A) confirmed the presence of cubic fluorite type structure with fine crystallinity [11, 12, 49]. Ceria and

ceria-zirconia solid solution crystallized in a cubic phase that matches respectively with the PDF file of CeO_2 (PDF 34-0394, cell parameter, a=5.4113 Å) and that of $Ce_{0.75}Zr_{0.25}O_2$ (PDF 28-0271, a=5.3494 Å). The compositions doped with Nd showed also a cubic structure without any trace of other segregated phases. The XRD of $CeZrNd_{0.07}$ shows the same profile as CeZr solid solution while in the XRD profiles of $CeZrNd_{0.2}$ peaks are slightly shifted with respect to the undoped phases (Figure 5.4) confirming that Nd enters into the fluorite lattice. After impregnation with nickel, all spectra exhibited a very small peak at 2θ = 43.28 degrees (Figure 5.5) corresponding to the (200) plane of cubic nickel oxide (PDF 78-0429). The small intensity of this peak suggests that NiO is well dispersed on the supports and seems to have no effect on the crystal structure of support materials (Figure 5.3B). These results are in good agreement with literature, in which it is reported that cubic phase catalysts have better dispersion for Ni as compared to other phase structures [4, 6, 12-14, 47].

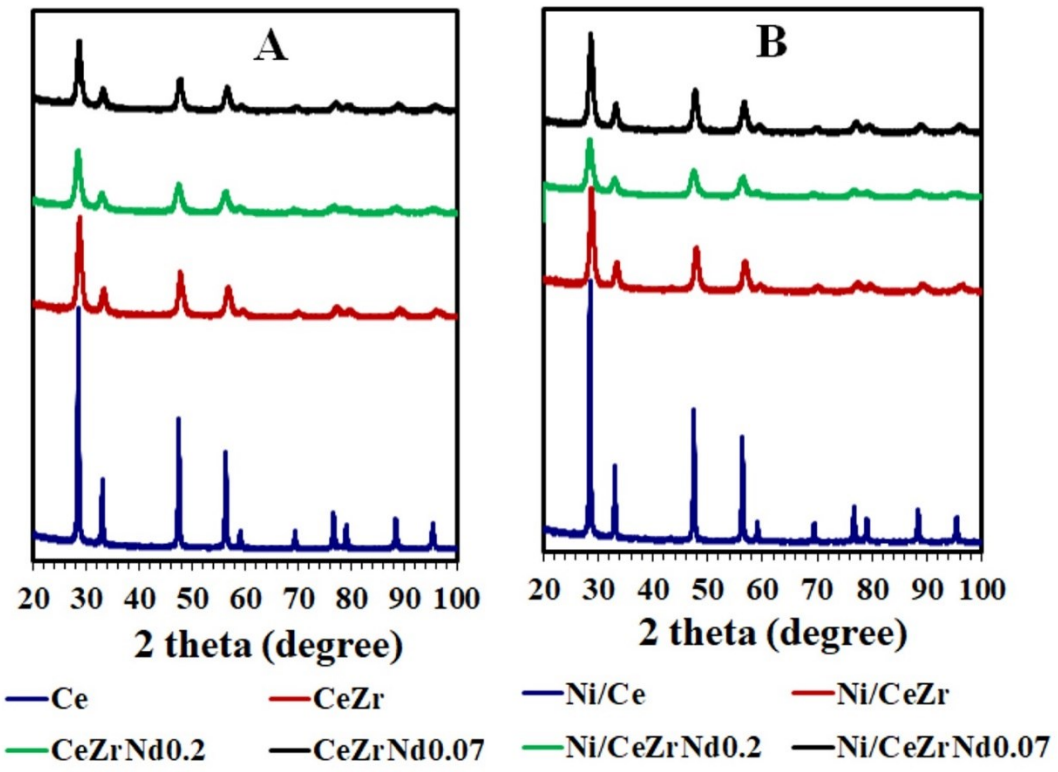

Figure 5.3. Comparison of XRD of Ce, CeZr, $CeZrNd_{0.2}$ and $CeZrNd_{0.07}$ samples with and without nickel: (A) after calcination at 800°C, (B) after impregnation of Ni and calcination at 800°C.

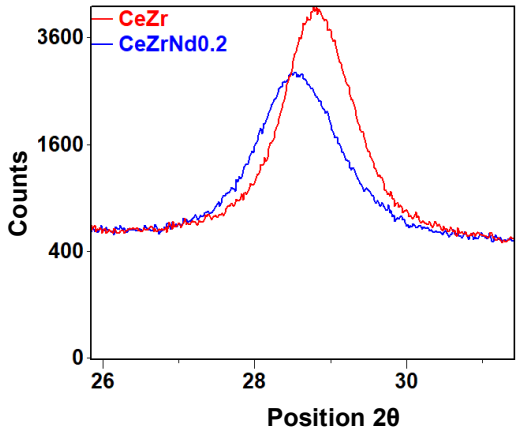

Figure 5.4. Details of comparison between CeZr and $CeZrNd_{0.2}$ in the 2θ range between 24 and 32 degrees, showing the shift of the main peak due to the insertion of Nd into the fluorite structure.

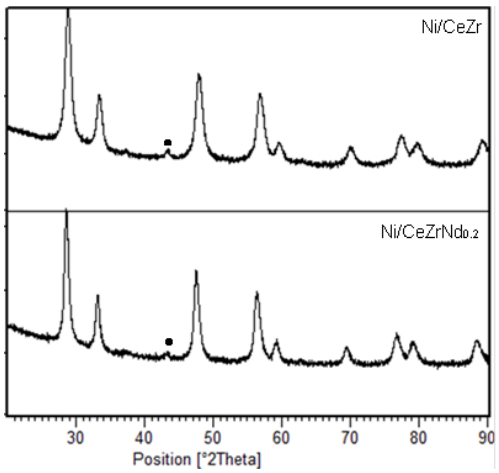

Figure 5.5. XRD patterns of Ni/support catalysts (Ni/CeZr and $Ni/CeZrNd_{0.2}$); black dot indicates nickel phase.

XRD patterns were also collected for CeZr, $CeZrNd_{0.2}$ and $CeZrNd_{0.07}$ compositions calcined at higher temperature (950-1030ºC) to get same surface area of all supports (20-25 m^2/g) which is equal to the surface area of CeO_2. XRD patterns of supports and catalysts (Figure 5.6 (A, B)) exhibited the same behavior which was observed for supports and Ni catalysts with high surface area. These results shows that

the samples prepared by surfactant assisted method are more stable even at higher calcination temperature [4]. Moreover, low surface area did not affect the crystallinity.

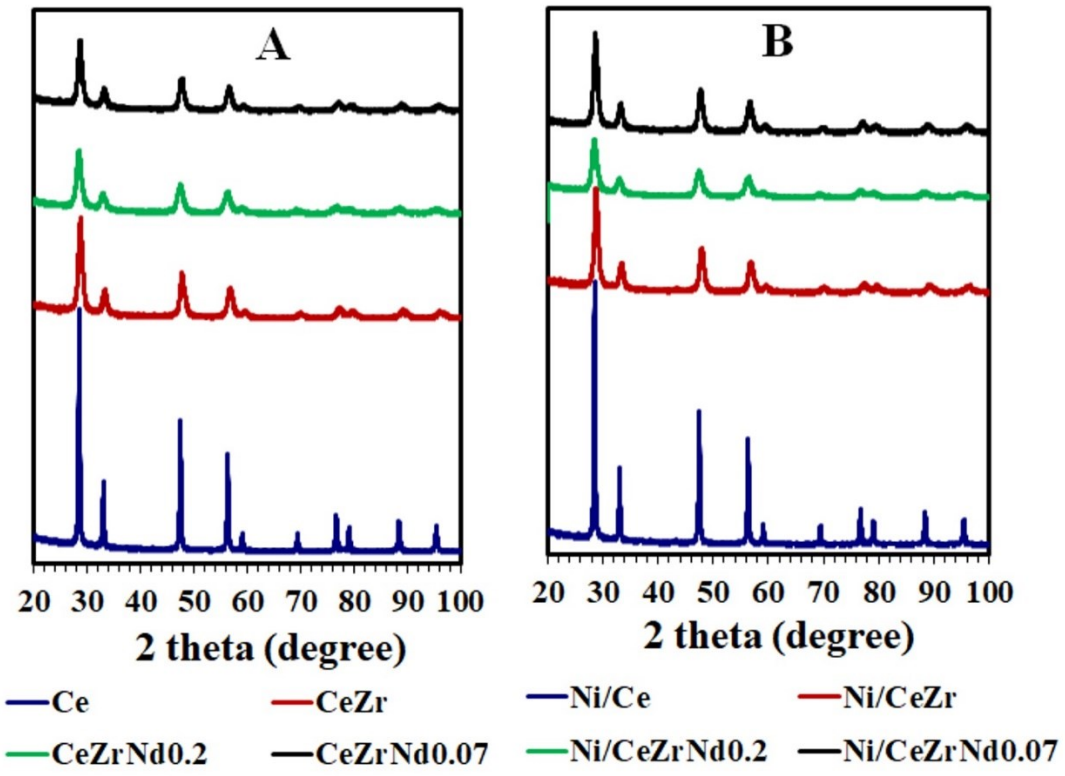

Figure 5.6. Comparison of XRD of Ce, CeZr, $CeZrNd_{0.2}$ and $CeZrNd_{0.07}$ samples with and without nickel: (A) after calcination at different temperatures (800-1030ºC), (B) after impregnation of Ni and calcination at 800°C.

5.1.3. TPR

TPR profiles of Ce, CeZr, $CeZrNd_{0.2}$ and $CeZrNd_{0.07}$ supports (Figure 5.7A) and the corresponding Ni catalysts (Figure 5.7B) have been investigated by H_2-TPR. It was observed that undoped materials show a classical multi-model profiles [15, 16]. It can be seen (Figure 5.7A) that CeO_2 shows two distinct reduction peaks, a small peak at 500°C ascribable to the surface reduction while second broad peak at 800°C related to the bulk reduction of the bulk Ce^{4+} ion. The smaller crystallites of CeO_2 are reduced first at lower temperature due to the lower enthalpy of reduction while the bulk reduction of CeO_2 occurred at higher temperature (> 750ºC) [17, 18]. CeZr, on the other hand showed complex reduction pattern with overlapped peaks distinguishable at 400, 500 and 800°C

related to nanostructural and compositional surface heterogeneity and the high temperature peak at 800°C attributed to the surface and in the bulk reduction of CeO_2 [19]. Compared to the CeZr, $CeZrNd_{0.2}$ and $CeZrNd_{0.07}$ compositions show lower degree of reduction of Ce^{4+} to Ce^{3+}. These results agree well with previous findings and requires further investigations to be fully understood [20, 21]. In these oxides the addition of extra vacancies due to the presence of Nd^{3+} may lead to a high vacancies concentration, which in turns may aggregate in less mobile clusters.

The Ni impregnated catalysts (Figure 5.7B) showed three to four reduction peaks not univocally interpreted in the literature [22]. An appropriate interaction between metal and support possibly increases the Ni reducibility. The Ni reducibility is basically because of an electronic interaction between CeO_2 and Ni^{30}, as Ce is rich in d-orbitals and Ni has unfilled d orbitals. Therefore, Ni can easily accept the d-electrons from Ce resulting an increase in the d-electron density of Ni 3. The peak in the range of 200-260°C are attributed to the reduction of free nanocrystallites of NiO, while the peaks around 300-450°C related to the reduction of larger Ni crystallites and to those Ni species strongly interacting with the support. Generally, the first three peaks at lower temperatures are attributed to the reduction of NiO with different particle sizes and strongly interacting with the support. Table 3 presented the quantitative results of TPR profiles and it was observed that the H_2 uptake is higher in Ni catalysts compared to their bare supports. Ce support and Ni/Ce catalyst have lower H_2 uptake and show lower degree of reduction. On the other hand, CeZr support and Ni/CeZr has higher H_2 uptake and higher degree of reduction when compared to other catalyst. Among CeZrNd compositions, $CeZrNd_{0.07}$ shows higher degree of reduction as compared to $CeZrNd_{0.2}$.

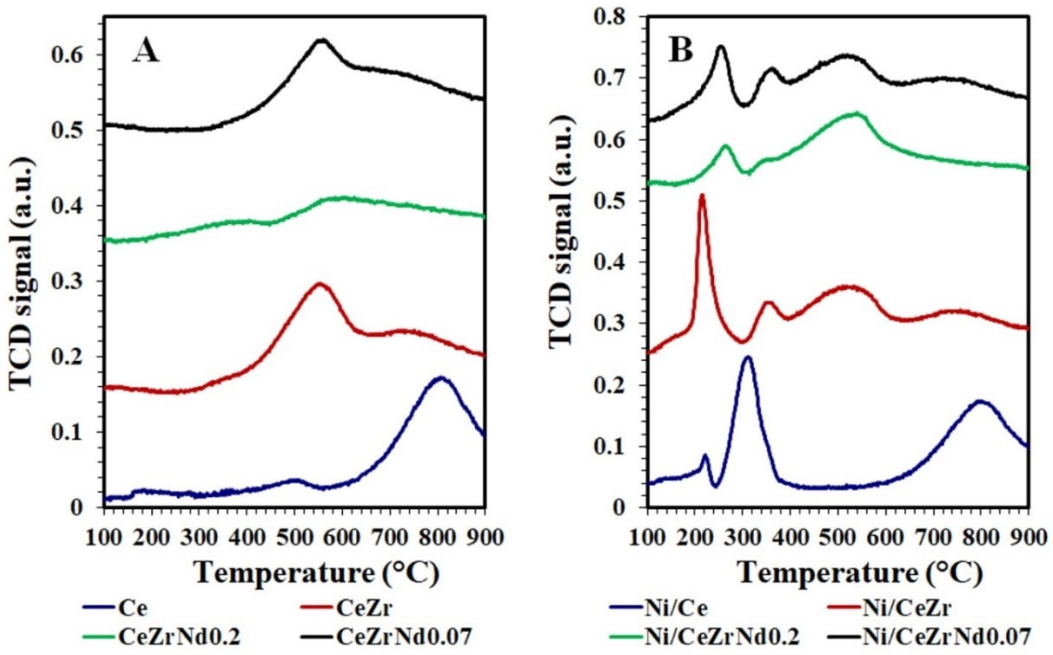

Figure 5.7. Comparison of TPR of Ce, CeZr, $CeZrNd_{0.2}$ and $CeZrNd_{0.07}$ samples with and without nickel: (A) after calcination at 800°C, (B) after impregnation of Ni and calcination at 800°C.

Table 3. Quantitative results from TPR profiles of the of Ce, CeZr, $CeZrNd_{0.2}$ and $CeZrNd_{0.07}$ supports and Ni supported catalysts at same calcination temperature (800°C).

Samples (mL/g)Supports	Supports H_2 uptake (mL/g)[a]	Degree of reduction of supports[b] (%)	Ni catalysts H_2 uptake (mL/g)[c]	Degree of reduction of Ni catalysts[b] (%)
Ni/Ce	24.5	38	29.3	45
Ni/CeZr	30.4	55	37.0	53
$Ni/CeZrNd_{0.2}$	18.9	43	30.0	42
$Ni/CeZrNd_{0.07}$	26.0	48	47.8	83

a-measured from integration of TPR calibrated profiles of Figure 5.7A.

b-calculated as the ratio of moles of H_2 consumed and those theoretically consumed for the complete reduction of the reducible species present in a sample, i.e. Ce^{4+} moles or the sum of Ce^{4+} moles and Ni^{2+} moles. The reactions considered in the calculation are $2CeO_2 + H_2 \leftrightarrow H_2O + Ce_2O_3$; $NiO + H_2 \leftrightarrow Ni + H_2O$

c- measured from integration of TPR calibrated profiles of Figure 5.7B.

d-expected values for a complete reduction of NiO i.e. (13.5 mL/g) and a partial reduction of support according to the values reported in the 2nd column.

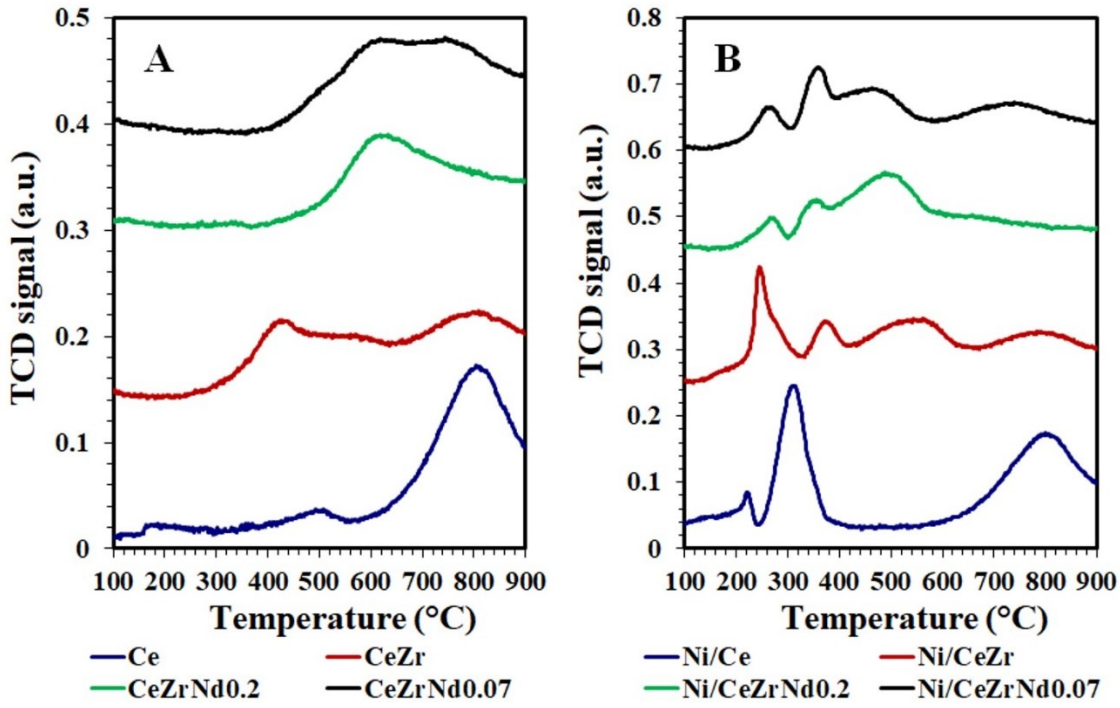

Figure 5.8. Comparison of TPR of Ce, CeZr, $CeZrNd_{0.2}$ and $CeZrNd_{0.07}$ samples with and without nickel: (A) after calcination at different temperatures (800-1030ºC), (B) after impregnation of Ni and calcination at 800 °C.

Table 4. Quantitative results from TPR profiles of the of Ce, CeZr, $CeZrNd_{0.2}$ and $CeZrNd_{0.07}$ supports and Ni supported catalysts at different calcination temperatures (800-1030ºC).

Samples (mL/g)Supports	Supports H_2 uptake (mL/g)[a]	Degree of reduction of supports[b] (%)	Ni catalysts H_2 uptake (mL/g)[c]	Degree of reduction of Ni catalysts[b] (%)
Ni/Ce	24.5	38	29.3	45
Ni/CeZr_950	26.5	48	35.7	51
$Ni/CeZrNd_{0.2}$_990	18.4	42	28.3	40
$Ni/CeZrNd_{0.07}$_1030	23.5	43	32.2	56

a-measured from integration of TPR calibrated profiles of Figure 5.8A.

b-calculated as the ratio of moles of H_2 consumed and those theoretically consumed for the complete reduction of the reducible species present in a sample (already described above)

c- measured from integration of TPR calibrated profiles of Figure 5.8B.

In order to investigate the effect of higher calcination temperature and to observe the catalytic activity at same surface area, CeZr, $CeZrNd_{0.2}$ and $CeZrNd_{0.07}$ supports were subjected to different calcination temperature (950-1030ºC) and characterized by H_2-TPR. The TPR profiles are illustrated in Figure 5.8 (A, B) and quantitative results are presented in Table 4. After comparing results at different surface area and at same surface area, it was observed that $CeZrNd_{0.2}$ and $CeZrNd_{0.07}$ supports after calcination at higher temperature (same surface area) show more broad and defined reduction peaks in comparison to the supports calcined at 800ºC. Furthermore, a decrease in the reduction degree of CeZr and $CeZrNd_{0.07}$ supports was observed at higher calcination temperature, 950ºC and 1030ºC respectively. A major difference in degree of reduction of $Ni/CeZrNd_{0.07}$ catalysts was observed at higher calcination temperature (low surface area) so it can be concluded that somehow lower morphological properties and higher calcination temperature can affect the reduction degree of supports and corresponding Ni catalysts. This could be due to the agglomeration of Ni particles at higher calcination temperature.

5.1.4. CO_2-TPD

CO_2-temperature programmed desorption (CO_2-TPD) experiments were carried out using CO_2 as a probe gas to investigate the strength of basic sites of Ce, CeZr, $CeZrNd_{0.2}$ and $CeZrNd_{0.07}$ supports along with Ni catalysts and results are illustrated in Figure 5.9, A and B respectively. The degree of acidity and basicity of the materials and/or catalysts is usually measured as a function of temperature range where the chemisorbed probe gas would be desorbed. The strength of basic sites using CO_2 as a probe gas depends on the CO_2 adsorption peaks located at different temperatures, i.e. the desorption peaks at 50-200ºC corresponds to weak basic site where as intermediate (200-400 ºC), strong (400-650 ºC) and very strong (>650 ºC) basic sites can be estimated from the area under CO_2 desorption patterns [53]. The presence of basic sites could improve the adsorption of acidic CO_2 which provides more oxygen species on the surface of catalyst for the gasification of intermediate carbonaceous species formed as a result of CH_4 decomposition during dry reforming reaction that would result to decrease coke formation and possibly increase the catalytic activity [48]. The higher conversion of CO_2

also favored the reduction of carbon deposition on catalyst surface by reverse Boudouard reaction ($CO_2 + C \rightarrow 2CO$) [11].

It is clear from Figure 5.9A that the fresh supports provided the lowest basicity therefore, showing lowest CO_2 adsorption. Moreover, it was found that the addition of Nd generally contributes to decrease the basicity of the supports, which when doped are mainly characterized by the presence of Lewis basic sites of weak strength (T < 200 °C) [54, 55]. Nd_2O_3 is more basic than CeO_2 and ZrO_2 [56] therefore, this change could be related to the surface vacancies introduced through the structural doping. In comparison to original support materials (without Ni) (Fig 5.9 A) Ni impregnation increases strong basic sites as inferred by the presence of an additional peak at higher temperature (between 500-630°C). It is interesting to observe that the intensity and the position of this additional peak was changing with the composition of the support.

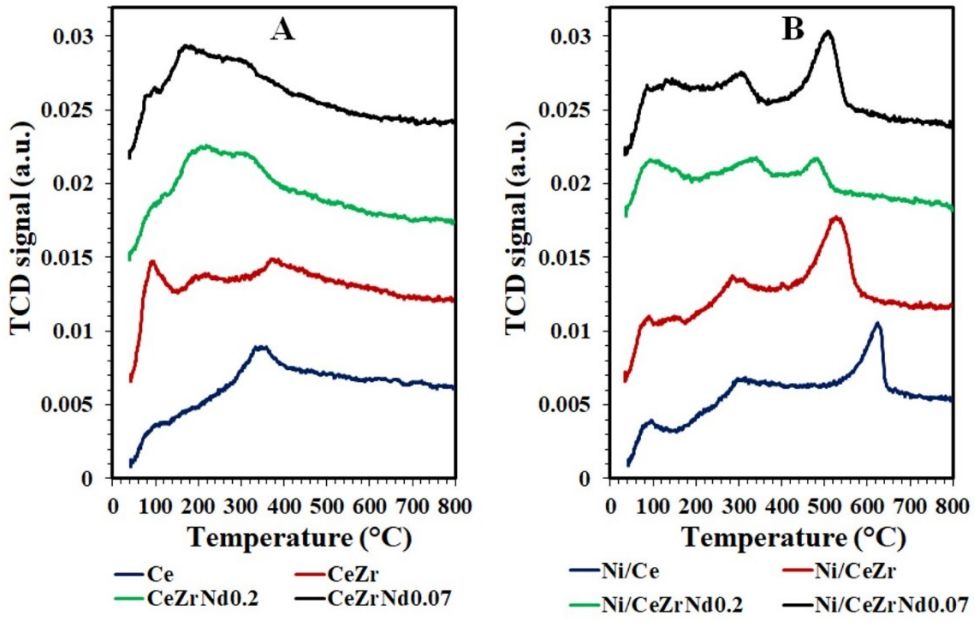

Figure 5.9. Comparison of CO_2-TPD of Ce, CeZr, $CeZrNd_{0.2}$ and $CeZrNd_{0.07}$ samples with and without nickel: (A) after calcination at 800°C, (B) after impregnation of Ni and calcination at 800°C.

The doping of ceria with Zr or Nd shifts the peak position at temperature lower than 600 °C and in Nd doped catalysts the peak intensity is related to the amount of Nd. It was observed that a large amount of neodymium contributes to create on the surface of catalysts a higher amount of mild strength Lewis basic sites (T ≈ 300 °C).

The CO_2 desorption experiments were also conducted for Ce, CeZr, $CeZrNd_{0.2}$ and $CeZrNd_{0.07}$ supports along with Ni catalysts at same surface area and results are illustrated in Figure 5.10 (A, B). By comparing the CO_2-TPD at different and same surface area, no remarkable difference was observed for the basic properties of supports or Ni catalysts.

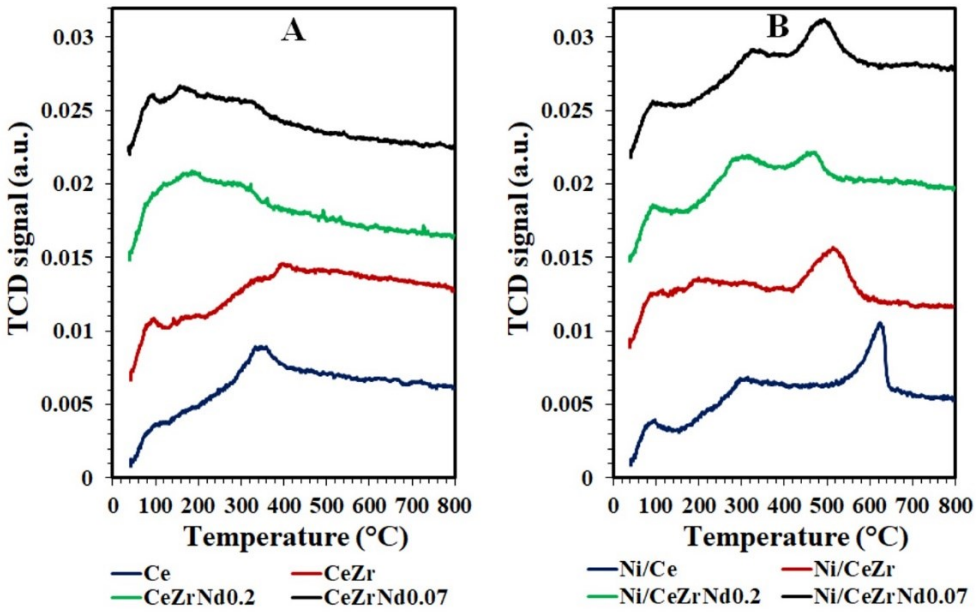

Figure 5.10. Comparison of CO_2-TPD of Ce, CeZr, $CeZrNd_{0.2}$ and $CeZrNd_{0.07}$ samples with and without nickel: (A) after calcination at different temperatures (800-1030ºC), (B) after impregnation of Ni and calcination at 800°C.

5.1.5. CO-chemisorption

Metal dispersion is an important characteristic of metal catalysts which can be defined as the fraction of active phase atoms present on the surface of support materials**.** The chemisorption using hydrogen or carbon monoxide is the most widespread technique to measure dispersion, reported in many investigations because it can be carried out

easily using simple apparatus (a detailed discussion of the method is already reported in chapter 4) [26, 27].

The metal dispersion (Table 5) was estimated on reduced samples by CO chemisorption measurements.

Table 5. Metal dispersion on Ni supported Ce, CeZr, $CeZrNd_{0.2}$ and $CeZrNd_{0.07}$ catalysts at different calcination temperatures.

Composition	Name	Temp/Time Calcination (°C/h)	Dispersion (%)
Ni/CeO_2	Ni/Ce	800/3	0.59
$Ni/Ce_{0.80}Zr_{0.20}O_2$	Ni/CeZr	800/3	1.08
$Ni/Ce_{0.80}Zr_{0.20}O_2$	Ni/CeZr_950	950/3	1.58
$Ni/Ce_{0.64}Zr_{0.16}Nd_{0.2}O_{1.9}$	$Ni/CeZrNd_{0.2}$	800/3	1.28
$Ni/Ce_{0.64}Zr_{0.16}Nd_{0.2}O_{1.9}$	$Ni/CeZrNd_{0.2}$_990	990/3	1.44
$Ni/Ce_{0.80}Zr_{0.13}Nd_{0.07}O_{1.96}$	$Ni/CeZrNd_{0.07}$	800/3	1.56
$Ni/Ce_{0.80}Zr_{0.13}Nd_{0.07}O_{1.96}$	$Ni/CeZrNd_{0.07}$_1030	1030/3	1.93

It is clear (Table 5) that the dispersion percent is low which could be due to the strong interaction of Ni crystallites with the support. Because of this interaction the surface electronic density of Ni particles can change affecting the chemisorption of CO. Moreover, the use of a surfactant during the synthesis of the supports leads to the formations of a large fraction of micropores where a part of NiO particles could be encapsulated and not any more accessible [7]. In fact, CeZr supports are formed by small crystallites rich in surface defects able to stabilize Ni precursors, and thus hindering Ni crystallites growth [6]. Moreover, the metal dispersion is higher when CeZr/CeZrNd compositions are calcined above 800°C. This means that CeZr oxides require temperatures above 800°C to stabilize their morphological and textural properties, i.e. to close the residual microporosity and to obtain large pores suitable for a more homogeneous Ni distribution [1, 7, 26]. The filling of pores with the metal causes a decrease of surface area of catalysts that depends on their composition and their thermal

history. Among all catalysts, the higher metal dispersion was observed for $Ni/CeZrNd_{0.07}$ calcined at 1030ºC temperature. The chemisorption values cited in literature are comparable with our study [7, 28, 29, 57].

5.1.6. Catalytic tests

The catalytic tests were carried out with a 0.66 CO_2/CH_4 ratio in the temperature range of 550-750ºC.

5.1.6.1.1. Effect of temperature

Figure 5.11 presents the CH_4 conv % (A), CO_2 conv % (B) and H_2/CO ratio (C) of Ni/Ce, Ni/CeZr, $Ni/CeZrNd_{0.2}$ and $Ni/CeZrNd_{0.07}$ catalysts (at different surface area) with 3.5% Ni in the temperature range of 550-750ºC. The obtained results show that the overall conversion percent of CH_4 and CO_2 is increasing with the increase of reaction temperature. The higher CO_2 conversion reveals that the DRM reaction is influenced by reverse water gas shift reaction (RWGS) [4]. Furthermore, RWGS reaction is favored at low temperature (<700ºC) and CO_2 can easily react with H_2 to give CO. The consumption of H_2 production due to RWGS resulted in H_2/CO product ratio less than unity [46]. It should be noted that H_2/CO product ratio is also increasing with the increase of reaction temperature from 550-750ºC [30, 31]. It was noted (Figure 5.11) that the catalytic activity of all catalysts shows minor activity towards CH_4 conversion, which was below the thermodynamic value in the entire range (550 to 750°C) of temperature. On the other hand, CO_2 conversion was found to be higher and reached the thermodynamic value for $Ni/CeZrNd_{0.07}$ at 750°C. It was observed that, in comparison to pure ceria, Zr addition affects CH_4 and CO_2 conversion in the range of lower temperatures (550-650°C); on the contrary Nd doping slightly decreases CH_4 conversion, with little or no influence on CO_2 conversion. On the other hand, it seems that the presence of Nd improves both CH_4 and CO_2 conversion of $Ni/CeZrNd_{0.2}$ and $Ni/CeZrNd_{0.07}$ catalysts in the entire range of temperatures (550-750°C) investigated. This different behavior suggests that the dry reforming reaction in these catalysts is ruled by a bi-functional mechanism in which CO_2 is activated at the metal-support interface and the CH_4 on the surface of metal particles [48]. The higher CO_2 conversion expecially for $Ni/CeZrNd_{0.07}$ catalyst in comparison to Ni/CeZr catalyst suggested that Nd doping has significant effect on redox properties of support which in turn favors the reduction of

carbon deposition on the surface of catalysts by reverse Boudouard reaction ($CO_2 + C \rightarrow 2CO$) as indicated by CO_2-TPD results. Based on the catalytic results it was noted that RWGS is highly promoted for all catalysts especially at lower temperature (<700ºC), yielding to lower H_2/CO ratio (CO_2+H_2↔ CO + H_2O RWGS) [2, 30]. In addition, both the CO and H_2 yields increase with the increase of reaction temperatures and H_2 yield is lower than CO (Figure 5.12 (A, B)). In comparison to all tested catalysts the highest CO and H_2 yields (Figure 5.12 (A, B) were obtained for Ni/CeZrNd$_{0.07}$. This trend is due to the effect of RWGS reaction [47, 49].

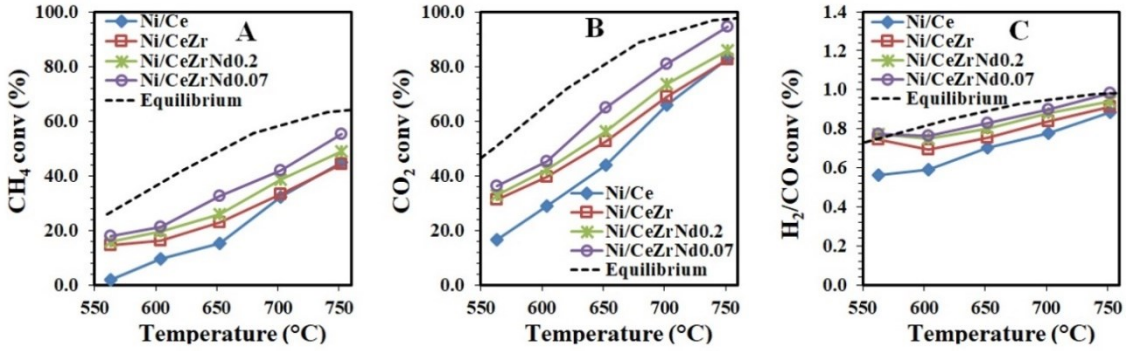

Figure 5.11. Effect of temperature on the catalytic activity of Ni/Ce, Ni/CeZr, Ni/CeZrNd$_{0.2}$ and Ni/CeZrNd$_{0.07}$ catalysts (at different surface area) with 3.5% Ni impregnation and 0.6 (CO_2/CH_4) molar ratio: (A) CH_4 conv (%), (B) CO_2 conv (%), (C) H_2/CO ratio.

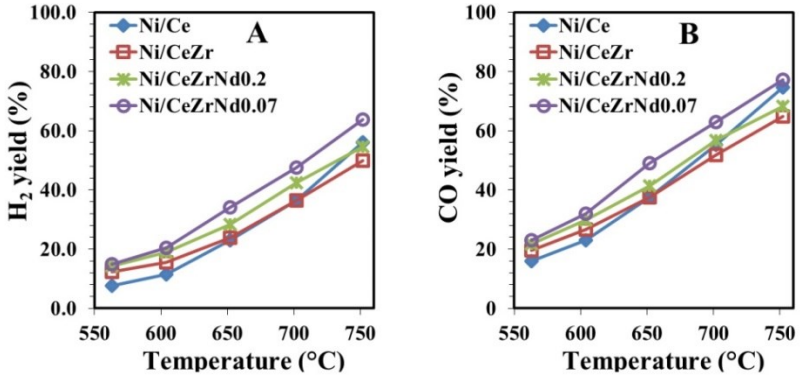

Figure 5.12. Effect of temperature on H_2 and CO yields of Ni/Ce, Ni/CeZr, Ni/CeZrNd$_{0.2}$ and Ni/CeZrNd$_{0.07}$ catalysts (at different surface area) with 3.5% Ni impregnation: (A) H_2 yield (%), (B) CO yield (%).

Moreover, among all tested catalysts, Ni/Ce catalyst has lower H_2/CO ratio due to the lower CO and H_2 yield while Ni/CeZrNd$_{0.07}$ has highest H_2/CO ratio (0.98) and reached the thermodynamic value (equilibrium) which seems to indicate that the co-presence of Zr and Nd inhibits the RWGS and thus increases the H_2/CO ratio and ultimately higher catalytic activity is obtained.

The catalytic tests were performed for Ni/CeZr, Ni/CeZrNd$_{0.2}$ and Ni/CeZrNd$_{0.07}$ catalysts at same surface area (20-25 m^2/g) in order to investigate how morphological properties influence the catalytic activity and results are illustrated in Figure 5.13 (A, B, C) and Figure 5.14 (A, B) . The comparative study at different surface area and at same surface area suggested that all catalysts showing same catalytic activity in term of CH_4 and CO_2 conversions which mean that higher calcination and lower surface properties did not affect the catalytic behaviour for DRM reaction. As indicated by BET and XRD results that the materials prepared by surfactant assisted method are more stable even at higher calcination temperature and low surface area did not affect the crystallinity of materials.

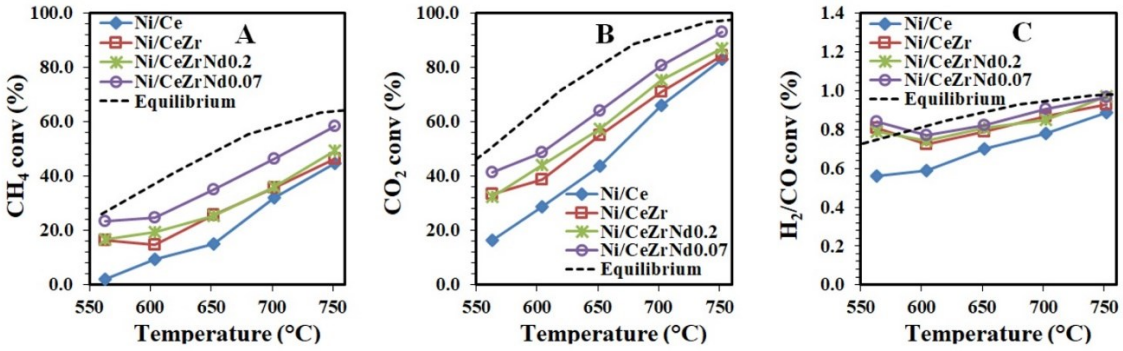

Figure 5.13. Effect of temperature on the catalytic activity of Ni/Ce, Ni/CeZr, Ni/CeZrNd$_{0.2}$ and Ni/CeZrNd$_{0.07}$ catalysts (at same surface area) with 3.5% Ni impregnation and 0.6 (CO_2/CH_4) molar ratio: (A) CH_4 conv (%), (B) CO_2 conv (%), (C) H_2/CO ratio.

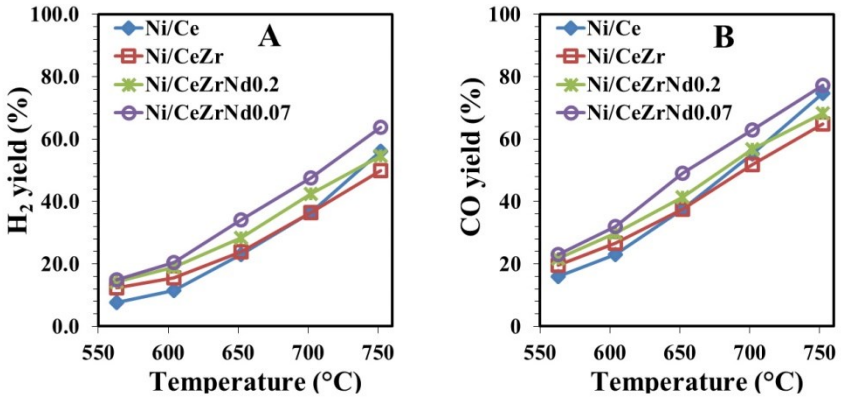

Figure 5.14. Effect of temperature on H_2 and CO yields of Ni/Ce, Ni/CeZr, Ni/CeZrNd$_{0.2}$ and Ni/CeZrNd$_{0.07}$ catalysts (at same surface area) with 3.5% Ni impregnation: (A) H_2 yield (%), (B) CO yield (%).

5.1.6.2. Effect of time

The reaction results for CH_4 and CO_2 conversions and H_2/CO ratio with time on stream (8 h) at 650ºC temperature were performed for Ni/Ce, Ni/CeZr, Ni/CeZrNd$_{0.2}$ and Ni/CeZrNd$_{0.07}$ catalysts (at different and same surface area) over 3.5% Ni impregnation and results are illustrated in Figure 5.15 (A, B, C) and Figure 5.16 (A, B, C). The conversion of CH_4 and CO_2 were measured in steady state conditions. In order to investigate the stability of catalysts towards carbon deposition, initially, Ni/CeZrNd$_{0.07}$ and Ni/ZrNd$_{0.2}$ catalysts were tested continuously at 650°C for 24 h and then for 8 h time on stream. By comparing the obtained results at different times on stream, both catalysts were found to be stable in term of CH_4, CO_2 and H_2/CO ratio. Therefore, it was decided to continue further investigation regarding stability of catalysts by considering 8 h time on stream. Figure 5.15 (A, B, C) and Figure 5.16 (A, B, C) demonstrate the stability of all catalysts during 8 hours of DRM reaction. Sokolov et al [58] found that mesoporous supports could resist the carbon formation due to strong interaction between Ni and mesoporous support and highly dispersed NiO species. As a result, Ni/La_2O_3-ZrO_2 mesoporous catalyst did not lose its activity and stability even for 180 h reaction time. These results indicate that mesoporosity, strong metal-support interaction and presence of active Ni particles favor the activity and stability of catalysts during DRM reaction [59-61].

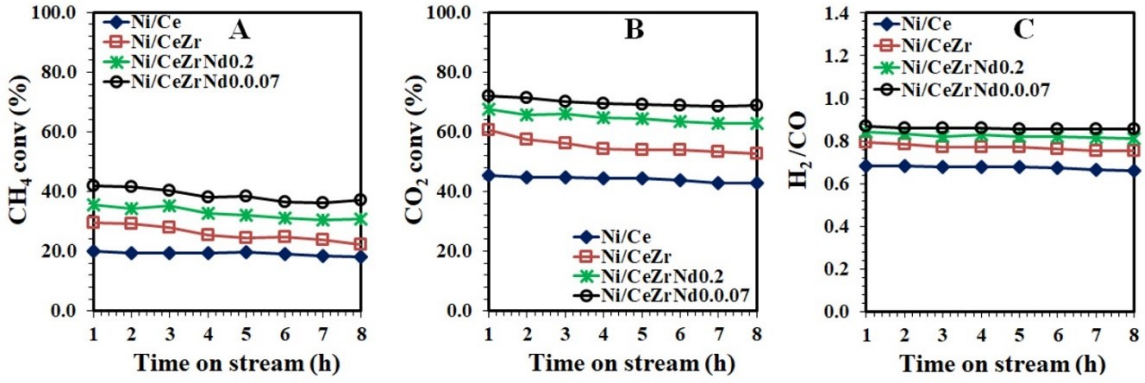

Figure 5.15. Effect of time on the catalytic activity of Ni/Ce, Ni/CeZr, Ni/CeZrNd$_{0.2}$ and Ni/CeZrNd$_{0.07}$ catalysts (at different surface area) with 3.5% Ni impregnation and 0.6 (CO_2/CH_4) molar ratio: (A) CH_4 conv (%), (B) CO_2 conv (%), (C) H_2/CO ratio.

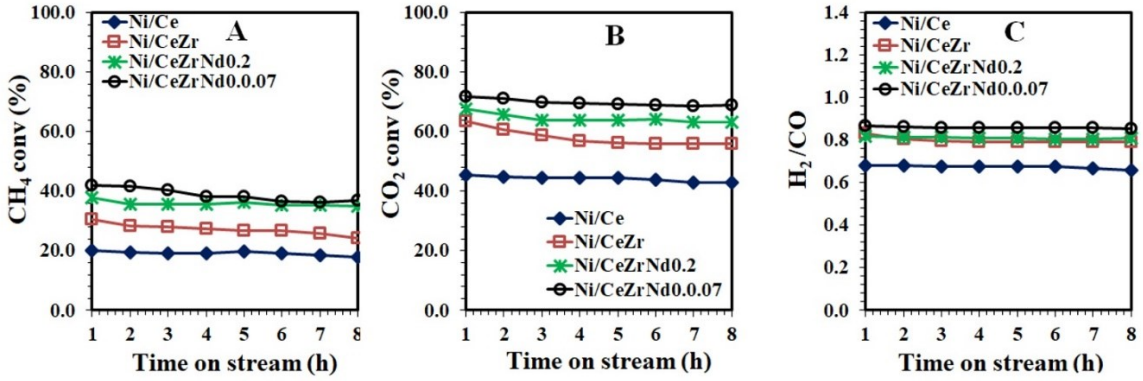

Figure 5.16. Effect of time on the catalytic activity of Ni/Ce, Ni/CeZr, Ni/CeZrNd$_{0.2}$ and Ni/CeZrNd$_{0.07}$ catalysts (at same surface area) with 3.5% Ni impregnation and 0.6 (CO_2/CH_4) molar ratio: (A) CH_4 conv (%), (B) CO_2 conv (%), (C) H_2/CO ratio.

5.1.7. Carbon formation

In order to investigate the deactivation processes related to carbon deposition, the Ni/Ce, Ni/CeZr, Ni/CeZrNd$_{0.2}$ and Ni/CeZrNd$_{0.07}$ catalysts (at different and same surface area) were tested continuously for 8 h at 650°C followed by quantification of the amount of carbon formed by thermogravimetric analysis under air and results are presented in

Figure 5.17 (A, B) and Table 6. The carbon accumulation is proportional to the activity of the catalysts and it occurs mainly in the first hours of testing (a 24 h test leads to an accumulation of 44 wt% of carbon on CeZrNd0.07_1030). The process is probably the main responsible of the deactivation observed in the first three hours of test, and it affects methane conversion more than CO_2 conversion. Despite the different amounts of carbon deposited, all the catalysts resulted to be stabilized with time (Figure 5.15 and 5.16) which suggests that the removal kinetics of carbon from the active sites is fast [2]. The initial hours are more important in order to observe the deactivation of catalysts and results are in good agreement with literature [6, 62]. It can be seen (Table 6) that the samples containing zirconium accumulate more carbon (27-37%) in comparison to ceria catalyst (22%). To further verify the carbon formation analyzed via TGA analysis, a more precise analytical technique of CHNS analysis was used for selected samples (Ni/CeZr, $Ni/CeZrNd_{0.2}$ and $Ni/CeZrNd_{0.07}$ catalysts calcined at 800ºC, after 8 h of testing at 650°C) and results are presented in Table 7. The results revealed that the carbon formation measured through CHNS analysis was 4-7% higher than that of TGA analysis. However, this difference could be acceptable because CHNS analysis is more precise and accurate compared to TGA analysis.

Table 6. Amount of carbon formation of exhausted Ni/Ce, Ni/CeZr, $Ni/CeZrNd_{0.2}$ and $Ni/CeZrNd_{0.07}$ catalysts after 8 h of testing at 650°C via TGA analysis.

Sample Name	Temp/Time Calcination (ºC)	Time on stream (h)	Carbon formed (%)
Ni/Ce	800/3h	8	22
Ni/CeZr	800/3h	8	27
Ni/CeZr	950/3h	8	31
$Ni/CeZrNd_{0.2}$	800/3h	8	30
$Ni/CeZrNd_{0.2}$	990/3h	8	27
$Ni/CeZrNd_{0.07}$	800/3h	8	37
$Ni/CeZrNd_{0.07}$	1030/3h	8	36

Table 7. Amount of carbon formation of exhausted Ni/CeZr, Ni/CeZrNd$_{0.2}$ and Ni/CeZrNd$_{0.07}$ catalysts after 8 h of testing at 650°C via CHNS analysis.

Sample Name	Temp/Time Calcination (°C)	Time on stream (h)	Carbon formed (%)
Ni/CeZr	800/3h	8	31
Ni/CeZrNd$_{0.2}$	800/3h	8	37
Ni/CeZrNd$_{0.07}$	800/3h	8	44

The TPO profile of Ce catalyst shows a tailed peak centered at 580°C, while two overlapped peaks, one at 450°C and the other at 580°C, characterize the profile of Ni/CeZr and Ni/CeZrNd$_{0.2}$. The TPO profiles of Ni/CeZrNd$_{0.07}$ catalysts with higher surface area showing two peaks, on at 450°C and other at 535°C while low surface area sample showing one broad and sharp peak centered at 530°C. The overall analysis showed that the gasification of carbon occurred between 450-580°C temperatures.

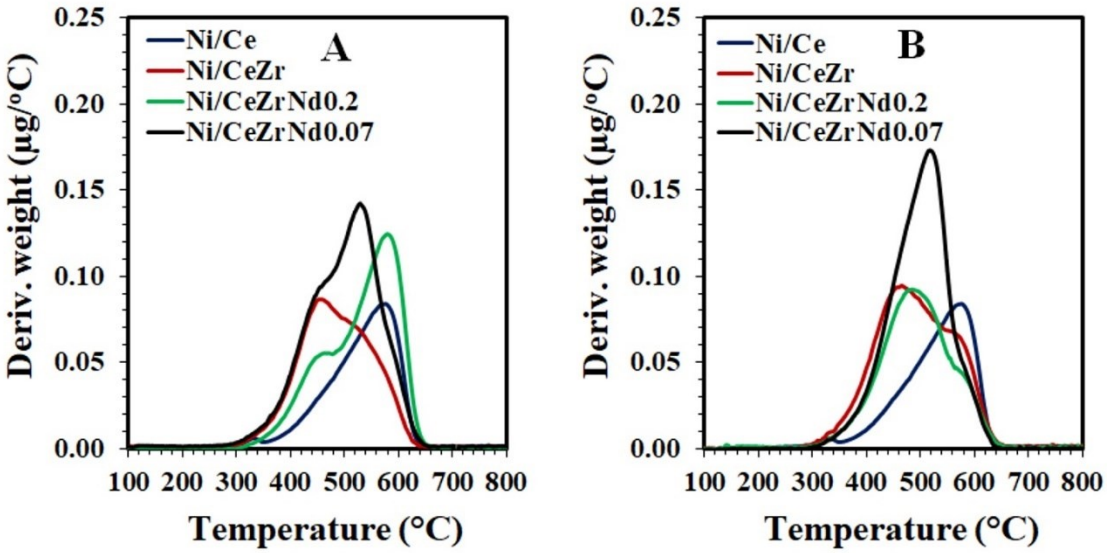

Figure 5.17. Thermogravimetric profiles of spent catalysts; Ni/Ce, Ni/CeZr, Ni/CeZrNd$_{0.2}$ and Ni/CeZrNd$_{0.07}$: (A) at different surface area and (B) at same surface area.

It is reported in literature that during DRM reaction over Ni based catalysts; different amount of carbon deposited onto the surface of catalysts which depends on the morphology, size and dispersion of Ni on the surface of support [2, 10, 11, 63-65]. There are several studies that categorize the type of carbon deposited on Ni based catalysts; Ni catalyzes the formation of whiskers and fibers of carbon, which can be oxidized above 500°C [66]. In the view of Makri et al (2016) work, large differences in DRM catalytic activity was observed for Ni supported on two differently prepared ceria-zirconia materials which could be also be explained by an effect of the different oxide compositions on the abundance of oxygen vacancies and on the participation of labile surface/subsurface lattice oxygen around the Ni particles, which may be a key for the removal of carbon near or at the metal support interface. It is inferred that in the investigated compositions the presence of Zr and/or Nd contributes to depress the formation of graphitic carbon in favor of less refractory forms of carbon [67]. This is correlated to a faster kinetics of oxidation as a consequence of doping. The doping with Zr and/or Nd increases oxygen exchange properties of ceria providing more labile lattice oxygen for the oxidation process. On the other hand, co-doping enhances the availability of surface oxidant species and the metal-support interaction, making feasible other paths for the removal of carbon. These results highlighted that the mesoporous support materials can stabilize active Ni particles and provide more accessible Ni active centers which ultimately increase the catalytic activity and stability during DRM reaction [58, 59, 61].

5.2. Discussion

Ni catalysts supported on ceria-zirconia (CeZr) mixed oxides doped with neodymium (Nd) have been synthesized via surfactant assisted co-precipitation method with surfactant/cation (S/C) ratio molar ratio of 0.25 and tested for DRM reaction in the temperature range of 550-750ºC. In order to understand better the effect of Nd doping along with zirconia, all physicochemical properties were studied by comparing ceria (CeO_2) support with undoped CeZr and CeZr mixed oxides doped with Nd. Furthermore, the catalysts were subjected to different calcinations temperatures (950ºC-1030ºC) to obtain the same surface area as CeO_2 support (22 m^2/g) to understand the effect of texture

properties on the catalytic activity of DRM reaction. BET results showed that addition of surfactant has a significant effect on textural properties. It was observed that the addition of surfactant led to an increase in the specific surface area and pore size distribution which shows high thermal stability of sample which remained stable at relatively high calcination temperatures (950^{o}C-1030^{o}C). Moreover, surfactant assisted method increases the fraction of pores maintaining the mesoporosity of samples which allow the higher Ni dispersion into the pores and shows positive effect towards dry reforming reaction. It was also observed that Nd doping affected the textural properties and crystallinity of CeO_2 causing a decrease of the dimension of crystallites from 298 Å to 178 Å and an increase of the pore volume. Opposite and less significant effects were observed for CeZr where the addition of Nd leads to a coalescence of crystallites and merging of the pores. XRD patterns of supports and catalysts exhibited the same behavior at lower and high surface areas which means that higher calcination temperature did not affect the structure and crystallinity. The small intensity of this peak suggests that NiO is well dispersed on the supports and seems to have no effect on the shape of support materials. TPR results showed that in comparison to CeZr, $CeZrNd_{0.2}$ and $CeZrNd_{0.07}$ compositions show lower degree of reduction of Ce^{4+} to Ce^{3+} which means that the addition of extra vacancies due to the presence of Nd^{3+} may lead to a high vacancies concentration, which in turns may aggregate in less mobile clusters and requires further investigations to be fully understood. Moreover, degree of reduction of $Ni/CeZrNd_{0.07}$ catalyst was found to be higher (83%) in comparison to Ni/CeZr and $Ni/CeZrNd_{0.2}$. After comparing TPR results at same surface area, a major difference in degree of reduction of $Ni/CeZrNd_{0.07}$ (56%) calcined catalyst was observed. This could be due to the agglomerations of Ni particles at higher calcination temperature. The strength of basic sites was investigated by CO_2-TPD analysis and revealed that Ni impregnation gives rise to strong basic sites (peak between 500-630°C), as compared to support materials. Moreover, it was found that the addition of Nd generally contributes to decrease the basicity of the supports, it is known that Nd_2O_3 is more basic than the CeO_2 and ZrO_2 therefore, this change could be related to the surface vacancies introduced through the structural doping. CO_2-TPD analysis also showed that the surface area (lower or higher) has no remarkable effect for the basic properties of supports and corresponding Ni catalysts. CO chemisorption measurements

were conducted to observe the metal dispersion (Ni) and it was observed that the overall metal dispersion is low for all tested catalysts which may be due to the higher stability of NiO particles deposited on support surface which results in the lower amount of metal migration towards active molecules or due to the to the formations of a large fraction of micropores where a part of NiO particles could be encapsulated and not any more accessible. Moreover, the metal dispersion was higher when CeZr/CeZrNd compositions were calcined at higher temperature (>800°C). This means that CeZr oxides require higher temperatures to stabilize their morphological and textural properties, i.e. to close the residual microporosity and to obtain large pores suitable for a more homogeneous Ni distribution. Among all catalysts, the higher metal dispersion was observed for $Ni/CeZrNd_{0.07}$ (1.93) calcined at 1030ºC temperature.

The DRM activity was tested with CO_2/CH_4 molar ratio of 0.6 (biogas composition) in the temperature range of 550-750ºC. It was observed that the catalytic activity of all catalysts showing minor activity towards CH_4 conversion (below the thermodynamic value) while CO_2 conversion was found to be higher in the entire range (550 to 750°C) and reached to the thermodynamic value in case of $Ni/CeZrNd_{0.07}$ catalyst at 750°C. The catalytic results showed that, in comparison to pure ceria, Zr addition increase the CH_4 and CO_2 conversion especially at lower temperature (< 700ºC) and the presence of Nd improves both the CH_4 and CO_2 conversion of $Ni/CeZrNd_{0.2}$ and $Ni/CeZrNd_{0.07}$ catalysts. Among all tested catalysts, Ni/Ce catalyst has lower H_2/CO ratio while $Ni/CeZrNd_{0.07}$ has highest H_2/CO ratio (≈ 1) and reached the thermodynamic value. This means that the co-presence of Zr and Nd inhibits the reverse water gas shift reaction and increase the H_2/CO ratio and ultimately higher catalytic activity is obtained.

Stability tests were carried out at 650ºC for 8 h to investigate the deactivation processes related to carbon deposition. It was observed that carbon accumulation is proportional to the activity of the catalysts and it occurs mainly in the first hours of testing. Despite the different amounts of carbon deposited, all the catalysts were found to be stable with time which suggested that the removal kinetics of carbon from the active sites is fast. The TPO showed that the gasification of carbon occurred between 450-580ºC which means that the presence of Zr and/or Nd contributes to depress the formation of

graphitic carbon, as Zr and/or Nd increases oxygen exchange properties of ceria providing more labile lattice oxygen for the oxidation process and the availability of surface oxidant species and the metal-support interaction, making feasible other paths for the removal of carbon. These results highlighted that the mesoporous support materials can stabilize active Ni particles and provide more accessible Ni active centers which ultimately increase the catalytic activity and stability during DRM reaction.

5.3. Conclusions

This study investigated for the first time the catalytic activities of Ni catalysts supported on CeO_2 and CeO_2-ZrO_2 mixed oxides doped with Nd for low temperature (600-800ºC) DRM reaction. Based on textural properties, it was observed that the addition of surfactant (lauric acid S/C=0.25) led to an increase in the specific surface area and pore size distribution and shows high thermal stability of sample. In order to compare the catalytic activity at different and same surface area, CeZr, $CeZrNd_{0.2}$ and $CeZrNd_{0.07}$ were subjected to high calcination temperature (950ºC-1030ºC) and were found to be stable. XRD analysis confirmed the presence of cubic fluorite type structure with fine crystallinity. The small intensity of NiO peak suggests that NiO is well dispersed on the supports and seems to have no effect on the crystal structure of support materials. Based on these results it was concluded that surfactant assisted method increases the fraction of pores maintaining the mesoporosity of samples which can stabilize the active Ni nanoparticles and provide more Ni active centers and hence enhance the catalytic activity towards DRM reaction. TPR results showed a strong metal-support interaction and the degree of reduction of $Ni/CeZrNd_{0.07}$ catalyst was found to be higher (83%) in comparison to Ni/CeZr and $Ni/CeZrNd_{0.2}$. After comparing TPR results at same surface area, a major difference in the degree of reduction of $Ni/CeZrNd_{0.07}$ (56%) catalysts was observed which could be due to the agglomeration of Ni particles at higher calcination temperature; therefore, further investigations are required to fully understand this phenomenon. CO_2-TPD analysis revealed that Ni impregnation leads to the formation of strong basic sites (peak between 500-630°C) which could improve the adsorption of acidic CO2 and provide more oxygen species for the removal of carbon formed as a result of CH4 decomposition and/or Boudouard reaction. CO chemisorption

measurements revealed higher metal dispersion when CeZr/CeZrNd compositions were calcined at higher temperature (>800°C). This means that CeZr oxides require higher temperatures to stabilize their morphological and textural properties, i.e. to close the residual microporosity and to obtain large pores suitable for a more homogeneous Ni distribution. Among all catalysts, the higher metal dispersion was observed for $Ni/CeZrNd_{0.07}$ (1.93) calcined at 1030°C temperature. The catalytic results showed that, in comparison to pure ceria, Zr addition increases the CH_4 and CO_2 conversion especially at lower temperature (<700°C) and the presence of Nd improves both the CH_4 and CO_2 conversion of $Ni/CeZrNd_{0.2}$ and $Ni/CeZrNd_{0.07}$ catalysts. Among all tested catalysts, Ni/Ce catalyst has lower H_2/CO ratio while $Ni/CeZrNd_{0.07}$ has highest H_2/CO ratio (≈ 1) and reached the thermodynamic value. This means that the co-presence of Zr and Nd inhibits the reverse water gas shift reaction and increase the H_2/CO ratio and ultimately higher catalytic activity is obtained. Despite the different amounts of carbon deposited, all catalysts were found to be stable during 8 hours time on stream which indicates that the presence of Zr and/or Nd contributes to depress the formation of graphitic carbon by increasing oxygen exchange properties of ceria which provide more labile lattice oxygen for the oxidation process. Based on these results it is concluded that mesoporosity of materials, strong metal-support interaction, presence of active Ni particles and availability of surface oxidant species favours the activity and stability of catalysts during DRM reaction.

Currently, actual mechanism of Nd doping onto CeZr materials is unclear because the effect of Nd as a dopant on CeO_2 and CeO_2-ZrO_2 materials investigated for the first time to study the catalytic activities of Ni catalysts for DRM reactions. Moreover, DRM is a complex process where main reaction ($CH_4 + CO_2 \rightarrow 2CO + 2H_2O$) is accompanied by other parallel-side reactions (reverse water gas reaction, Boudouard reaction and methane cracking) which can cause a decrease in the yield of products and the deactivation of catalysts due to the carbon deposition. Moreover, formation and removal of carbon species occur simultaneously. Therefore, in order to understand the effect of Nd on ceria and ceria-zirconia mixed oxide supports and their interaction with Ni, further investigation will be carried out by planning different experiments and characterization by using some advanced techniques such as Raman, FTIR, XPS etc.

Chapter No: 06

Results and Discussion

Comparison between $CeNd_{0.2}$ and $ZrNd_{0.2}$

Effect of Neodymium onto ceria (CeO_2) and zirconia (ZrO_2) supports for the development of Ni supported catalysts

6. Introduction

It has been demonstrated that Ni catalysts supported on ceria (Ni/CeO_2) and zirconia (Ni/ZrO_2) are active and exhibit good catalytic activity in term of DRM. The previous literature also reported that in comparison to CeO_2 and ZrO_2 supports, CeO_2-ZrO_2 mixed oxides leads to relatively higher activity and stability due to higher oxygen storage capacity, redox property and higher thermal stability [3, 12, 16, 22, 23, 46-52]. Therefore, in order to further enhance the catalytic activity of Ni/ZrO_2 as well as Ni/CeO_2, there is a need to improve the structural and physiochemical properties of CeO_2 and ZrO_2 supports. Recently, Pappecena et al [2] investigated for the first time the catalytic activities of Ni/CeO_2 and Ni/CeO_2-ZrO_2 doped with Nd in term of dry reforming of methane. They have concluded that co-doping of CeO_2 with Nd and Zr can possibly control the morphological and redox properties which in turn improve the catalytic activity of DRM reaction. Moreover, it was also observed that presence of Nd promotes the surface oxygen mobility of CeO_2 based materials which in turn supresses the carbon formation on catalyst surface making it more stable. Roh et al [49] investigated the effect of Ni/ZrO_2 catalysts for DRM and concluded that it has lower activity and deactivated with the time on stream. Naeem et al [11] observed that Ni/ZrO_2 synthesized via surfactant assisted method exhibited lower catalytic activity towards DRM in comparison to Ni/ZrO_2 catalyst synthesized via polyol process.

Based on literature and our previous knowledge [2], the main focus is to improve the ZrO_2 and CeO_2 support through Nd doping to unveil the morphological and redox properties for actual evaluation of the catalytic performance in term of DRM reaction. To the best of our knowledge, the doping of CeO_2 and ZrO_2 with Nd is here investigated for the first time and not reported in literature.

6.1. Results and discussions

6.1.1. BET surface area

The BET surface area, pore volume and pore size distribution of the supports prepared with a 0.25 S/C molar ratio, along with nickel (Ni) catalysts are summarized in Table 1 and Figure 6.1.

Table 1. BET surface area, pore volume and pore diameter of $CeNd_{0.2}$ and $ZrNd_{0.2}$, Ce, Zr and Nd with and without nickel at different calcination temperatures.

Compositions	Name	Temp/Time Calcination (°C)	Surface Area (m^2/g)	Pore Volume (cm^3/g)	Pore Diameter (Å)
$Ce_{0.8}Nd_{0.2}O_{1.9}$	$CeNd_{0.2}$	800/3h	25.3	0.22	279
$Ni/Ce_{0.8}Nd_{0.2}O_{1.9}$	$Ni/CeNd_{0.2}$	800/1h	18.9	0.195	307
$Zr_{0.8}Nd_{0.2}O_{1.9}$	$ZrNd_{0.2}$	800/3h	67.5	0.33	146
$Ni/Zr_{0.8}Nd_{0.2}O_{1.9}$	$Ni/ZrNd_{0.2}$	800/1h	53.8	0.29	160
$Zr_{0.8}Nd_{0.2}O_{1.9}$	$ZrNd_{0.2}$	1030/3h	25.2	0.17	208
$Ni/Zr_{0.8}Nd_{0.2}O_{1.9}$	$Ni/ZrNd_{0.2}$	800/1h	15.2	0.13	255
CeO_2	Ce	800/3h	22	0.195	295
Ni/CeO_2	Ni/Ce	800/1h	19	0.180	316
ZrO_2	Zr	800/3h	6.3	0.07	417
Ni/ZrO_2	Ni/Zr	800/1h	6.4	0.14	634
Nd_2O_3	Nd	800/3h	8.1	0.170	473
Ni/Nd_2O_3	Ni/Nd	800/1h	4.0	0.095	435

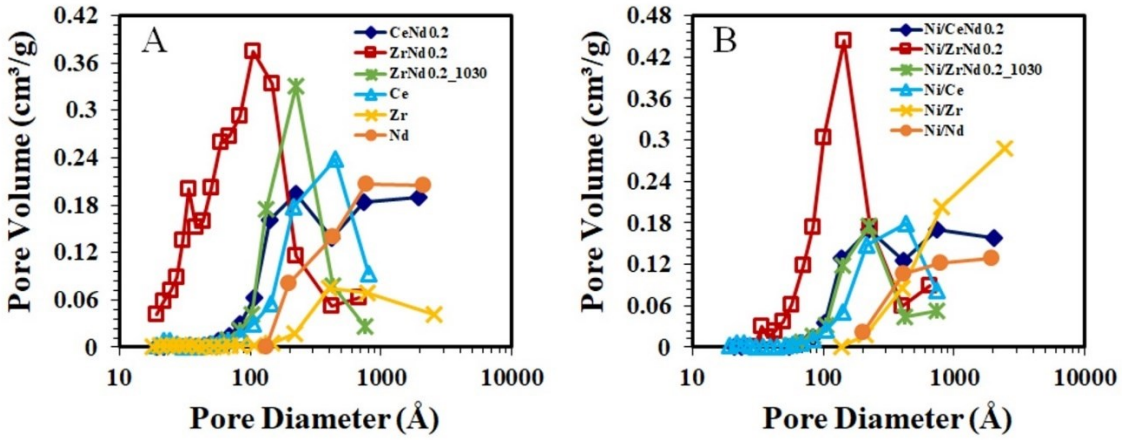

Figure 6.1. Comparison of pore size distribution of $CeNd_{0.2}$ and $ZrNd_{0.2}$, Ce, Zr and Nd samples with and without nickel: (A) after calcination at different temperatures, (B) after impregnation of Ni and calcination at 800°C.

BET surface area of ZrO_2 doped with Nd ($ZrNd_{0.2}$) was found to be higher (67.5 m^2/g) as compared to pure CeO_2 (22 m^2/g) and CeO_2 doped with Nd ($CeNd_{0.2}$ = 25.3 m^2/g) supports calcined at 800°C. On the other hand, 6.3 m^2/g and 8.1 m^2/g surface areas were obtained for ZrO_2 and Nd_2O_3 respectively which is very low. Furthermore, $ZrNd_{0.2}$ shows higher pore volume (0.3cm^3/g) in comparison to Ce and $CeNd_{0.2}$ (≈0.2 cm^3/g). Ni metal loading (3.5%) onto support materials leads to the significant decrease in the surface area [12]. It can be seen [Table 1] that the relative reduction of surface area with the loading of Ni metal did not affect the pore volume of Ni/Ce, Ni/$CeNd_{0.2}$ and Ni/$ZrNd_{0.2}$ catalysts compared to their pure supports [12, 48]. It is clear from obtained BET results (Table 1) that Nd doping has a higher effect on the morphological properties of ZrO_2 in comparison to CeO_2. In order to compare the effect of Nd doping on Ce and Zr supports and to understand better if structural properties can directly affect the catalytic activity, $ZrNd_{0.2}$ was subjected to higher calcinations temperature (1030°C) to get same BET surface area as Ce and $CeNd_{0.2}$ (20-25 m^2/g). All synthesized materials were found to be mesoporous (Figure 6.1) which shows that the surfactant assisted method maintains the mesoporosity of samples which allows higher Ni dispersion into the pores and shows positive effect towards dry reforming reaction (detailed discussion already explained in chapter 4) [1, 4, 6, 8-10]. Moreover, it was interesting to note that Nd doping increases the textural properties of Zr rather than Ce material. After Nd doping, a drastic increase in BET surface area of Zr from 6.3 m^2/g to 67.5 m^2/g was observed. Mustu et al [4] prepared ZrO_2 materials via surfactant assisted method and their observed pore volume and pore diameters values are lower compared to our reported values. Moreover, Roh et al [28] also reported that Ni/ZrO_2 catalysts prepared by co-precipitation method shows higher textural properties compared to impregnation method. Therefore, it is worthy to say that both surfactant assisted co-precipitation method of preparation and Nd doping strongly improve the textural properties of Zr-based material.

6.1.2. XRD

XRD analysis was carried out to understand the effect of Ce, Zr, Nd, $CeNd_{0.2}$ and $ZrNd_{0.2}$ materials on the phases and crystallinity with and without Ni impregnation, and results are shown in Figure 6.2 (A, B). It is confirmed from the diffractograms that oxides

of Ce and mixed oxides of $CeNd_{0.2}$ and $ZrNd_{0.2}$ (Figure 6.2 A) are cubic [11, 12, 49] whereas monoclinic and hexagonal phases were observed for Zr and Nd oxides, respectively. It was observed that the XRD profile of $CeNd_{0.2}$ is slightly shifted with respect to the undoped ceria phase confirming that Nd enters into the fluorite lattice (Figure 6.3). Ni (3.5%) was well dispersed and often not detectable (Figure 6.2 B). Furthermore, Ni impregnation on Ce and $CeNd_{0.2}$ showed a very small peak at $2\theta = 42.38$ degree (Figure 6.4) corresponding to (200) plane of cubic NiO which suggests that NiO is well dispersed on supports [4, 6, 12-14, 47]. Moreover, it was observed that due to Nd doping the monoclinic phase of Zr changed to cubic phase which showed that doping of Nd has a higher effect on the crystallinity of Zr material compared to Ce. These results are in good agreement with literature in which it is reported that Ni species are highly dispersed on cubic phase of support materials compared to other phase structures [4, 6, 14]. Furthermore, $Ni/ZrNd_{0.2}$ catalyst with higher and lower surface area i,e 53.8 m^2/g and 15.2 m^2/g respectively shows the same diffractograms without any minor and/major difference and Ni was well dispersed and not detectable.

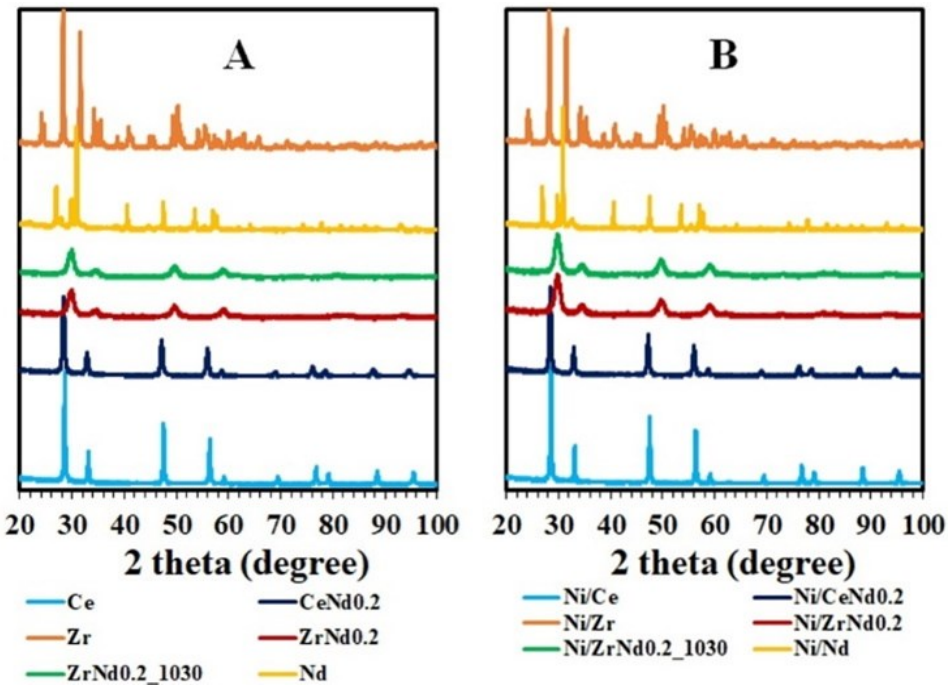

Figure 6.2. Comparison of XRD of Ce, Zr, Nd, $CeNd_{0.2}$ and $ZrNd_{0.2}$ samples with and without nickel: (A) after calcination at different temperature, (B) after impregnation of Ni and calcination at 800°C.

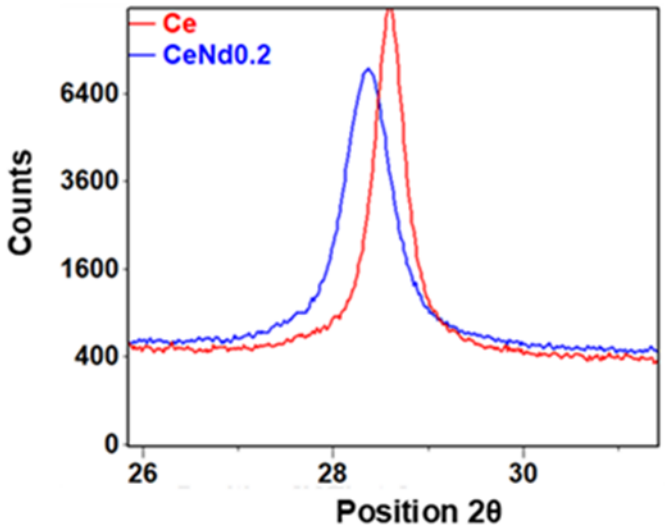

Figure 6.3. Details of comparison between Ce and $CeNd_{0.2}$ in the 2θ range between 24 and 32 degrees, showing the shift of the main peak due to the insertion of Nd into fluorite structure.

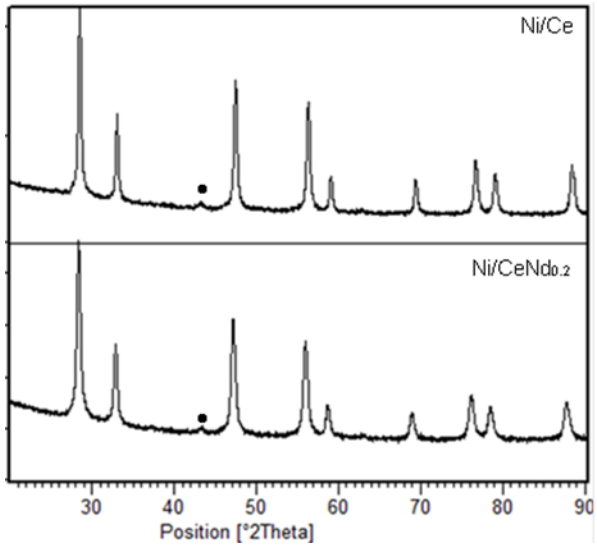

Figure 6.4. XRD patterns of Ni/support catalysts (Ni/Ce and $Ni/CeNd_{0.2}$); black dot indicates nickel phase.

After studying the morphological and textural properties, it was decided to continue further investigations by considering $CeNd_{0.2}$ and $ZrNd_{0.2}$ materials in order to explore the effect of Nd onto Ce and Zr supports.

6.1.3. TPR

The TPR patterns obtained from $CeNd_{0.2}$ and $ZrNd_{0.2}$ mixed oxides support prepared by surfactant assisted method with and without Ni impregnation are presented in Figure 6.5 (A, B). The TPR profile of $CeNd_{0.2}$ (Figure 6.5A) consisted of two broad peaks, the first peak at 300°C is attributed to surface reduction while the second peak around 700°C assigned to the bulk reduction of ceria [17, 18]. On the other hand, $ZrNd_{0.2}$ support is non-reducible. Figure 6.5B describes the TPR patterns of $Ni/CeNd_{0.2}$ and $Ni/ZrNd_{0.2}$ catalysts. In case of $Ni/CeNd_{0.2}$, the first and second peak located at 120°C and 250°C assigned to NiO reduction while the third peak around 350°C is ascribed to the reduction of NiO species strongly interacting with support. It is known that NiO can easily be reduced in the presence of ceria [22-25].

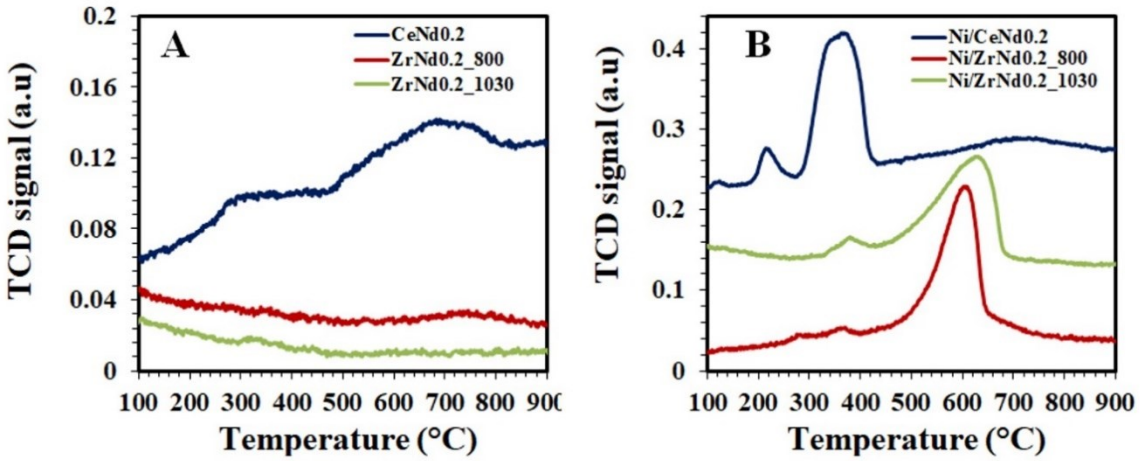

Figure 6.5. Comparison of TPR profiles of $ZrNd_{0.2}$ and $CeNd_{0.2}$ samples with and without nickel: (A) after calcination at different temperature, (B) after impregnation of Ni and calcination at 800°C.

On the other hand, $Ni/ZrNd_{0.2}$_800 (high surface area) shows a short peak around 370°C and one broad peak appeared at 615°C while $Ni/ZrNd_{0.2}$_1030 (low surface area) shows a short peak at 385°C and one broad peak at 650°C. The peaks at < 600°C can be assigned to free NiO species while the broad reduction peak of NiO species at higher temperature (<600°C) are attributed to the complex reduction of NiO and relatively strong interaction between Ni and $ZrNd_{0.2}$ support. Moreover, $Ni/ZrNd_{0.2}$_1030 at lower surface area (15.2 m^2/g) has shown almost the same TPR pattern in comparison to

$Ni/ZrNd_{0.2}$_800 with high surface area, which means that higher calcination temperature did not affect significantly the reduction behavior. The TPR profiles of $Ni/ZrNd_{0.2}$ catalysts showed the reduction peak at higher temperature (<600ºC) as compared to literature [28] which confirmed that Ni metal has strong interaction with $ZrNd_{0.2}$ support.

6.1.4. CO_2-TPD

CO_2-temperature programmed desorption (CO_2-TPD) experiments were conducted using CO_2 as a probe gas to investigate the strength of basic sited present in catalysts and the results are presented in Figure 6.6 (A, B).

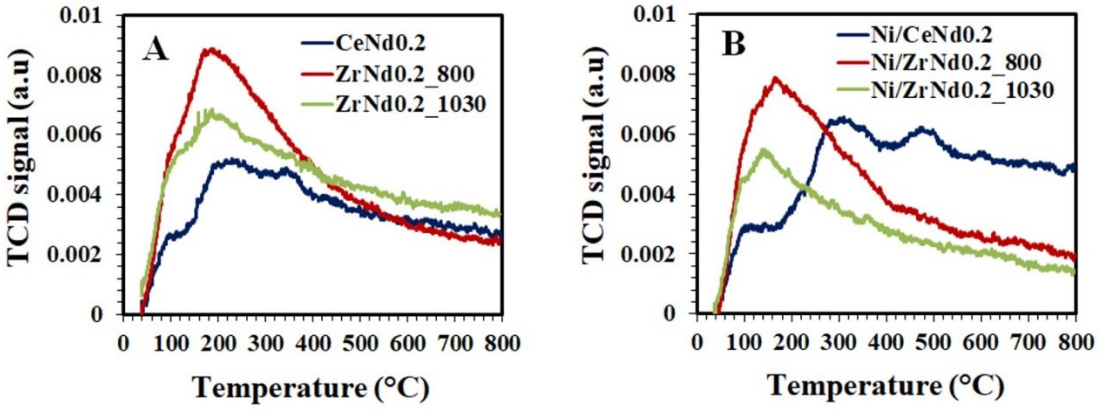

Figure 6.6. Comparison of CO_2-TPD profiles of $ZrNd_{0.2}$ and $CeNd_{0.2}$ samples with and without nickel: (A) after calcination at different temperature, (B) after impregnation of Ni and calcination at 800°C.

The strength of basic sites depends on the CO_2 adsorption peaks located at different temperatures [11, 68-70]. It is obvious from Figure 6.6A that the fresh supports provided the lowest basicity therefore, showing lowest CO_2 adsorption. On the other hand (Figure 6.6B) $Ni/CeNd_{0.2}$ shows two distinct peaks, one is around 308ºC which is related to intermediate (200-400ºC) while the second one at relatively higher temperature around 476ºC corresponds to strong (400-600ºC) basic sites while $Ni/ZrNd_{0.2}$ shows 1 broad peak at lower temperature around 163ºC which is related to the weak (50-200ºC) basic sites [70, 71]. $ZrNd_{0.2}$ with lower surface area (15.2 m^2/g) has shown the same CO_2-TPD profile with a broad peak at lower temperature (150ºC) which means that higher calcination temperature (1030ºC) has no effect on the strength of basic sites, but only on

the amount of CO_2 adsorbed/released. Based on CO_2-TPD results it was observed that in comparison to $Ni/CeNd_{0.2}$ (intermediate and strong basic sites) $Ni/ZrNd_{0.2}$ possess very weak basic sites which is not an appropriate property for DRM reaction. But it is important to note that the activity, stability and carbon resistance properties of DRM reaction do not depend only on the basic properties but also depends on other factors including metal support interaction, surface area, pore size distribution, metal dispersion and reduction behavior of catalysts [60, 72, 73].

6.1.5. CO pulse chemisorption

It is reported that the active metal dispersion is one of the important factors in order to improve the catalytic performance of materials during DRM reactions (a detailed discussion already explained in chapter 4 and 5) [26, 27]. Therefore, CO pulse chemisorption measurements were carried out to gain insight into the metal (Ni) dispersion onto $ZrNd_{0.2}$ and $CeNd_{0.2}$ support and results are presented in Table 2. It is clear that metal dispersion of $Ni/ZrNd_{0.2}$ and $Ni/CeNd_{0.2}$ is the same. In addition, a significant decrease was observed when $ZrNd_{0.2}$ was calcined at higher temperature (1030^{o}C). This means that $ZrNd_{0.2}$ oxides require temperatures around 800°C to stabilize their morphological and textural properties for a more homogeneous Ni distribution [1, 7, 26]. The chemisorption values cited in literature are comparable with our study [7, 28, 29, 57].

Table 2. Ni metal dispersion onto $CeNd_{0.2}$ and $ZrNd_{0.2}$ at different calcination temperatures.

Sample Name	Temp/Time Calcination (^{o}C)	Dispersion (%)
$Ni/CeNd_{0.2}$	800/3h	1.0
$Ni/ZrNd_{0.2}$	800/3h	0.95
$Ni/ZrNd_{0.2}$	1030/3h	0.71

6.1.6. Catalytic tests

6.1.6.1. Effect of temperature

The catalytic performance of Ni/CeNd$_{0.2}$, Ni/ZrNd$_{0.2}$, Ni/Ce, Ni/Zr and Ni/Nd catalysts in term of CO_2 and CH_4 conversion and H_2/CO product ratio at different temperatures (550-750ºC) is presented in Figure 6.7 (A, B, C).

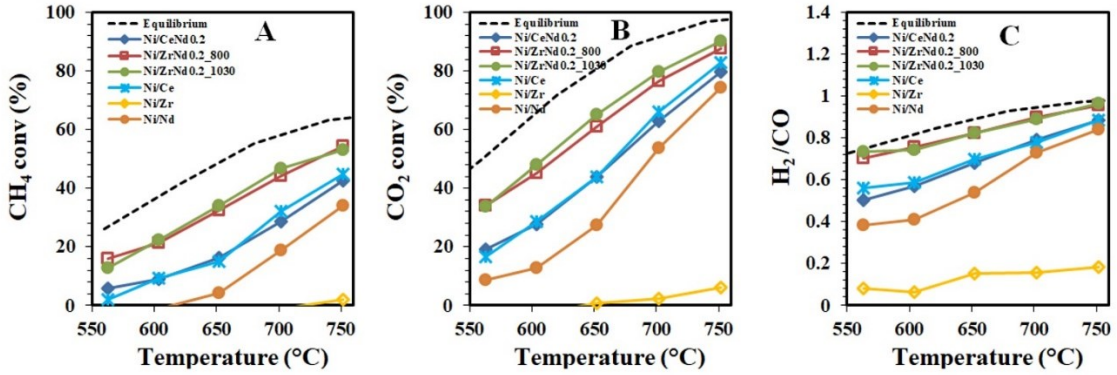

Figure 6.7. Effect of temperature on the catalytic activity of Ni/CeNd$_{0.2}$, Ni/ZrNd$_{0.2}$, Ni/Ce, Ni/Zr and Ni/Nd catalysts with 3.5% Ni impregnation and 0.6 (CO_2/CH_4) molar ratio: (A) CH_4 conv (%), (B) CO_2 conv (%), (C) H_2/CO ratio.

The overall conversion percent of CO_2 was found to be higher than CH_4 conversion due to the occurrence of RWGS [4]. A detailed investigation was already reported in chapter 4 and chapter 5. The results show that Ni/Ce and Ni/CeNd$_{0.2}$ have the same catalytic activity while Ni/ZrNd$_{0.2}$ shows higher efficiencies in term of CO_2 and CH_4 conversion and higher H_2/CO (≈1) product ratio, and reaches the thermodynamic value at temperature >700°C. Furthermore, Ni/Nd shows very low catalytic activity at lower temperature (< 650ºC). On the other hand, compared to all tested catalysts Ni/Zr showed no catalytic activity. It was also observed that Ni/ZrNd$_{0.2}$ shows the same catalytic activity at lower and higher surface area, which means that texture properties did not affect the catalytic performances in term of DRM reaction. These results indicated that Nd doping strongly influence the catalytic activity of zirconia rather than ceria doped Nd and undoped Zr catalysts. The presence of Nd into Zr lattice inhibits the RWGS and thus increases the H_2/CO ratio and ultimately higher catalytic activity is obtained. Moreover, TPR results indicate that the metal/support interaction between Ni and ZrNd$_{0.2}$

is stronger than Ni and $CeNd_{0.2}$. $ZrNd_{0.2}$ support was subjected to higher calcination temperature (1030°C) and it shows higher thermal stability at very high calcination temperature (1030°C). XRD results also revealed that Nd doping has changed the monoclinic phase of Zr to cubic phase which indicates that the doping of Nd affects more the crystallinity of Zr material compared to Ce. Ni is better dispersed on cubic phase compared to other phase structures [4, 6, 14]. Furthermore, $ZrNd_{0.2}$ with higher and lower surface area i,e 53.8 m^2/g and 15.2 m^2/g respectively shows the same diffractograms without any minor and/major difference and Ni is well dispersed and often not detectable. Based on these results it is worthy to say that the higher metal support interaction and better stability associated with $ZrNd_{0.2}$ support is the reason of its higher catalytic activity.

6.1.6.2. Effect of time

The long-term tests over Ni/$ZrNd_{0.2}$ and Ni/$CeNd_{0.2}$ were conducted at 650°C for 8 h to determine their stabilities and results are presented in Figure 6.8 (A, B, C). A detailed discussion is already reported in chapter 5. It was noted that both catalysts, Ni/$ZrNd_{0.2}$ and Ni/$CeNd_{0.2}$ are stable and active during the course of reaction. The reason for the stabilities of catalysts might be Nd doping which can decrease the particle size of NiO and possibly eliminate the deposited carbon from the surface of catalysts and improve their stability for DRM reaction. Moreover, mesoporosity, strong metal-support interaction and presence of active Ni particles favor the activity and stability of catalysts during DRM reaction [2, 59-61].

During long term durability tests, it was observed that the conversion percent of CH_4 and CO_2 is higher at 650°C in comparison to the catalytic conversion observed during catalytic tests conducted at different temperatures (Figure 6.7(A, B, C)). Therefore, it was decided to start durability test from 550°C and then maintained at 650°C and results are presented in Figure 6.9 (A, B, C). Ni/$ZrNd_{0.2}$ catalyst was found to be more stable in comparison to Ni/$CeNd_{0.2}$. This means that in case Ni/$CeNd_{0.2}$, the carbon formation occurs during the initial hours at lower temperature which decrease the catalytic activity, while to conduct the catalytic experiment at higher temperature (>650°C) can possibly increase the catalytic performance in term of DRM reaction. The

initial hours are more important in order to observe the deactivation of catalysts and results are in good agreements with literature [6, 62].

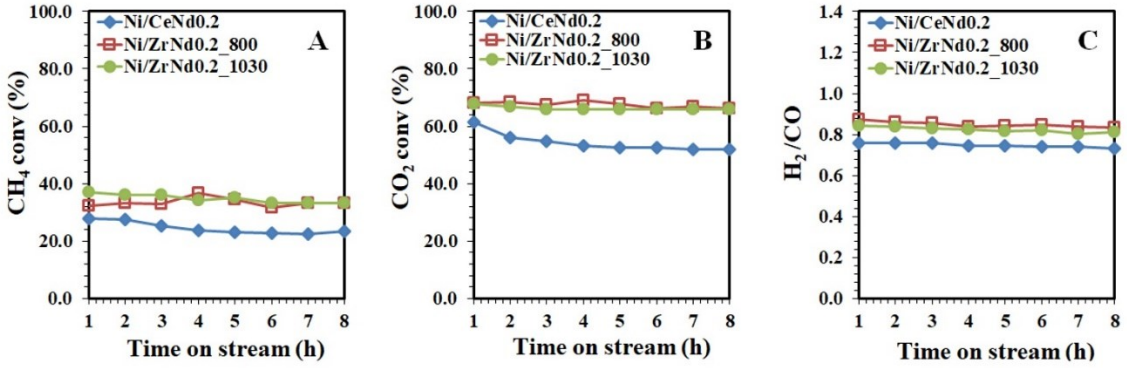

Figure 6.8. Effect of time on the catalytic activity of $Ni/CeNd_{0.2}$ and $Ni/ZrNd_{0.2}$ catalysts with 3.5% Ni impregnation, 0.6 (CO_2/CH_4) molar ratio at 650°C for 8 h: (A) CH_4 conv (%), (B) CO_2 conv (%), (C) H_2/CO ratio.

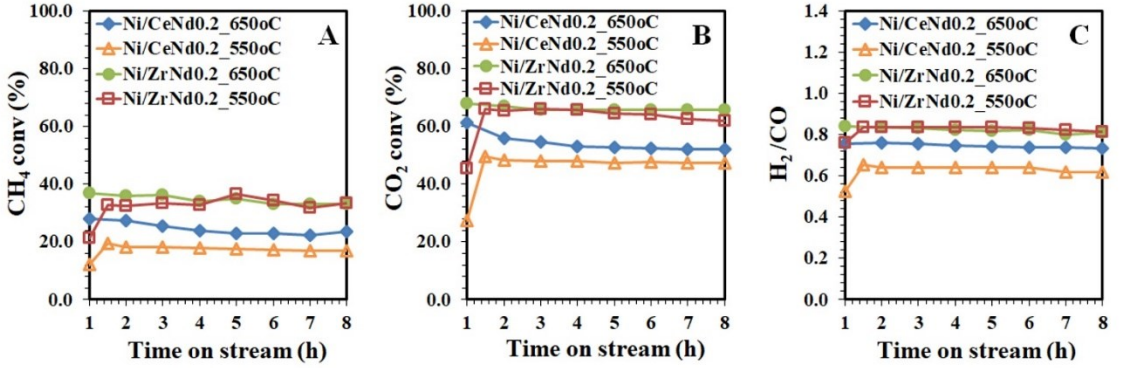

Figure 6.9. Effect of time on the catalytic activity of $Ni/CeNd_{0.2}$ and $Ni/ZrNd_{0.2}$ catalysts with 3.5% Ni impregnation, 0.6 (CO_2/CH_4) molar ratio at different temperatures (550-650°C) for 8 h: (A) CH_4 conv (%), (B) CO_2 conv (%), (C) H_2/CO ratio.

6.1.7. Carbon formation

The amount of carbon deposition over spent catalysts after 8 h TOS was investigated by TGA analysis and results are presented in Table 3 and Figure 6.10. It can be seen (Table 3) that Ni/ZrNd0.2_800, Ni/ZrNd0.2_1030 and Ni/CeNd0.2_800 catalysts have same carbon deposition while Ni/ZrNd0.2 has higher catalytic activity as compared

to $Ni/CeNd_{0.2}$. It is important to note that all catalysts show low carbon deposition (<20%) which indicates that Nd doping can possibly decrease the carbon deposition during DRM reaction [2].

Table 3. Amount of carbon formation of spent $Ni/CeNd_{0.2}$ and $Ni/ZrNd_{0.2}$ catalysts after 8 h of testing at 650°C via TGA analysis.

Sample Name	Temp/Time Calcination (°C)	Carbon Formed (%)
$Ni/CeNd_{0.2}$	800/3h	17
$Ni/ZrNd_{0.2}$	800/3h	19
$Ni/ZrNd_{0.2}$	1030/3h	18

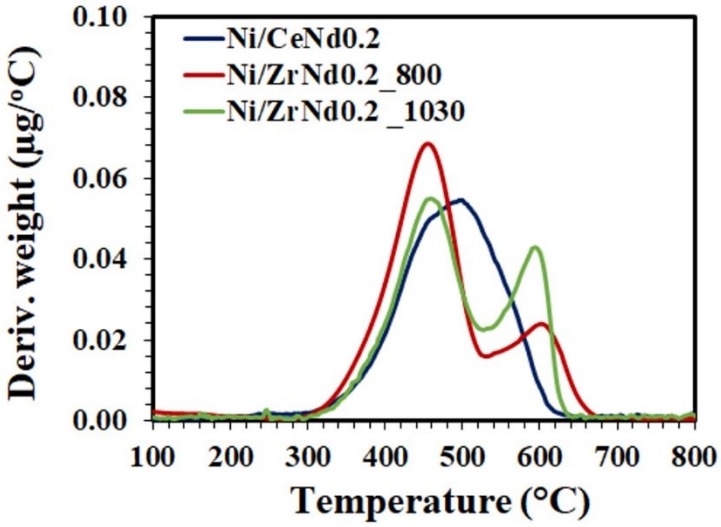

Figure 6.10. Thermogravimetric profiles of spent $Ni/CeNd_{0.2}$ and $Ni/ZrNd_{0.2}$ catalysts after 8 h of testing at 650 °C.

It is reported in literature that during DRM reaction over Ni based catalysts different amount of carbon deposited onto the surface of catalysts which depends on the morphology, size and dispersion of Ni on the surface of support [2, 10, 11, 63-65]. It is

known that methane is decomposed first on the active metal sites to produce reactive surface carbonaceous species which can be easily oxidized to CO by reacting with oxygen species which are produced from the dissociation of CO_2 [31]. On the other hand, the gasification of graphitic carbon involves relatively more effort due to the encapsulation of Ni particles. The TPO profile (Figure 6.10) of $Ni/CeNd_{0.2}$ catalyst shows a broad peak centered at 480°C, while in case of $Ni/ZrNd_{0.2}$_800 and $Ni/ZrNd_{0.2}$_1030 two peaks, one centered at 460°C and the other at 610°C were observed. Hence, the TPO analysis showed that the gasification of carbon occurred between 450-610ºC temperatures. Despite the different amounts of carbon deposited, all the catalysts resulted to be stabilized with time which suggests that the removal kinetics of carbon from the active sites is fast and initial hours are more important in order to observe the deactivation of catalysts [2, 6, 62].

6.1.7.1. SEM analysis

The carbon deposition was determined on spent $Ni/CeNd_{0.2}$ and $Ni/ZrNd_{0.2}$ catalysts using SEM analysis are presented in Figure 6.11 (A, B).

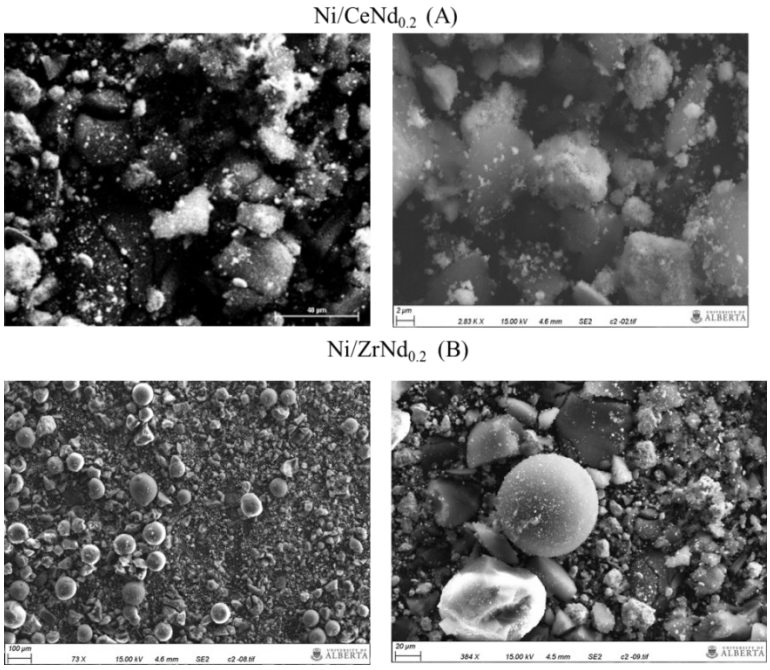

Figure 6.11. SEM images of spent $Ni/CeNd_{0.2}$ and $Ni/ZrNd_{0.2}$ catalysts after 24 h of testing at 800°C.

These images showed traces of carbon but no filamentous carbon existed on the surface of $Ni/CeNd_{0.2}$ and $Ni/ZrNd_{0.2}$ catalysts. SEM results showed that presence of Nd contributes to depress the formation of graphitic carbon in favor of less refractory forms of carbon [67]. The doping of Nd increases oxygen exchange properties providing more labile lattice oxygen for the oxidation process and the metal-support interaction, making feasible other paths for the removal of carbon.

6.1.8. Effect of nickel (Ni) loading

6.1.8.1 BET

The BET surface area, pore volume and pore size distribution of $CeNd_{0.2}$ and $ZrNd_{0.2}$ catalysts with different Ni loading are summarized in Table 4. It can be seen that all catalysts show almost the same BET surface ranging between 15-22 m^2/g. The purpose of the study is to observe the effect of Ni loading on the catalytic activity of $CeNd_{0.2}$ and $ZrNd_{0.2}$ catalysts at same surface area in term of DRM reaction. A detailed discussion and explanation already explained in chapter 4, 5 and in the section 6.1.1 of chapter 6.

Table 4. BET surface area, pore volume and pore diameter of $Ni/CeNd_{0.2}$ and $Ni/ZrNd_{0.2}$ catalysts with different Ni percentages (1%, 3.5% and 7%).

		Temp/Time	Surface Area	Pore Volume	Pore Diameter
Compositions	**Name**	**Calcination (°C)**	**(m^2/g)**	**(cm^3/g)**	**(Å)**
$Ce_{0.8}Nd_{0.2}O_{1.9}$	$CeNd_{0.2}$	800/3h	25.3	0.22	279
$1\%Ni/Ce_{0.8}Nd_{0.2}O_{1.9}$	$1\%Ni/CeNd_{0.2}$	800/1h	16.7	0.126	290
$3.5\%Ni/Ce_{0.8}Nd_{0.2}O_{1.9}$	$3.5\%Ni/CeNd_{0.2}$	800/1h	18.9	0.195	307
$7\%Ni/Ce_{0.8}Nd_{0.2}O_{1.9}$	$7\%Ni/CeNd_{0.2}$	800/1h	15.48	0.22	407
$Zr_{0.8}Nd_{0.2}O_{1.9}$	$ZrNd_{0.2}$	1030/3h	25.2	0.177	208
$1\%Ni/Zr_{0.8}Nd_{0.2}O_{1.9}$	$1\%Ni/ZrNd_{0.2}$	1030/1h	22.3	0.169	219
$3.5\%Ni/Zr_{0.8}Nd_{0.2}O_{1.9}$	$3.5\%Ni/ZrNd_{0.2}$	1030/1h	15.2	0.13	255
$7\%Ni/Zr_{0.8}Nd_{0.2}O_{1.9}$	$7\%Ni/ZrNd_{0.2}$	1030/1h	20.4	0.23	295

6.1.8.2. XRD

XRD analysis of Ni/$CeNd_{0.2}$ and Ni/$ZrNd_{0.2}$ (impregnation with 7% Ni) confirmed that the spectra of both catalysts exhibited a clear peak at 2θ = 43.28 degrees (Figure 6.12) corresponding to the (200) plane of cubic nickel oxide. A detailed discussion and explanation already explained in chapter 4, 5 and in the section 6.1.2 of chapter 6.

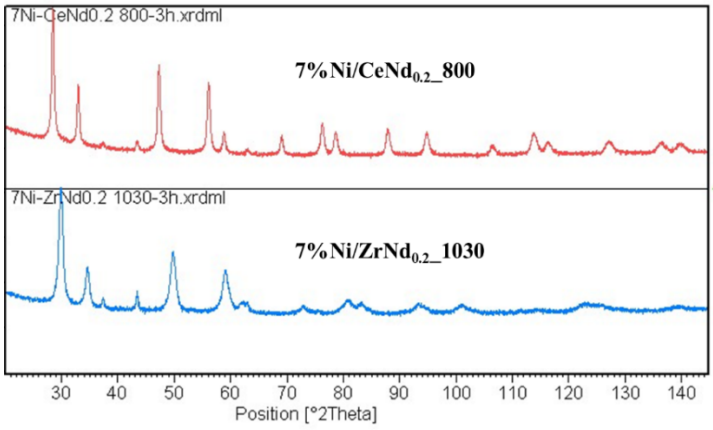

Figure 6.12. XRD patterns of $CeNd_{0.2}$ and $ZrNd_{0.2}$ at same surface area with 7%Ni impregnation.

6.1.8.3. TPR

The TPR patterns of $CeNd_{0.2}$ and $ZrNd_{0.2}$ supports with different percentages of Ni loading are presented in Figure 6.13.

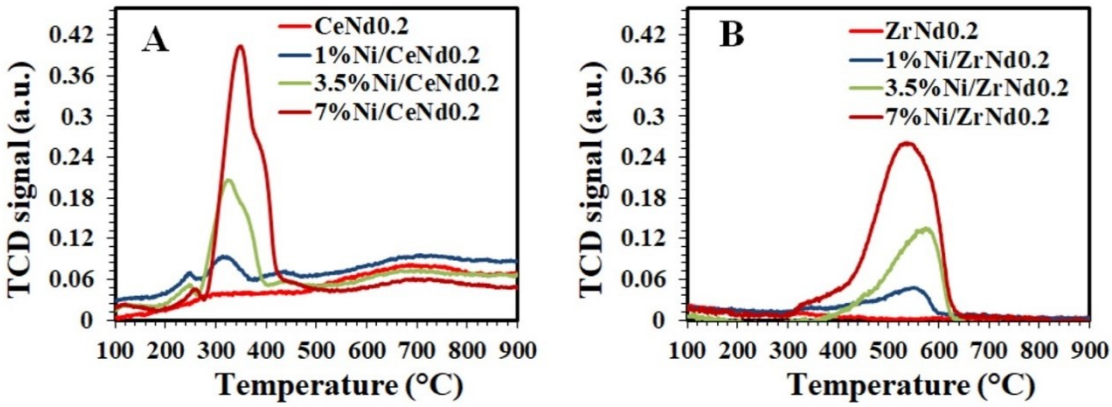

Figure 6.13. Comparison of TPR profiles at same surface area with different Ni percentages (1%, 3.5% and 7%): (A) $CeNd_{0.2}$ and (B) $ZrNd_{0.2}$.

A detailed explanation regarding TPR spectra of $CeNd_{0.2}$ and $ZrNd_{0.2}$ supports along with Ni catalysts is already described in section 6.1.3. Figure 6.13 shows that peak intensities increase with increasing Ni loading from 1-7%.

6.1.8.4. CO pulse chemisorption

CO pulse chemisorption measurements were carried out to investigate the effect of metal (Ni) dispersion on $ZrNd_{0.2}$ and $CeNd_{0.2}$ catalysts with different percentages of Ni loading (1%, 3.5% and 7%) and results are presented in Table 5. A detailed discussion and explanation already explained in chapter 4, 5 and in the section 6.1.5 of chapter 6. It can be seen (Table 5) that both $Ni/CeNd_{0.2}$ and $Ni/ZrNd_{0.2}$ with 3.5% of Ni loading showing high metal dispersion in comparison to 1% and 7%. This means that 1% is a small amount of Ni for impregnation while higher Ni loading (7%) blocking the active sites of support. Radlik et al (2015) [74] reported that in case of 2-4% of Ni loading, NiO crystallites were completely reduced to Ni^0 which cause the higher dispersion of small Ni crystallites on the surface of support. On the other hand, with higher Ni loading (10%), large Ni particles formed due to the formation of NiO agglomerates which ultimately decrease the active sites due to the blockage of pores.

Table 5. Comparison of Ni dispersion on $CeNd_{0.2}$ and $ZrNd_{0.2}$ catalysts with different Ni percentages: 1%, 3.5% and 7%.

Sample Name	Ni loading (%)	Temp/Time Calcination (°C)	Dispersion (%)
$Ni/CeNd_{0.2}$	1	800/3h	0.17
$Ni/CeNd_{0.2}$	3.5	800/3h	1.0
$Ni/CeNd_{0.2}$	7	800/3h	0.42
$Ni/ZrNd_{0.2}$	1	1030/3h	0.26
$Ni/ZrNd_{0.2}$	3.5	1030/3h	0.71
$Ni/ZrNd_{0.2}$	7	800/3h	0.52
$Ni/ZrNd_{0.2}$	7	1030/3h	0.59

6.1.8.5. Catalytic test

6.1.8.5.1 Effect of temperature

In order to optimize the best percentage of Ni loading onto the support materials, the DRM reaction was carried out with Ni/ZrNd$_{0.2}$ and Ni/CeNd$_{0.2}$ catalysts and results are presented in Figure 6.14 (A, B, C) and Figure 6.15 (A, B, C).

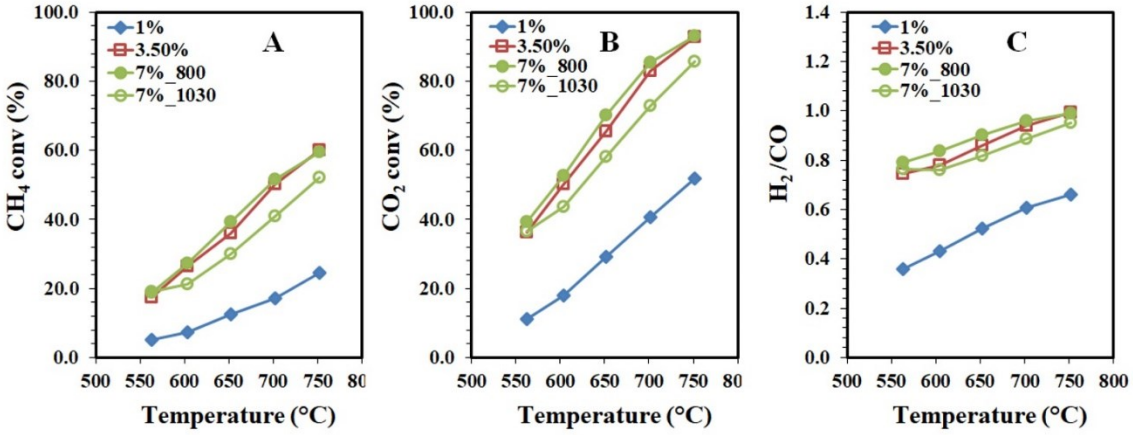

Figure 6.14. Comparison of catalytic tests of Ni/ZrNd$_{0.2}$ catalyst with different Ni percentages (1%, 3.5% and 7%): (A) CH_4 conv (%), (B) CO_2 conv (%), (C) H_2/CO ratio.

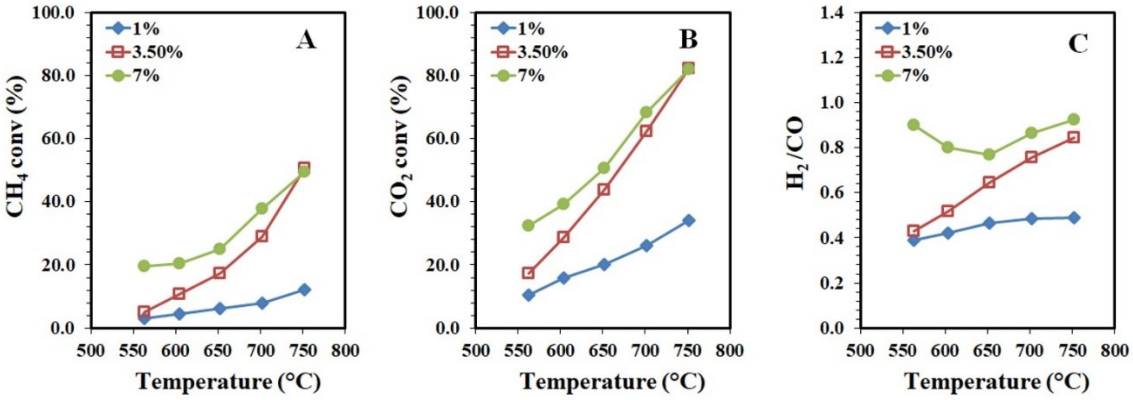

Figure 6.15. Comparison of catalytic tests of Ni/CeNd$_{0.2}$ catalyst with different Ni percentages (1%, 3.5% and 7%): (A) CH_4 conv (%), (B) CO_2 conv (%), (C) H_2/CO ratio.

It was observed that both CO_2 and CH_4 conversion increased with the increase of Ni loading from 1% up to 3.5%. At high surface area (53.8m^2/g) of Ni/$ZrNd_{0.2}$, the conversion efficiencies of CO_2 and CH_4 were found to be same at 3.5 % and 7% Ni loading while a decrease in conversion efficiencies was observed for Ni/$ZrNd_{0.2}$ at lower surface area (15.2 m^2/g) (Figure 6.14 (A, B, C). The lower catalytic activity of Ni/$ZrNd_{0.2}$_1030^oC could be due to the blockage of active sites due to higher Ni impregnation on lower surface area support [74]. On the other hand, the catalytic activity of Ni/$CeNd_{0.2}$ was found to increase with the increase of Ni loading from 1%-7% and the same catalytic activity was observed with 3.5% and 7% at 750^oC temperature Figure 6.15 (A, B, C). Moreover, both for Ni/$CeNd_{0.2}$ and Ni/$ZrNd_{0.2}$ catalysts, higher Ni loading (7%) terminated the catalytic reaction due to the blockage of reactor with large amount of carbon deposition.

Based on above results, it was concluded that 3.5% of Ni loading is a good percentage both for Ni/$CeNd_{0.2}$ and Ni/$ZrNd_{0.2}$ catalysts in term of DRM reaction. On the other hand, higher Ni loading decrease the catalytic activity due to the formation of large Ni clusters which cause serious carbon deposition [64, 75]. The large amount of carbon deposited on the inner wall of reactor around the catalyst bed clogged the reactor which ultimately terminates the experiment [74]. This is confirmed by TPO analysis of Ni/$CeNd_{0.2}$ and Ni/$ZrNd_{0.2}$ catalysts (7% Ni loading) where carbon deposition was found to be 49% and 37% respectively.

6.2. Discussion

The previous literature reported that in comparison to CeO_2 and ZrO_2 supports, CeO_2-ZrO_2 mixed oxides leads to relatively higher activity and stability due to higher oxygen storage capacity, redox property and higher thermal stability [3, 12, 16, 22, 23, 46-52]. Therefore, in order to further enhance the catalytic activity of Ni/ZrO_2 as well as Ni/CeO_2, there is a need to improve the structural and physiochemical properties of CeO_2 and ZrO_2 supports. It can be accomplished either by employing an appropriate surfactant during their synthesis or doping them with an effective dopant such as Nd. The application of surfactant may delay the precipitation of ceria/zirconia which in turn increases their surface area. Similarly, dopant may act as connecting bridge between the

molecules of support, yielding an extended surface area. Based on literature and our previous knowledge [2], the main focus is to improve the ZrO_2 and CeO_2 support through Nd doping to unveil the morphological and redox properties for actual evaluation of the catalytic performance in term of DRM reaction. Therefore, Ni catalysts supported on CeO_2 and ZrO_2 doped with neodymium (Nd) have been synthesized via surfactant assisted co-precipitation method with surfactant/cation (S/C) ratio molar ratio of 0.25 and tested for DRM reaction in the temperature range of 550-750^oC. In order to compare the effect of Nd doping on CeO_2 and ZrO_2 supports and to understand better if structural properties can directly affect the catalytic activity, $ZrNd_{0.2}$ was subjected to higher calcinations temperature (1030^oC) to get same BET surface area as $CeNd_{0.2}$ (25 m^2/g). This has been verified by BET results that the surface area of Zr and Nd is very low (6.3 m^2/g and 8.1 m^2/g respectively) while after doping of Zr with Nd it was observed that the surface area of $ZrNd_{0.2}$ is 67.5 m^2/g which is 11 times more than the surface of area of Zr. Moreover, all synthesized materials were found to be mesoporous which shows that the surfactant assisted method maintains the mesoporosity of samples which allow the higher Ni dispersion into the pores and shows positive effect towards dry reforming reaction. XRD results confirmed that oxides of $CeNd_{0.2}$ and $ZrNd_{0.2}$ are cubic and Ni impregnation on $CeNd_{0.2}$ showed a very small peak at $2\theta = 42.38$ degree corresponding to (200) plane of cubic NiO which suggests that NiO is well dispersed on supports Moreover, it was interesting to observe that after Nd doping, the monoclinic phase of Zr changed to cubic phase which is considered as suitable phase for better Ni dispersion. These results show that doping of Nd effects more the crystallinity of ZrO_2 material as compared to CeO_2. Furthermore, $ZrNd_{0.2}$ with higher and lower surface area i,e 53.8 m^2/g and 15.2 m^2/g respectively shows the same diffractograms without any minor and/major difference and Ni was well dispersed and not detectable which means that $Ni/ZrNd_{0.2}$ catalyst is stable even at high calcination temperature (1030^oC). TPR results indicated that Ni has strong affinity with $ZrNd_{0.2}$ support as compared to $CeNd_{0.2}$ because NiO reduces to Ni^0 at relatively high temperature (> 600^oC) which attributed to the complex reduction of NiO and relatively strong interaction between Ni and $ZrNd_{0.2}$ support. Moreover, $Ni/ZrNd_{0.2}$_1030 at lower surface area (15.2 m^2/g) has shown almost the same TPR pattern in comparison to $Ni/ZrNd_{0.2}$_800 with high surface area (53.8 m^2/g), which means

that higher calcination temperature did not affect the reduction behavior. Furthermore, CO_2-TPD results revealed that in comparison to Ni/$CeNd_{0.2}$ (intermediate and strong basic sites) Ni/$ZrNd_{0.2}$ possess very weak basic sites. CO pulse chemisorption results indicated that the Ni dispersion onto $ZrNd_{0.2}$ and $CeNd_{0.2}$ support is the same. In addition, a significant decrease was observed when $ZrNd_{0.2}$ was calcined at higher temperature (1030^{o}C). This means that $ZrNd_{0.2}$ oxides require temperatures above 800°C to stabilize their morphological and textural properties for a more homogeneous Ni distribution.

The catalytic results show that Ni/$ZrNd_{0.2}$ has higher CO_2 and CH_4 conversion with higher H_2/CO ratio (≈1) as compared to Ni/$CeNd_{0.2}$ whereas Ni/Ce and Ni/$CeNd_{0.2}$ show the same catalytic activity which is noticeable because both catalyst have similar physiochemical properties and therefore exhibit similar catalytic performance for DRM reaction. Carbon deposition was found almost the same on Ni/$ZrNd_{0.2}$ and Ni/$CeNd_{0.2}$ (19 and 17 wt% respectively) which means that removal kinetics for deposited carbon is fast and that could be one of the reasons for long term stability of both catalysts. It was also observed that at low temperature (<650^{o}C) more carbon accumulates on Ni/$CeNd_{0.2}$ compared to Ni/$ZrNd_{0.2}$ and this has been verified by performing long term durability test under two different conditions, and it was found that Ni/$ZrNd_{0.2}$ catalyst is more stable than Ni/$CeNd_{0.2}$. To investigate the effect of Ni loading, Ni/$ZrNd_{0.2}$ and Ni/$CeNd_{0.2}$ catalysts were studied by varying the Ni loading from 1-7%. It was observed that the best Ni percentage to impregnate $ZrNd_{0.2}$ and $CeNd_{0.2}$ supports is 3.5%. It was also observed that 1% is very low percentage to improve the catalytic activity of both catalysts in term of DRM reaction while at higher Ni percentage (7%) accumulates more carbon on the catalysts surface which can cause the blockage of reactor and decrease the catalytic performance especially at low temperature studies. This was confirmed by studying the long term stability tests with 7% of Ni impregnation and 49% and 37% carbon formation was observed over Ni/$CeNd_{0.2}$ and Ni/$ZrNd_{0.2}$ catalysts respectively. SEM analysis showed carbon deposition but no filamentous carbon was found on the surfaces of Ni/$CeNd_{0.2}$ and Ni/$ZrNd_{0.2}$ catalysts which mean that the doping of Nd increases oxygen exchange properties by providing more labile lattice oxygen for the oxidation process and the metal-support interaction making feasible other paths for the removal of carbon. In

order to understand the kinetic mechanism of $Ni/CeNd_{0.2}$ and $Ni/ZrNd_{0.2}$, DRIFT experiments were conducted under H_2 and CO_2 flow. The results showed the presence of carbonates on the surface of $Ni/CeNd_{0.2}$ while formats were formed in case of $Ni/ZrNd_{0.2}$. Based on DRIFT study it was concluded that in the presence of only carbonates and formats it is difficult to understand the actual kinetics of reaction (results did not presented in thesis because experiments are in progress). The comparison between $Ni/CeNd_{0.2}$ and $Ni/ZrNd_{0.2}$ has shown that Nd doping affects more strongly structural, textural and redox properties of zirconia rather than those of ceria. To understand better why $Ni/ZrNd_{0.2}$ showed higher activity in term of DRM, further investigation is needed which is in progress and soon will be published.

6.3. Conclusion

To the best of our knowledge, the doping of CeO_2 and ZrO_2 with Nd has been investigated for the first time to study the catalytic activities of Ni catalysts at low temperature (600-800^{o}C) for DRM reaction. Based on textural properties, it was observed that the addition of surfactant (lauric acid S/C=0.25) led to an increase in the specific surface area and pore size distribution and shows high thermal stability of synthesized sample. Both $CeNd_{0.2}$ and $ZrNd_{0.2}$ materials were found to be mesoporous which shows that the surfactant assisted method maintains the mesoporosity of samples which allow the higher Ni dispersion into the pores and shows positive effect towards dry reforming reaction. After Nd doping, a drastic increase in BET surface area of Zr from 6.3 m^2/g to 67.5 m^2/g was observed which is 11 times more than the surface of area of Zr. Moreover, $ZrNd_{0.2}$ was subjected to higher calcination temperature (1030^{o}C) and found to be stable. Therefore, it was concluded that Nd doping improves the textural properties of ZrO_2 rather than CeO_2 material. XRD results confirmed that oxides of $CeNd_{0.2}$ and $ZrNd_{0.2}$ are cubic and $Ni/CeNd_{0.2}$ catalyst showed a very small peak at 2θ = 42.38 degree corresponding to (200) plane of cubic NiO which suggests that NiO is well dispersed on supports. Moreover, it was interesting to observe that after Nd doping the monoclinic phase of Zr changed to cubic phase which is considered as suitable phase for better Ni dispersion compared to other phase structures. TPR results revealed that in comparison to $Ni/CeNd_{0.2}$ catalysts, $Ni/ZrNd_{0.2}$ showed a broad peak at higher temperature (>600^{o}C)

attributed to the complex reduction of NiO and relatively strong interaction between Ni and $ZrNd_{0.2}$ support. Moreover, Ni/$ZrNd_{0.2}$_1030 at lower surface area (15.2 m^2/g) has shown almost the same TPR pattern in comparison to Ni/$ZrNd_{0.2}$_800 with high surface area, which means that higher calcination temperature did not affect the reduction behavior. These results confirmed that Ni metal has strong interaction with $ZrNd_{0.2}$ support. CO_2-TPD results showed that in comparison to Ni/$CeNd_{0.2}$ (intermediate and strong basic sites) Ni/$ZrNd_{0.2}$ possess very weak basic sites which is not an appropriate property for DRM reaction. But, it is important to note that the activity, stability and carbon resistance properties of DRM reaction do not depend only on the basic properties but also depends on the other factors including metal support interaction, surface area, pore size distribution, metal dispersion and reduction behavior of catalysts. Moreover, metal dispersion of Ni/$ZrNd_{0.2}$ and Ni/$CeNd_{0.2}$ is similar but Ni/$ZrNd_{0.2}$ showed higher efficiencies in term of CO_2 and CH_4 conversion and higher H_2/CO (≈1) product ratio, reaches the thermodynamic value at temperature >700°C compared to Ni/$CeNd_{0.2}$. This seems to indicate that the presence of Nd into Zr lattice inhibits the RWGS and thus increases the H_2/CO ratio and ultimately higher catalytic activity is obtained. TPO analysis indicated that all catalysts show low carbon deposition (<20%). Despite the different amounts of carbon deposited, all the catalysts resulted to be stabilized with time which suggests that the removal kinetics of carbon from the active sites is fast. The reason for the stabilities of catalysts might be Nd doping which can decrease the particle size of NiO and possibly eliminate the deposited carbon from the surface of catalysts and improve their stability for DRM reaction. Among 1-7% Ni loading, 3.5% of Ni loading was found to be a good percentage both for Ni/$CeNd_{0.2}$ and Ni/$ZrNd_{0.2}$ catalysts in term of DRM reaction because higher Ni loading (7%) decrease the catalytic activity due to the formation of large Ni clusters which cause the serious carbon deposition. The large amount of carbon deposited on the inner wall of reactor around the catalyst bed clogged the reactor which ultimately terminates the experiment. Based on these results it is worthy to conclude mesoporosity, strong metal-support interaction, presence of active Ni particles and better stability associated with $ZrNd_{0.2}$ support is the reason for its higher catalytic activity. Therefore, it can be concluded that ZrO_2 support doped with Nd can be a valid strategy to enhance the activity of Ni and to balance the properties needed for the

simultaneous activation of CH_4 and CO_2 and for the development of a carbon resistant catalyst. $Ni/ZrNd_{0.2}$ has shown some distinct properties but exhibiting higher activity and low carbon deposition in term DRM reaction so its actual mechanism has to be verified to take advantage of this catalyst for many other industrial applications including fuel cell technology.

Future goals

Currently, the actual mechanism of Nd doping remains quite unclear because the effect of Nd as a dopant on CeO_2, ZrO_2 and CeO_2-ZrO_2 materials on the catalytic activity of Ni catalysts for DRM reaction would need further investigation. Moreover, DRM is a complex process where the main reaction ($CH_4 + CO_2 \rightarrow 2CO + 2H_2O$) is accompanied by other parallel-side reactions (reverse water gas reaction, Boudouard reaction and methane cracking) which can cause a decrease in the yield of products and the deactivation of catalysts due to the carbon deposition. In addition, formation and removal of carbon species occur simultaneously. Therefore, in order to understand the effect of Nd on CeO_2, ZrO_2 and CeO_2-ZrO_2 supports and their interaction with Ni, further investigation will be carried out by planning different experiments and characterization by using some advanced techniques such as Raman, FTIR, XPS etc and soon will be published.

References

1. Alvar, E.N. and M. Rezaei, *Mesoporous nanocrystalline MgAl2O4 spinel and its applications as support for Ni catalyst in dry reforming.* Scripta Materialia, 2009. **61**(2): p. 212-215.
2. Pappacena, A., et al., *The Role of Neodymium in the Optimization of a Ni/CeO2 and Ni/CeZrO2 Methane Dry Reforming Catalyst.* Inorganics, 2018. **6**(2): p. 39.
3. Kumar, P., Y. Sun, and R.O. Idem, *Nickel-based ceria, zirconia, and ceria–zirconia catalytic systems for low-temperature carbon dioxide reforming of methane.* Energy & Fuels, 2007. **21**(6): p. 3113-3123.
4. Mustu, H., et al., *Effect of synthesis route of mesoporous zirconia based Ni catalysts on coke minimization in conversion of biogas to synthesis gas.* International Journal of Hydrogen Energy, 2015. **40**(8): p. 3217-3228.
5. Pappacena, A., et al., *Development of a modified co-precipitation route for thermally resistant, high surface area ceria-zirconia based solid solutions*, in *Studies in Surface Science and Catalysis*2010, Elsevier. p. 835-838.
6. Wolfbeisser, A., et al., *Methane dry reforming over ceria-zirconia supported Ni catalysts.* Catalysis Today, 2016. **277**: p. 234-245.
7. Zhang, J. and F. Li, *Coke-resistant Ni@ SiO2 catalyst for dry reforming of methane.* Applied Catalysis B: Environmental, 2015. **176**: p. 513-521.
8. Rezaei, M., et al., *CO2 reforming of CH4 over nanocrystalline zirconia-supported nickel catalysts.* Applied Catalysis B: Environmental, 2008. **77**(3-4): p. 346-354.
9. Yang, W., et al., *CO2 reforming of methane to syngas over highly-stable Ni/SBA-15 catalysts prepared by P123-assisted method.* International Journal of Hydrogen Energy, 2016. **41**(3): p. 1513-1523.
10. Sokolov, S., et al., *Effect of calcination conditions on time on-stream performance of Ni/La2O3–ZrO2 in low-temperature dry reforming of methane.* International Journal of Hydrogen Energy, 2013. **38**(36): p. 16121-16132.
11. Naeem, M.A., et al., *Hydrogen production from methane dry reforming over nickel-based nanocatalysts using surfactant-assisted or polyol method.* International Journal of Hydrogen Energy, 2014. **39**(30): p. 17009-17023.

12. Kumar, P., Y. Sun, and R.O. Idem, *Comparative study of Ni-based mixed oxide catalyst for carbon dioxide reforming of methane.* Energy & Fuels, 2008. **22**(6): p. 3575-3582.
13. Toops, T.J., A.B. Walters, and M.A. Vannice, *Methane combustion over La2O3-based catalysts and γ-Al2O3.* Applied Catalysis A, General, 2002. **233**(1-2): p. 125-140.
14. Cai, W., et al., *Highly dispersed nickel-containing mesoporous silica with superior stability in carbon dioxide reforming of methane: The effect of anchoring.* Materials, 2014. **7**(3): p. 2340-2355.
15. Monaco, F., A. Lanzini, and M. Santarelli, *Making synthetic fuels for the road transportation sector via solid oxide electrolysis and catalytic upgrade using recovered carbon dioxide and residual biomass.* Journal of Cleaner Production, 2018. **170**: p. 160-173.
16. Aramouni, N.A.K., et al., *Catalyst design for dry reforming of methane: Analysis review.* Renewable and Sustainable Energy Reviews, 2018. **82**: p. 2570-2585.
17. Giordano, F., et al., *A model for the temperature-programmed reduction of low and high surface area ceria.* Journal of catalysis, 2000. **193**(2): p. 273-282.
18. Piras, A., A. Trovarelli, and G. Dolcetti, *Remarkable stabilization of transition alumina operated by ceria under reducing and redox conditions.* Applied Catalysis B: Environmental, 2000. **28**(2): p. L77-L81.
19. Trovarelli, A., *Structural and oxygen storage/release properties of CeO2-based solid solutions.* Comments on Inorganic Chemistry, 1999. **20**(4-6): p. 263-284.
20. Andriopoulou, C., et al., *Structural and Redox Properties of Ce1–x Zr x O2− δ and Ce0. 8Zr0. 15RE0. 05O2− δ (RE: La, Nd, Pr, Y) Solids Studied by High Temperature in Situ Raman Spectroscopy.* The Journal of Physical Chemistry C, 2017. **121**(14): p. 7931-7943.
21. Mikulova, J., et al., *Properties of cerium–zirconium mixed oxides partially substituted by neodymium: Comparison with Zr–Ce–Pr–O ternary oxides.* Journal of Solid State Chemistry, 2006. **179**(8): p. 2511-2520.
22. Kambolis, A., et al., *Ni/CeO2-ZrO2 catalysts for the dry reforming of methane.* Applied Catalysis A: General, 2010. **377**(1-2): p. 16-26.

23. Chen, J., et al., *Effect of preparation methods on structure and performance of Ni/Ce0. 75Zr0. 25O2 catalysts for CH4–CO2 reforming.* Fuel, 2008. **87**(13-14): p. 2901-2907.
24. Takeguchi, T., S.-n. Furukawa, and M. Inoue, *Hydrogen spillover from NiO to the large surface area CeO2–ZrO2 solid solutions and activity of the NiO/CeO2–ZrO2 catalysts for partial oxidation of methane.* Journal of Catalysis, 2001. **202**(1): p. 14-24.
25. Montoya, J.A., et al., *Methane reforming with CO2 over Ni/ZrO2–CeO2 catalysts prepared by sol–gel.* Catalysis Today, 2000. **63**(1): p. 71-85.
26. Perrichon, V., et al., *Metal dispersion of CeO2–ZrO2 supported platinum catalysts measured by H2 or CO chemisorption.* Applied Catalysis A: General, 2004. **260**(1): p. 1-8.
27. Zecchina, A. and S. Califano, *The Development of Catalysis.* A History of Key Processes and Personas in Catalytic Science and Technology. Hoboken: Wiley, 2017.
28. Roh, H.-S., K.Y. Koo, and W.L. Yoon, *Combined reforming of methane over co-precipitated Ni–CeO2, Ni–ZrO2 and Ni–Ce0. 8Zr0. 2O2 catalysts to produce synthesis gas for gas to liquid (GTL) process.* Catalysis Today, 2009. **146**(1-2): p. 71-75.
29. Italiano, C., et al., *CO and CO2 methanation over Ni catalysts supported on CeO2, Al2O3 and Y2O3 oxides.* Applied Catalysis B: Environmental, 2020. **264**: p. 118494.
30. Barroso-Quiroga, M.M. and A.E. Castro-Luna, *Catalytic activity and effect of modifiers on Ni-based catalysts for the dry reforming of methane.* International Journal of Hydrogen Energy, 2010. **35**(11): p. 6052-6056.
31. Liu, H., et al., *Effects of Nd, Ce, and La modification on catalytic performance of Ni/SBA-15 catalyst in CO2 reforming of CH4.* Chinese Journal of Catalysis, 2014. **35**(9): p. 1520-1528.
32. Delimitis, A., *IV Yentekakis, G. Goula, P. Panagiotopoulou, A. Katsoni, E. Diamadopoulos, D. Mantzavinos &.* Top Catal, 2015. **58**: p. 1228-1241.

33. Pereñiguez, R., et al., *LaNiO3 as a precursor of Ni/La2O3 for CO2 reforming of CH4: Effect of the presence of an amorphous NiO phase.* Applied Catalysis B: Environmental, 2012. **123**: p. 324-332.
34. Ayodele, B.V., et al., *Production of CO-rich hydrogen from methane dry reforming over lanthania-supported cobalt catalyst: kinetic and mechanistic studies.* International Journal of Hydrogen Energy, 2016. **41**(8): p. 4603-4615.
35. Bradford, M. and M. Vannice, *CO2 reforming of CH4.* Catalysis Reviews, 1999. **41**(1): p. 1-42.
36. Bradford, M.C. and M.A. Vannice, *Catalytic reforming of methane with carbon dioxide over nickel catalysts I. Catalyst characterization and activity.* Applied Catalysis A: General, 1996. **142**(1): p. 73-96.
37. Wei, J. and E. Iglesia, *Mechanism and site requirements for activation and chemical conversion of methane on supported Pt clusters and turnover rate comparisons among noble metals.* The Journal of Physical Chemistry B, 2004. **108**(13): p. 4094-4103.
38. Wang, Y.-H., H.-M. Liu, and B.-Q. Xu, *Durable Ni/MgO catalysts for CO2 reforming of methane: Activity and metal–support interaction.* Journal of Molecular Catalysis A: Chemical, 2009. **299**(1-2): p. 44-52.
39. Song, C. and W. Pan, *Tri-reforming of methane: a novel concept for synthesis of industrially useful synthesis gas with desired H2/CO ratios using CO2 in flue gas of power plants without CO2 separation.* Am Chem Soc Div Fuel Chem Prepr, 2004. **49**(1).
40. Nagaoka, K., et al., *Carbon deposition during carbon dioxide reforming of methane—comparison between Pt/Al2O3 and Pt/ZrO2.* Journal of Catalysis, 2001. **197**(1): p. 34-42.
41. Souza, M.M., D.A. Aranda, and M. Schmal, *Reforming of methane with carbon dioxide over Pt/ZrO2/Al2O3 catalysts.* Journal of Catalysis, 2001. **204**(2): p. 498-511.
42. Xu, J. and M. Saeys, *Improving the coking resistance of Ni-based catalysts by promotion with subsurface boron.* Journal of Catalysis, 2006. **242**(1): p. 217-226.

43. Juan-Juan, J., M. Román-Martínez, and M. Illán-Gómez, *Nickel catalyst activation in the carbon dioxide reforming of methane: effect of pretreatments.* Applied Catalysis A: General, 2009. **355**(1-2): p. 27-32.
44. Takahashi, R., et al., *CO2-reforming of methane over Ni/SiO2 catalyst prepared by homogeneous precipitation in sol–gel-derived silica gel.* Applied Catalysis A: General, 2005. **286**(1): p. 142-147.
45. Verykios, X.E., *Catalytic dry reforming of natural gas for the production of chemicals and hydrogen.* International Journal of Hydrogen Energy, 2003. **28**(10): p. 1045-1063.
46. Wang, Y., et al., *Low-temperature catalytic CO2 dry reforming of methane on Ni-based catalysts: a review.* Fuel Processing Technology, 2018. **169**: p. 199-206.
47. Goula, M., et al., *Syngas production via the biogas dry reforming reaction over Ni supported on zirconia modified with CeO2 or La2O3 catalysts.* international journal of hydrogen energy, 2017. **42**(19): p. 13724-13740.
48. Makri, M., et al., *Effect of support composition on the origin and reactivity of carbon formed during dry reforming of methane over 5 wt% Ni/Ce1− xMxO2− δ (M= Zr4+, Pr3+) catalysts.* Catalysis Today, 2016. **259**: p. 150-164.
49. Roh, H.-S., et al., *Carbon dioxide reforming of methane over Ni incorporated into Ce–ZrO2 catalysts.* Applied Catalysis A: General, 2004. **276**(1-2): p. 231-239.
50. Sukonket, T., et al., *Influence of the catalyst preparation method, surfactant amount, and steam on CO2 reforming of CH4 over 5Ni/Ce0. 6Zr0. 4O2 catalysts.* Energy & Fuels, 2011. **25**(3): p. 864-877.
51. Horváth, A., et al., *Methane dry reforming with CO2 on CeZr-oxide supported Ni, NiRh and NiCo catalysts prepared by sol–gel technique: relationship between activity and coke formation.* Catalysis Today, 2011. **169**(1): p. 102-111.
52. Ocampo, F., et al. *CO2 methanation over Ni-Ceria-Zirconia catalysts: effect of preparation and operating conditions*. in *IOP Conference Series: Materials Science and Engineering*. 2011. IOP Publishing.
53. Al-Fatesh, A.S., et al., *Sustainable production of synthesis gases via state of the art metal supported catalytic systems: an overview.* Journal of the Chinese Chemical Society, 2013. **60**(11): p. 1297-1308.

54. Binet, C., M. Daturi, and J.-C. Lavalley, *IR study of polycrystalline ceria properties in oxidised and reduced states.* Catalysis Today, 1999. **50**(2): p. 207-225.
55. Wang, W., et al., *Crystal structures, acid–base properties, and reactivities of CexZr1− xO2 catalysts.* Catalysis Today, 2009. **148**(3-4): p. 323-328.
56. Sato, S., et al., *Basic properties of rare earth oxides.* Applied Catalysis A: General, 2009. **356**(1): p. 57-63.
57. Mebrahtu, C., et al., *CO2 methanation over Ni catalysts based on ternary and quaternary mixed oxide: A comparison and analysis of the structure-activity relationships.* Catalysis Today, 2018. **304**: p. 181-189.
58. Sokolov, S., et al., *Stable low-temperature dry reforming of methane over mesoporous La2O3-ZrO2 supported Ni catalyst.* Applied Catalysis B: Environmental, 2012. **113**: p. 19-30.
59. Li, S. and J. Gong, *Strategies for improving the performance and stability of Ni-based catalysts for reforming reactions.* Chemical Society Reviews, 2014. **43**(21): p. 7245-7256.
60. Naeem, M.A., et al., *Syngas production from dry reforming of methane over nano Ni polyol catalysts.* International Journal of Chemical Engineering and Applications, 2013. **4**(5): p. 315.
61. Seo, H.O., *Recent scientific progress on developing supported Ni catalysts for dry (CO2) reforming of methane.* Catalysts, 2018. **8**(3): p. 110.
62. Dębek, R., et al., *Ni-containing Ce-promoted hydrotalcite derived materials as catalysts for methane reforming with carbon dioxide at low temperature–on the effect of basicity.* Catalysis Today, 2015. **257**: p. 59-65.
63. Bobin, A., et al., *Mechanism of CH 4 dry reforming on nanocrystalline doped ceria-zirconia with supported Pt, Ru, Ni, and Ni–Ru.* Topics in Catalysis, 2013. **56**(11): p. 958-968.
64. Zanganeh, R., M. Rezaei, and A. Zamaniyan, *Dry reforming of methane to synthesis gas on NiO–MgO nanocrystalline solid solution catalysts.* International Journal of Hydrogen Energy, 2013. **38**(7): p. 3012-3018.

65. Nagaraja, B.M., et al., *Potassium-doped Ni–MgO–ZrO 2 catalysts for dry reforming of methane to synthesis gas.* Topics in Catalysis, 2013. **56**(18-20): p. 1686-1694.
66. Argyle, M. and C. Bartholomew, *Heterogeneous catalyst deactivation and regeneration: a review.* Catalysts, 2015. **5**(1): p. 145-269.
67. Bartholomew, C.H., *Carbon deposition in steam reforming and methanation.* Catalysis Reviews Science and Engineering, 1982. **24**(1): p. 67-112.
68. Wu, H., et al., *Ni-based catalysts for low temperature methane steam reforming: recent results on Ni-Au and comparison with other bi-metallic systems.* Catalysts, 2013. **3**(2): p. 563-583.
69. Junke, X., et al., *Characterization and analysis of carbon deposited during the dry reforming of methane over Ni/La2O3/Al2O3 catalysts.* Chinese Journal of Catalysis, 2009. **30**(11): p. 1076-1084.
70. García, V., et al., *Effect of MgO addition on the basicity of Ni/ZrO2 and on its catalytic activity in carbon dioxide reforming of methane.* Catalysis Communications, 2009. **11**(4): p. 240-246.
71. Al-Fatesh, A. and A. Fakeeha, *Effects of calcination and activation temperature on dry reforming catalysts.* Journal of Saudi Chemical Society, 2012. **16**(1): p. 55-61.
72. Koo, K.Y., et al., *Combined H2O and CO2 reforming of CH4 over nano-sized Ni/MgO-Al2O3 catalysts for synthesis gas production for gas to liquid (GTL): Effect of Mg/Al mixed ratio on coke formation.* Catalysis Today, 2009. **146**(1-2): p. 166-171.
73. Koo, K.Y., et al., *Combined H2O and CO2 reforming of CH4 over Ce-promoted Ni/Al2O3 catalyst for gas to liquid (GTL) process: Enhancement of Ni–CeO2 interaction.* Catalysis Today, 2012. **185**(1): p. 126-130.
74. Radlik, M., et al., *Dry reforming of methane over Ni/Ce0. 62Zr0. 38O2 catalysts: Effect of Ni loading on the catalytic activity and on H2/CO production.* Comptes Rendus Chimie, 2015. **18**(11): p. 1242-1249.
75. Zanganeh, R., M. Rezaei, and A. Zamaniyan, *Preparation of nanocrystalline NiO–MgO solid solution powders as catalyst for methane reforming with carbon*

dioxide: Effect of preparation conditions. Advanced Powder Technology, 2014. **25**(3): p. 1111-1117.

Appendix

Ni/Ceria zirconia doped with neodymium as an anodic catalyst for intermediate-temperature solid oxide fuel Cells (IT-SOFCs)

7. Introduction

The increasing electric power demand and fast consumption of fossil fuels require highly efficient and green energy conversion technologies. The alternatives to fossil fuel are wind power, hydro-power, wave power, solar energy and power which are derived from renewable fuel such as biomass, waste gas, etc. Amongst other technologies, fuel cell technology has attracted great attention in recent years as it is one of the most promising and highly efficient technology for converting the chemical energy of fuel (usually hydrogen and hydrocarbons) into electric power. Based on the electrolyte materials used, fuel cells are divided into (i) alkaline fuel cell (AFC), (ii) proton exchange membrane fuel cell (PEMFC), (iii) phosphoric acid fuel cell (PCFC), (iv) molten carbonate fuel cell (MCFC) and (v) solid oxide fuel cell (SOFC). Among these type of cells, the solid oxide fuel cells have been widely investigated due to their capability of being powdered not only by hydrogen but also by methane (CH_4) hydrocarbons or renewable fuels such as biogas or alcohols. SOFCs operate in the temperature range of 550-1000ºC, showing the potential to perform simultaneously reforming reactions in their anode compartment (internal reforming mode). The DRM reaction is highly endothermic (ΔH = 247.3 kJ/mol) and usually carried out at temperature higher than 800°C to attain a reasonable yield of syngas [1].

In SOFCs the heat necessary to DRM reaction can be in part provided by the electrochemical reaction. The syngas resulting from the internal DRM process can be directly used to produce electricity. Such a system has tremendous potential to mitigate the effect of greenhouse gases [2, 3]. However suitable catalysts are requested. Nickel-based cermets are widely used as anode support for SOFCs running under hydrogen fuel because of the high catalytic activity and good electronic conductivity of nickel (Ni). However, when IT-SOFC are working with carbon-fuel severe carbon deposition due to Ni presence is one of the major problems which can affect the electrochemical properties of the anode for fuel oxidation, causing structure instability and anode breaking [14]. To consider this problem, it is necessary to introduce a material which can suppress the carbon deposition and improve the structural stability of the SOFC.

Ceria zirconia based mixed oxides were demonstrated to be a promising component for IT-SOFC anode, showing suitable performance regarding mixed (electronic and ionic) conductivity, thermal and redox stability and catalytic properties towards alternative fuels [4-7]. It is also reported that nanostructured ceria doped with Nd leads to the further enhancement in ionic conductivity of ceria based electrolytes and anodes [8]. In this work of thesis neodymium has been demonstrated to be an affective dopant for CeO_2 and ZrO_2 to develop a carbon resistant Ni supported catalyst of DRM. Therefore, it has been explored the possible applications of these materials as components of SOFC anode in cooperation with the research group of Prof. Thomas Etsell, university of Alberta, Canada.

7.1. Research activity and results

7.1.1. YSZ based systems

The present work explores the configuration of cathode and anode materials and in the fabrication of yttria stabilized zirconia (YSZ) based fuel cells [9, 10] to build a SOFC at intermediate temperature (< 800^{o}C) to improve the stability and cell life of fuel cell and to decrease the fabrication cost [2, 11]. Zirconia (ZrO_2) was found to be an important ceramic material used in various advanced applications such as mechanical, electronic, biomedical, optical and thermal devices. ZrO_2 is considered as a crucial material in the form of cubic YSZ (ZrO_2 doped with Y_2O_3) in ceramic fuel cells, which shows higher performance compared to its polymer counterparts. Torabi et al [12] and Amir et al [13] investigated the morphology of porous yttria stabilized zirconia (YSZ) and it was concluded that porosity can greatly affect the surface area, density of three phase boundary and hence can improve the electrochemical performance of fuel cells.

7.1.2. Configuration of cell

The cells are electrolyte supported. Figure 7.1 presents the configuration of prepared fuel cell which involves (i) Ni-YSZ (porous anode) (ii) YSZ (dense electrolyte) (iii) LSM ($La_{1-x}Sr_xMnO_{3-\delta}$)-YSZ (porous cathode). To provide better gas diffusion channels for electrochemical reactions, the anode and cathode structures must be porous

while YSZ electrolyte should be fully dense to prevent air and fuel mixing in the cell [14].

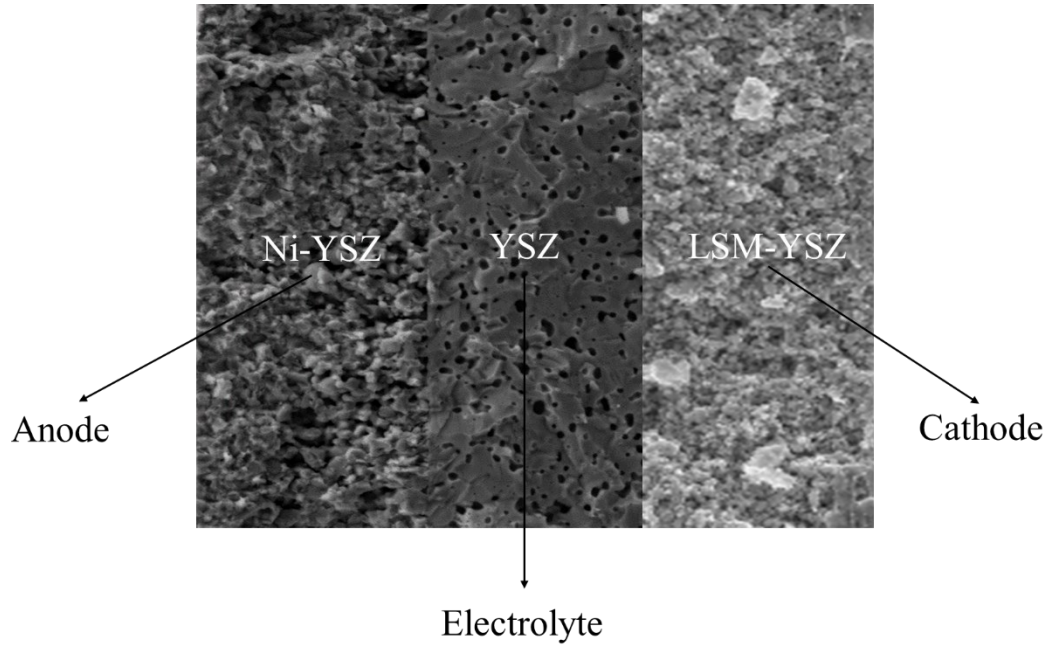

Figure 7.1. Configuration of electrolyte supported SOFC.

7.1.3. Experimental

Screen printing method was employed for the preparation of anode as well as for cathode. YSZ powder (Tosoh TZ-8Y, 8 mol% Y_2O_3) was mixed with water (1:1) and mixture was milled at 120 rmp for 72 h in a plastic bottle using 5mm zirconia balls and finally sintered at 1400°C for 3 h.

7.1.3.1. Preparation of Anode

50:50 vol % of NiO and YSZ were mixed with 60 wt % of solid loading using ink vehicle as a binder. Terpinol ethyl cellulose can also be used as a binder instead of ink vehicle but during our experiments we have observed that ink vehicle is a best binder for screen printing method. The samples were mixed in a plastic jar and ball milled using 5 mm ZrO_2 balls in a rotating mill (f=22.4 1/sec for 100 mins). The mass ratio of ZrO_2 balls to YSZ powder was set as 6:1 to provide sufficient load to crush the coarse powders. Ethanol was added to the mixture for homogenous mixing and at the end the mixture was

put under fume hood with continues stirring for the complete evaporation of ethanol. Finally, Ni-YSZ paste was incorporated onto dense YSZ electrolyte and sintered at 1300ºC/3h (Figure 7.2).

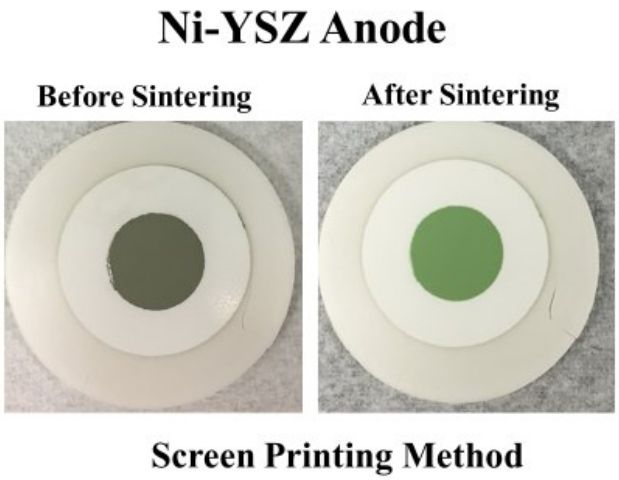

Figure 7.2. Ni-YSZ anode before and after sintering.

7.1.3.2. Preparation of Cathode

LSM-YSZ cathode was prepared with 50:50 vol % of LSM and YSZ by using the same procedure as for anode. Final LSM-YSZ paste was incorporated onto dense YSZ electrolyte and sintered at 1100ºC/3h (Figure 7.3).

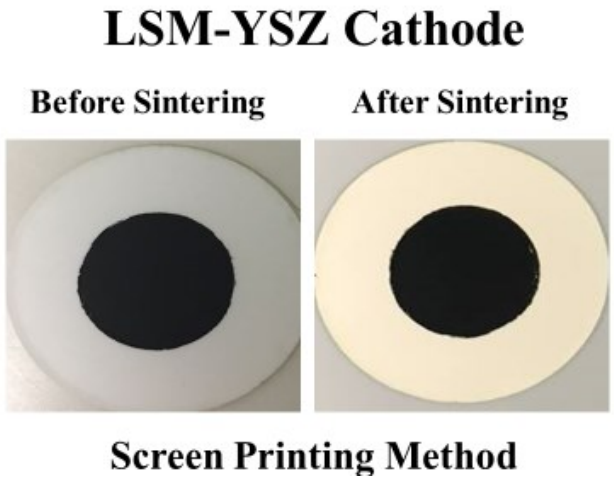

Figure 7.3. LSM-YSZ cathode before and after sintering.

7.1.3.3. Infiltration Method

$CeNd_{0.2}$ and $ZrNd_{0.2}$ were impregnated into Ni-YSZ anode scaffold using nitrate solutions. The desired amounts of $Ce_{0.8}Nd_{0.2}O_{1.9}$ ($CeNd_{0.2}$) and $Zr_{0.8}Nd_{0.2}O_{1.9}$ ($ZrNd_{0.2}$) using $Ce(NO_3)_3*6H_2O$, $ZrO(NO_3)_2$ and $Nd(NO_3)_3*6H_2O$ precursors were mixed with a small amount of a polymeric dispersant (Triton X-45, Union Carbide Chemicals and Plastics Co., Inc.) and water. The mixture was heated at 90°C temperature with continuous stirring and subsequently decompose to the oxides at 350°C, process was repeated for 6 time to make sure that Ni-YSZ anode scaffold is properly infiltrated and finally heated at 800°C to be sure they were single phase.

7.1.4. Results

7.1.4.1. SEM

In order to understand the effect of impregnation and to better investigate the number of impregnation steps, we first determine the impregnation of $CeNd_{0.2}$ into Ni-YSZ anode scaffold. Figure 7.4 and Figure 7.5 demonstrates the SEM images of Ni-YSZ anode after 3 steps of $CeNd_{0.2}$ impregnation and LSM-YSZ cathode respectively.

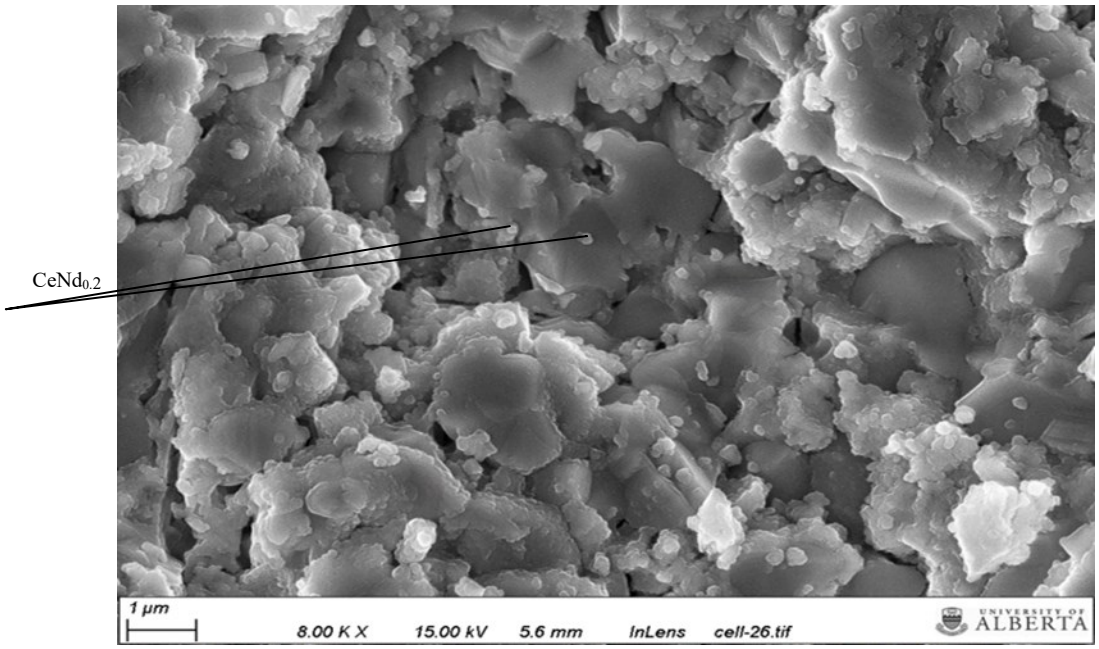

Figure 7.4. SEM image of Ni-YSZ anode after $CeNd_{0.2}$ infiltration.

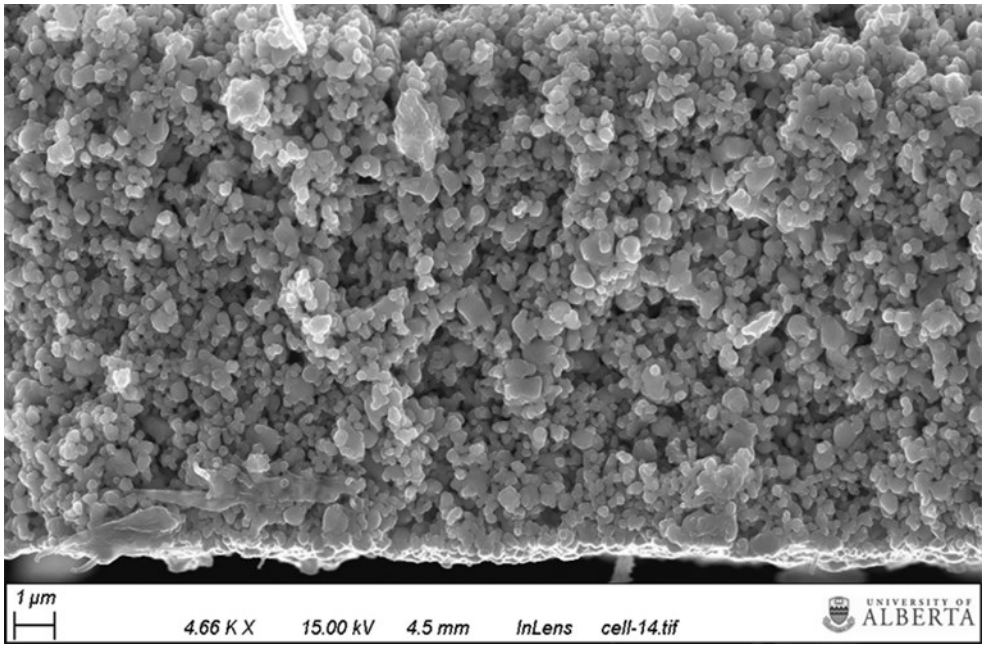

Figure 7.5. SEM image of LSM-YSZ cathode.

It can be seen from Figure 7.4 that $CeNd_{0.2}$ is homogenously dispersed onto Ni-YSZ scaffold.

Future goals

Two complete fuel cells with each catalyst were fabricated. The electrochemical performance will be studied with Electrochemical Impedance Spectroscopy in a symmetric cell in a single cell configuration using biogas as fuel. The behavior of catalysts will be evaluated for;

1. Their ability to catalyze the dry reforming reaction whereby approximately 50:50 mixture of CO and H_2 will be produced.
2. Their ability to avoid coke resulting from methane cracking.

References

1. Wang, Y., et al., *Low-temperature catalytic CO_2 dry reforming of methane on Ni-based catalysts: a review.* Fuel Processing Technology, 2018. **169**: p. 199-206.

2. Sandhu, N.K., et al., *Electrochemical performance of a short tubular solid oxide fuel cell stack at intermediate temperatures.* Applied energy, 2016. **183**: p. 358-368.

3. Jiang, Z., et al., *Turning carbon dioxide into fuel.* Philosophical Transactions of the Royal Society A: Mathematical, Physical and Engineering Sciences, 2010. **368**(1923): p. 3343-3364.

4. Song, S., R.O. Fuentes, and R.T. Baker, *Nanoparticulate ceria–zirconia anode materials for intermediate temperature solid oxide fuel cells using hydrocarbon fuels.* Journal of Materials Chemistry, 2010. **20**(43): p. 9760-9769.

5. Boaro, M., et al., *Effect of redox treatments on Ce0. 50Zr0. 50O2 based solid oxide fuel cell anodes.* Journal of power sources, 2014. **270**: p. 79-91.

6. Boaro, M., et al., *Study on Redox, Structural and Electrical Properties of Ce x Zr1− x O2 for Applications in SOFC Anodes.* Journal of The Electrochemical Society, 2011. **158**(2): p. P22-P29.

7. Zhao, K., et al., *NiMo-ceria-zirconia catalytic reforming layer for solid oxide fuel cells running on a gasoline surrogate.* Applied Catalysis B: Environmental, 2018. **224**: p. 500-507.

8. Uslu, İ., et al., *Synthesis and characterization of neodymium doped ceria nanocrystalline ceramic structures.* Ceramics International, 2012. **38**(6): p. 4943-4951.

9. Hanifi, A.R., et al., *Slip-cast and hot-solution infiltrated porous yttria stabilized zirconia (YSZ) supported tubular fuel cells.* Journal of Power Sources, 2014. **266**: p. 121-131.

10. Laguna-Bercero, M.A., et al., *High performance of microtubular solid oxide fuel cells using Nd 2 NiO 4+ δ-based composite cathodes.* Journal of Materials Chemistry A, 2014. **2**(25): p. 9764-9770.

11. Hanifi, A.R., et al., *Development of Redox Resistant Infiltrated Tubular SOFCs.* ECS Transactions, 2013. **57**(1): p. 1245-1257.

12. Torabi, A., et al., *Effects of porous support microstructure on performance of infiltrated electrodes in solid oxide fuel cells.* Journal of the Electrochemical Society, 2011. **159**(2): p. B201-B210.

13. Vincent, A.L., et al., *Preparation and characterization of an solid oxide fuel cell tubular cell for direct use with sour gas.* Journal of power sources, 2013. **240**: p. 411-416.

14. Hanifi, A.R., et al., *Effects of calcination and milling on surface properties, rheological behaviour and microstructure of 8 mol% yttria-stabilised zirconia (8 YSZ).* Powder technology, 2012. **231**: p. 35-43.

Carbon mass balance

Dry reforming tests were carried out with a 0.66 CO_2/CH_4 ratio with total volumetric flow of 80 mL/min, resulting in a GHSV of 8000 h^{-1}. Nitrogen was used as internal reference. The concentration of effluent gases (CO, H_2, CO_2 and CH_4) from reactor was analyzed by using a micro-gas chromatograph equipped with TCD detector. The conversions of CO_2 and CH_4 and H_2/CO ratios were calculated according to the following formulas, where the factor $\beta = [N_2]_{in}/[N_2]_{out}$ allows to take into account the changes of flow rate during the reaction. Reference samples are $Ni/CeZrNd_{0.2}$ and $Ni/CeZrNd_{0.07}$.

Formulas

$$X[CH_4]\% = ([CH_4]in-([CH_4]out* \beta))/[CH_4]in)*100$$

$$X[CO_2]\% = ([CO_2]in-([CO_2]out* \beta))/[CO_2]in)*100$$

$$H_2/CO = ([H_2]out* \beta)/([CO]out* \beta)$$

$$\text{Carbon balance} = ([CO]out* \beta)+([CH_4]out* \beta)+([CO_2]out* \beta))/ ([CH_4]in+[CO_2]in)*100$$

Table 1. Effect of time on the catalytic activity of Ni/CeZrNd$_{0.07}$ catalyst (at different surface area) with 3.5% Ni impregnation.

Time	N2 in	N2 out	H2 rest	H2 out	H2 corr	H2*β	CH4 in	CH4 out	CH4*β	CO2 in	CO2out	CO2*β	CO out	CO*β	conv CH4 (%)	conv CO2(%)	H2/CO	Carbon Balance
60	4.8086	3.647985	0.07	24.6316	24.56163	32.37597	42.4528	18.7131	24.66672	28.8329	6.137804	8.09056	28.31264	37.32037	42	72	0.87	98
120	4.8086	3.630862	0.07	24.1832	24.11324	31.93482	42.4528	19.11949	25.32125	28.8329	6.458159	8.552985	27.95897	37.02799	40	70	0.86	99
180	4.8086	3.604179	0.07	23.96001	23.89001	31.87341	42.4528	19.49686	26.01219	28.8329	6.606748	8.814548	27.78114	37.06486	39	69	0.86	101
240	4.8086	3.577596	0.07	23.81357	23.74357	31.91343	42.4528	19.8911	26.73536	28.8329	6.673353	8.969566	27.58207	37.0727	37	69	0.86	102
300	4.8086	3.620024	0.07	23.22303	23.15303	30.75496	42.4528	19.61799	26.05925	28.8329	6.687191	8.882822	27.59497	36.65533	39	69	0.84	100
360	4.8086	3.62258	0.07	23.43739	23.36739	31.01779	42.4528	20.23377	26.85823	28.8329	6.743351	8.951098	27.28059	36.21215	37	69	0.86	101
420	4.8086	3.57940	0.07	23.34169	23.27169	31.26346	42.4528	20.37924	27.3777	28.8329	6.789368	9.120914	27.15924	36.48602	36	68	0.86	102
480	4.8086	3.64631	0.07	23.21644	23.14644	30.52459	42.4528	20.26986	26.73107	28.8329	6.800102	8.967699	27.08277	35.71566	37	69	0.85	100

Table 2. Effect of time on the catalytic activity of Ni/CeZrNd$_{0.2}$ catalyst (at different surface area) with 3.5% Ni impregnation.

Time	N2 in	N2 out	H2 rest	H2 out	H2 corr	H2*β	CH4 in	CH4 out	CH4*β	CO2 in	CO2out	CO2*β	CO out	CO*β	conv CH4 (%)	conv CO2(%)	H2/CO	Carbon Balance
60	4.7131	3.545516	0.04	23.0274	22.98743	30.55748	42.4026	20.51264	27.26771	29.5589	7.194786	9.56412	27.28278	36.26734	36	68	0.84	102
120	4.7131	3.646197	0.04	21.8899	21.84991	28.24334	42.4026	20.97254	27.10925	29.5589	7.665873	9.90896	26.5987	34.38167	36	66	0.82	99
180	4.7131	3.579777	0.04	21.95404	21.91404	28.85181	42.4026	21.50606	28.31467	29.5589	7.885023	10.38134	26.41081	34.77221	33	65	0.83	102
240	4.7131	3.57461	0.04	21.71465	21.67465	28.57789	42.4026	21.71891	28.63624	29.5589	7.911763	10.43161	26.24844	34.60841	32	65	0.83	102
300	4.7131	3.590744	0.04	21.28151	21.24151	27.88095	42.4026	22.26229	29.2208	29.5589	8.204651	10.76917	25.86519	33.94985	31	64	0.82	103
360	4.7131	3.61839	0.04	20.98437	20.94437	27.28092	42.4026	22.34093	29.1	29.5589	8.265666	10.76638	25.84208	33.6604	31	64	0.81	102
420	4.7131	3.62853	0.04	20.65193	20.61193	26.77284	42.4026	22.58794	29.33948	29.5589	8.432158	10.95253	25.43238	33.03413	31	63	0.81	102
480	4.7131	3.605412	0.04	20.60241	20.56241	26.87979	42.4026	22.52881	29.45032	29.5589	8.44326	11.03728	25.29418	33.06529	31	63	0.81	102

REVIEW 1

Surname

RAZZAQ

Name

RABIL

Title of the Thesis

"Effect of Neodymium on the development of Ni supported catalysts for carbon dioxide reforming of methane."

Evaluator's data

Name

ANTONELLA

Surname

GLISENTI

E-mail

antonella.glisenti@unipd.it

Evaluator's institution

University of Padova Department of Chemical Sciences

First of all, I thank the reviewer for the positive evaluation of our study, and for productive advice for an improvement. Below you will find our reply to your comments and the corresponding actions taken.

(1). The student reported that the amount of surfactant influences the properties and catalytic attitude of the samples but no hypothesis concerning the reasons and the mechanism of formation of the compound. It appears that the S/C molar ratio = 0.25 allows to reach the better results and for higher values the structure collapses and pore close (Page 49) but why? Is there anything in literature connecting the surfactant and the pore structure? I suggest a more accurate evaluation, at least of literature.

Answer. Explained in chapter 4 page # 48-52.

(2). XRD data (pag 51); the graphs are with lines so thick that is difficult to evaluate the consideration the differences between patterns; it is better to indicate, moreover, where Ni is expected to contribute so to convince readers.

Answer. Corrected in chapter 4 page # 52-53

(3). TPR (pag 51) I suggest to gradually explain the TPR starting from CeO_2, CeZr and then the effect of adding Nd otherwise the importance of the result obtained is lost. Or Chapter concerning the simpler oxides (such as 5) can be reported before.

Answer. Corrected in chapter 4 page # 53-55

(4). In table 2 the Degree of reduction is not defined (it is defined in a successive chapter) and is not evident the quantitative discussion. I suggest to better describe this part and to compare the H_2 uptake with the expected one (explaining how is obtained the reference value).

Answer. All necessary changes have been made in chapter 4 page # 53-55 and detailed experiments were conducted and explained in detail from chapter 5.

(5). In CO-chemisorption all data are commented in 5 rows: I suggest the Student to explain the meaning of this measure and how chemisorption of CO can give Dispersion. I also suggest to indicate what dispersion means: are the reported values good or not? How they compare to literature values or to commercial catalysts?

Answer. Corrected in chapter 4 page # 55-56

(6). In fig. 4.5 which is the error-bar? Are the differences between the curves significant?

The error between different runs was found to be negligible (0.5-2%), therefore, no error bar is mentioned in plots (chapter 4 page # 58)

(7). In Chap. 4b both the effect of surfactant and doping are reported but a more detailed discussion on the catalytic results, connected to specific surface area or to the effect of dopants should be carried out.

Answer. Correction has been made in chapter 4

(8). In chapter 5 table 1 and 2 is difficult to rationalize the results because the calcination temperatures are not exactly comparable.

Answer. As explained in chapter 5 page # 66-69, the purpose of calcination at higher temperatures is to reduce surface area of materials to investigate the effect of catalytic activity at lower as well as higher surface area.

(9). At page 70 the sentence "Ni impregnation attributable to strong basic sites by an additional peak at higher temperature (between 500-630°C), when compared to original supports" is not clear to me.

Answer. This means that in comparison to original support materials (without Ni) (Fig 5.9 A) Ni impregnation increases strong basic sites as inferred by the presence of an additional peak at higher temperature (between 500-630°C) page # 77.

(10). Page 75 "This means that the co-presence of Zr and Nd inhibits the reverse water gas shift reaction and hence increase the H_2/CO ratio." Why?

Answer. Explained in chapter 5 page # 80-83.

(11). Paragraph 5.1.6.2; 8 hours are enough to judge the stability? Maybe the first hours are the more significant? Can the Student compare with literature or to commercial catalysts performance?

Answer. Explained in chapter 5 page # 83.

(12). Page 77 "The process is probably the main responsible of the deactivation observed in the first three hours of test, and it affects methane conversion more than CO_2 conversion" there are a lot of references in literature, concerning the amount and morphology of deposited Carbon and the effect on deactivation. I suggest a post reaction SEM investigation to evaluate the morphology of C.

Answer. Explained in chapter 5 page # 83-87. SEM analysis was conducted for $CeNd_{0.2}$ and $ZrNd_{0.2}$ catalysts chapter 6 page # 105-106 but it was difficult to investigate the nature

and type of carbon accumulation so now it is decided to characterize the samples with Raman spectroscopy as it is more advanced and it is easy to understand the nature of accumulated carbon on the surface of catalysts.

(13). Chap 6 Table 1 same consideration that for Chap. 5; the reasons of using this calcination temperature is not so evident and justified.

Answer. As already explained in chapter 5 page # 66-69, the purpose of calcination at higher temperatures is to reduce surface area of materials to investigate the effect of catalytic activity at lower as well as higher surface area.

(14). Page 91: "These results indicated that Nd doping strongly influence the catalytic activity of zirconia rather than ceria doped Nd and undoped Zr catalysts. " Why?

Answer. Explained in chapter 6 page # 93, discussions, conclusions and future goals, page # 110-115

(15). Page 95 "Furthermore, it can be seen (Table 3) that Ni/$ZrNd_{0.2}$_800, Ni/$ZrNd_{0.2}$_1030 and Ni/$CeNd_{0.2}$_800 catalysts having low carbon deposition" does not sound correct "The results can be indicated that Nd doping can possibly decrease the carbon deposition during DRM reaction" why?

Answer. SEM analysis was conducted for Ni/$CeNd_{0.2}$ and Ni/$ZrNd_{0.2}$ catalysts chapter 6 page # 105-106 but it was difficult to investigate the nature and type of carbon accumulation so now it is decided to characterize the samples with Raman spectroscopy as it is more advanced and it is easy to understand the nature of accumulated carbon on the surface of catalysts.

(16). Page 97 "This means that 1% is a small amount of Ni for impregnation and still there are active molecules onto support surface while higher Ni loading (7%) blocking the active sites of support." I expect that the deposition procedure can make a big difference in determining the "better" loading. Can the Student better discuss this point?

Answer. Explained in chapter 6 page # 109-110

(17). Page 100 "Moreover, Ni impregnation on Ce and $CeNd_{0.2}$ showed a very small peak at $2\theta = 42.38$ degree which corresponds to (200) plane of cubic NiO (PDF 78-0492). This suggests that NiO is well dispersed on Ce and $CeNd_{0.2}$ supports." A signal in XRD is not necessary meaning a high dispersion: highly dispersed nanoparticles I expect not to give rise do XRD contributions.

Answer. Explained in chapter 4, 5 and 6 (XRD).

(18). The appendix does not seem to me very relevant: in absence of electrochemical measures the reported data are just the deposition on YSZ of one of the prepared catalysts and the obtained morphology and compatibility is just a preliminary consideration.

Answer. This study is in process.

Future goals

Currently, the actual mechanism of Nd doping remains quite unclear because the effect of Nd as a dopant on CeO_2, ZrO_2 and CeO_2-ZrO_2 materials on the catalytic activity of Ni catalysts for DRM reaction would need further investigation. Moreover, DRM is a complex process where the main reaction ($CH_4 + CO_2 \rightarrow 2CO + 2H_2O$) is accompanied by other parallel-side reactions (reverse water gas reaction, Boudouard reaction and methane cracking) which can cause a decrease in the yield of products and the deactivation of catalysts due to the carbon deposition. In addition, formation and removal of carbon species occur simultaneously. Therefore, in order to understand the effect of Nd on CeO_2, ZrO_2 and CeO_2-ZrO_2 supports and their interaction with Ni, further investigation will be carried out by planning different experiments and characterization by using some advanced techniques such as Raman, FTIR, XPS etc and soon will be published.

REVIEW 2

Surname

RAZZAQ

Name

RABIL

Title of the Thesis

"Effect of Neodymium on the development of Ni supported catalysts for carbon dioxide reforming of methane."

Evaluator's data

Name

Albin

Surname

Pintar

E-mail

albin.pintar@ki.si

Evaluator's institution

National Institute of Chemistry, Ljubljana, Slovenia

First of all, I thank the reviewer for the positive evaluation of our study, and for productive advice for an improvement. Below you will find our reply to your comments and the corresponding actions taken.

(1). Experimental: It is shown in the graphical drawing of the experimental set-up that a glass quartz reactor was used to perform catalytic experiments. This is ok. But it is mentioned in the text that a stainless steel reactor was used. This is not ok, the metallic reactor wall could influence the data measured. This must be clarified.

Answer. Sorry that was a mistake. A quartz microreactor was used to carry out the catalytic experiments.

(2). CHNS elemental analysis must be used to exactly quantify the extent of coke formed on the catalyst surface. TGA analysis solely is not adequate for this purpose.

Answer. CHNS elemental analysis was carried out and explained in chapter 5 page # 85-86.

(3). No attempt was made in the thesis to close carbon mass balance. This must be done in order to demonstrate that the experimental data are of sufficient quality.

Answer. In order to check the accuracy of our GC data, we performed the carbon balance which shows that the error in our data was ± 5%, chapter 3 page # 46 and appendix section table 1 and table 2.

(4). No graph is shown in the thesis presenting the evolution of hydrogen and carbon monoxide during the reaction course. Do so for a few catalytic runs.

Answer. Graphs are plotted presenting the evolution of hydrogen and carbon monoxide, chapter 5 page # 80-83

(5). I can see that the conversion of CO_2 is much higher compared to the conversion of CH_4 in any of the runs. This shows that the extent of water formation through the side RWGS reaction is huge. I cannot agree with the conclusion that the extent of water formation was low. Surprisingly, H_2/CO ratios reported are high. Were the values of H_2/CO ratio calculated correctly? Please check.

Answer. Explained in chapter 5 page # 80-83. Yes, H_2/CO ratio values are calculated correctly according to the formula $H_2/CO = ([H_2]out * \beta) / ([CO]out * \beta)$ already mentioned in experimental section at page 46.

(6). Do you have a possibility to measure the extent of water formed during the reaction course? A conventional GC analyzer should be employed for this purpose instead of a microGC device.

Answer. At the moment is not possible but in future we will consider your point to understand better the extent of water formation during DRM reaction.

(7) Regarding the interpretation of results and discussion, the thesis must be rewritten. You have to try to clearly show (quantitative) structure-activity and structure-selectivity relationships in the thesis. Organize data correspondingly in tables and graphs as well.

Answer. Corrections have been made in thesis.

(8). Effect of neodymium on reaction activity and selectivity: please investigate and present how an increasing amount of neodymium in one of the supports examined influences the catalyst behavior. Such a dependency must be clearly presented in the thesis in order to support your hypothesis.

Answer. Explained in chapter 5 and 6 in discussions and conclusions parts. To understand the actual mechanism that how neodymium effects the activity and selectivity, experimental work is in progress which will take some time and results will be explained soon in our next publication.

(9). Character of coke formed: the extent of coking is high. However, besides TGA analysis and elemental CHNS analysis provide SEM images in the thesis showing the character of coke formed.

Answer. CHNS elemental analysis was carried out and explained in chapter 5 page # 85-86. SEM analysis was conducted for $CeNd_{0.2}$ and $ZrNd_{0.2}$ catalysts chapter 6 page # 105-106 but it was difficult to investigate the nature and type of carbon accumulation so now it is decided to characterize the samples with Raman spectroscopy as it is more advanced and it is easy to understand the nature of accumulated carbon on the surface of catalysts.

Future goals

Currently, the actual mechanism of Nd doping remains quite unclear because the effect of Nd as a dopant on CeO_2, ZrO_2 and CeO_2-ZrO_2 materials on the catalytic activity of Ni catalysts for DRM reaction would need further investigation. Moreover, DRM is a complex process where the main reaction ($CH_4 + CO_2 \rightarrow 2CO +$

$2H_2O$) is accompanied by other parallel-side reactions (reverse water gas reaction, Boudouard reaction and methane cracking) which can cause a decrease in the yield of products and the deactivation of catalysts due to the carbon deposition. In addition, formation and removal of carbon species occur simultaneously. Therefore, in order to understand the effect of Nd on CeO_2, ZrO_2 and CeO_2-ZrO_2 supports and their interaction with Ni, further investigation will be carried out by planning different experiments and characterization by using some advanced techniques such as Raman, FTIR, XPS etc and soon will be published.